Characterising Novel Human $CD8^+$ T Cell Responses to Influenza A Virus

Submitted by

MiaoJuan Huang

Bachelor of Medicine, Bachelor of Surgery

A thesis submitted in total fulfilment of the requirements for the degree of

Doctor of **P**hilosophy

Department of Biochemistry and Genetics
La Trobe Institute for Molecular Science (LIMS)
Faculty of Science, Health and Engineering

La Trobe University,
Victoria, Australia, 3086

August 2019

Table of Contents

Abbreviations

APCs	Antigen Presenting Cells
ARF	Alternative Reading Frame
ARFP	Alternative Reading Frame encoded peptides
β_2m	Beta 2 microglobulin
BFA	Brefeldin A
BLCLs	B-Lymphocyte Cell Lines
BSA	Bovine Serum Albumin
CCL	Chemokine (C-C motif) Ligand
cDCs	conventional DCs
CDR	Complimentary Determining Region
CMV	Cytomegalovirus
C-terminal	Carboxyl-terminal
Cα	TCR constant alpha chain
Cβ	TCR constant beta chain
DC	Dendritic Cell
DMSO	Dimethyl Sulfoxide
DRiPs	Defective Ribosomal Products
EBV	Epstein Barr Virus
ER	Endoplasmic Reticulum
ERAP	Endoplasmic Reticulum Aminopeptidase
FACS	Fluorescence Activated Cell Sorting
FCS	Fetal Calf Serum
FGF5	Fibroblast Growth Factor 5
Flt3	fms-like tyrosine kinase 3
GM-CSF	Granulocyte/Macrophage Colony-Stimulating Factor
gp75	Tyrosinase-related protein 1
HA	Hemagglutinin
HBV	Hepatitis B Virus
HIV	Human Immunodeficiency Virus
HSV	Herpes Simplex Virus
HLA	Human Leukocyte antigen
HLA-I	HLA Class I
HLA-II	HLA Class II
HPLC	High Performance Liquid Chromatography
h	Hour(s)
IAV	Influenza A Virus
IBV	Influenza B Virus
ICS	Intracellular Cytokine Staining
ICV	Influenza C Virus

IEDB	Immune Epitope Database
IFN-γ	Interferon gamma
IL-2	Interleukin-2
IU	International Unit
ITAMs	Immunoreceptor Tyrosine-based Activation Motifs
LCMV	Lymphocytic Choriomeningitis Virus
IgM	Immunoglobulin M
M1	Matrix protein 1
M2	Matrix protein 2
M-CSF	Macrophage-Colony Stimulating Factor
mDCs	monocyte-derived DCs
MHC-I	Major Histocompatibility Complex class I
MHC-II	Major Histocompatibility Complex class II
Min(s)	Minute(s)
MOI	Multiplicity of Infection
NA	Neuraminidase
NCBI	National Center for Biotechnology Information
NK	Natural Killer cell
NP	Nucleoprotein
NS1	Non-structural protein 1
NS2	Non-structural protein 2
N-terminal	Amino-terminal
ORFs	Open Reading Frames
pMHC-I	Peptide MHC-I complex
pMHC-II	Peptide MHC-II complex
PA-X	Polymerase acidic protein X
PB1	Polymerase Basic protein 1
PB1-F2	Polymerase Basic protein 1 Frame 2
PB1-N155	Polymerase Basic protein 1 N-terminal variant 155
PB1-N182	Polymerase Basic protein 1 N-terminal variant 182
PB1-N40	Polymerase Basic protein 1 N-terminal variant 40
PB2	Polymerase Basic protein 2
PBMCs	Peripheral Blood Mononuclear Cells
pDCs	plasmacytoid DCs
PE	Polyethylene
Pen/Strep	Penicillin, Streptomycin
PFU	Plaque-Forming Units
PHA	Phytohemagglutinin
pH1N1	2009 H1N1 influenza pandemic
PR8	Influenza A Virus strain (A/Puerto Rico/8/1934 H1N1)
PTMs	Post-translational Modifications

rVVs	Recombinant Vaccinia Viruses
RP-HPLC	Reversed Phase High Performance Liquid Chromatography
SLE	Systemic Lupus Erythematosus
TAPBPR	Tapasin-related protein
TAPs	Transporter associated with antigen processing
TCEP	Tris(2-Carboxyethyl)-Phosphine
TCR	T Cell Receptor
TFA	Trifluoroacetic Acid
TGF-β	Transforming Growth Factor β
TNF-α	Tumour Necrosis Factor alpha
Vα	TCR variable alpha chain
Vβ	TCR variable beta chain
WHO	World Health Organization

Abstract

Influenza A virus (IAV) infection triggers annual seasonal epidemics and sporadic pandemics outbreaks, resulting in significant morbidity and mortality globally. IAV-specific $CD8^+$ T cells play a vital role in virus clearance. They recognise specific peptide-MHC class I complexes (pMHC-I) on the surface of antigen presenting cells (APCs) with T cell receptors (TCRs). As they recognise highly conserved internal IAV antigens, there has been considerable interest in studying their protective role during IAV infection. Immunodominance has been studied for decades; however, little is known about the broad-based T cell responses to IAV in humans. Therefore, the specific goal of this thesis is to characterise novel $CD8^+$ T cell responses to IAV in a donor with broad-based IAV-specific $CD8^+$ T cell responses. In this thesis, I first established and optimised a novel $CD8^+$ T cell enrichment method based on $CD8^+$ T cell activation-induced CD3CD8 downregulation and successfully demonstrated that this method allows enriching a low purity polyclonal $CD8^+$ T cell population (**Chapter 3**). Based on this method, I then demonstrated the first case of broad-based $CD8^+$ T cell response to IAV and identified seven highly-conserved novel IAV epitopes including the first HLA-A*33:03 restricted IAV epitope (**Chapter 4**). Interestingly, I observed that the NP- and NS1-specific $CD8^+$ T cell responses were not fully elucidated using synthetic 18mer overlapping peptides. Next, the preliminary results in **Chapter 5** indicated that such $CD8^+$ T cells might recognise internally truncated pin-peptides, likely encoded by alternative reading frame (ARF). Together, this thesis demonstrates a novel approach for enriching rare antigen-specific $CD8^+$ T cells and exploring broad-based $CD8^+$ T cell response to IAV. Data presented in **Chapter 5** may ultimately lead to insights into the generation of ARF peptides or spliced ARF peptides during IAV infection.

Statement of Authorship

This thesis includes work by the author that has been published or accepted for publication as described in the text. Except where reference is made in the text of the thesis, this thesis contains no material published elsewhere or extracted in whole or in part from a thesis accepted for the award of any other degree or diploma. No other person's work has been used without due acknowledgement in the main text of the thesis. This thesis has not been submitted for the award of any degree or diploma in any other tertiary institution.

Signed: Miaojuan Huang 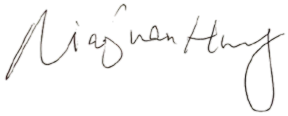

Date: 19/August/2019

Acknowledgements

This work was supported by a La Trobe University Postgraduate Research Scholarship and a La Trobe University Full Fee Research Scholarship. The last four years have been a fantastic journey for me to pursue what I truly believed and loved by exceptional support from a great team of people without whom this work would never be possible.

First and foremost, I would like to express my sincere gratitude to my primary supervisor Professor Weisan Chen for his patience, wisdom and immense knowledge to guide me through this wonderful PhD journey. He encouraged and motivated me to think independently and critically and to be undaunted by asking questions out of the box, and such inspiration shaped me as the scientist I am today. With his continued support and encouragement, the ups and downs of PhD research in the past four years has become more meaningful and worthwhile. I could have never imagined having a better supervisor for my PhD study, and I am thoroughly thankful to him for his guidance.

I would like to thank the rest of my progress committee: my co-supervisor Associate Professor Hamsa Puthalakath and my mentor Dr Ivan Poon. I appreciate their contributions to my research progress and supports for my milestone reports during my PhD study.

I would also like to thank my fellow lab mates for building an amazing working atmosphere, for your technical expertise and the stimulating discussions, and for all the great time we have had in the past four years. In particular, I would like to thank two former lab member, Kun Xiao, for teaching me all necessary lab skills; and Dr Damien Zanker for helping me in troubleshooting.

Last but not least, I would like to thank my family back in China, my Dad Yiqing and my Mum Xinghua for supporting me spiritually throughout my PhD study. I thank my sister Lijuan and her husband Wencong, my brother Jingwei and his beautiful fiancée Zhiwen for spending good, memorable time with me. In particular, I thank Zhiwen for kindly do the proofreading of this thesis.

To my fantastic fiancé Dr Rong Xu, I thank you from the bottom of my heart for always standing by my side, making me become a better, stronger and more self-confident person. I feel so blessed to have you in my life, and I am so excited about the steps we were talking to have a fantastic future together. A special thank you to my unborn baby girl. Sweetheart, it has been a magnificent journey to having you during my thesis writing. I can genuinely feel your hiccups, kicking and moving, and I know this is a lovely way you are trying to support Mummy to get through this tough time.

Furthermore, I want to commemorate this work to my beloved Grandpa and Grandma; you both are one of the driving force for me to complete this work. Dearest Grandpa, you are the only reason for making me attend medical school and pursuing my dream career. My beloved Grandma, I thank you for making my childhood a full of love, which helps me conquer all the difficulties in my life.

List of publications

Huang, M.; Zhang, J.; Chen, W. FACS isolation of low percentage human antigen-specific $CD8^+$ T cells based on activation-induced CD3 and CD8 downregulation. *Journal of Immunological Methods*. 472 (2019) 35-43

Huang, M.; Zanker, D.; Chen, W. Broad-based $CD8^+$ T cell shows an atypical immunodominance hierarchy during Influenza A virus infection. *Manuscript in preparation*

Chen, L.; Anthony, A.; Oveissi, S.; **Huang, M**.; Zanker, D.; Xiao, K.; Wu, C.; Zou, Q.; Chen, W. Broad-based $CD4^+$ T cell responses to influenza A virus in a healthy individual who lacks typical immunodominance hierarchy. *Frontiers in Immunology*. 2017 Apr 3; 8:375

List of Tables

List of Figures

Appendix

Chapter 1: General introduction

1.1 The overview of the immune system

Humans encounter potentially disease-causing pathogens such as bacteria and viruses in our daily life. Our immune system is composed of a group of cell types and some specific molecules, which together fight off harmful organisms and ensure our body disease-free. The immune response can be divided into the innate (natural) and the adaptive (acquired) responses (Chaplin, 2010).

1.2 Innate immune system

Innate immunity provides host defence through the activity of by using phagocytic cells (neutrophils, macrophages and dendritic cells), inflammatory mediator-releasing cells (mast cells), natural killer (NK) cells and molecular components such as complement, cytokines, and many physiological and chemical barriers (Delves et al., 2000; Parkin et al., 2001). The innate immunity is rapid in response to pathogens but generally lacks specificity and immunologic memory (Chaplin, 2010). Its most important role is to serve as the first line of defence while cells of the adaptive immune system undergo clonal expansion. Importantly, although innate and adaptive immunity are often described as separate and contrasting systems, they actually work together to eradicate pathogens.

1.2.1 Dendritic Cells

Dendritic cells (DCs) are the major professional antigen-presenting cells (APCs) derived from bone marrow precursors. Most importantly, DCs make a critical connection between the innate and the adaptive immune systems. They were first discovered by Ralph Steinman in 1973 (Steinman et al., 1973), since then DCs have been extensively studied, with a number of different subsets discovered (Steinman, 2012). The differentiation and function of DCs can be modulated through different growth factors and cytokines such as granulocyte/macrophage colony-stimulating factor (GM-CSF), macrophage-colony stimulating factor (M-CSF), fms-like tyrosine kinase 3 (Flt3) and transforming growth factor β (TGF-β) (Banchereau et al., 2000). Therefore, there are a large variety of DCs and they

perform diverse functions. Human DCs can be classified as plasmacytoid DCs (pDCs), conventional DCs (cDCs), and monocyte-derived DCs (mDCs) (K. Liu et al., 2010; Merad et al., 2013). DCs, as our immune sentinels, constantly survey through the blood and peripheral tissues looking for any invading pathogens (Guermonprez et al., 2002). Once they detect invaders they will sample their antigens and bring them to the local lymph nodes to activate both B cells and T cells. Alternatively, antigens enter lymph nodes via the circulation or lymph can be presented by the resident DCs to B and T cells (Banchereau et al., 1998). During Influenza A virus (IAV) infection, DCs can acquire antigen through two different mechanisms. The first is that DCs are directly infected by IAV and therefore produce IAV antigens (Bhardwaj et al., 1994; Hamilton-Easton et al., 1995) and the second is that DCs acquire IAV antigens via phagocytosis of virus particles or infected apoptotic cells or cell debris (Banchereau et al., 1998; Mori et al., 1995). DCs activate B cells by directly display viral antigens which are recognised by B-cell receptors (B cell surface antibodies). However, DCs activate T cells by displaying processed peptide fragments as peptide major histocompatibility complex class I (pMHC-I) or peptide MHC-II (pMHC-II) complexes on their surface through MHC-I or MHC-II antigen processing and presentation pathways. The MHC-I antigen presentation pathways will be further reviewed in below section 1.5.3.

1.3 Adaptive immune system

Upon virus infection, both innate and adaptive immune systems are activated. The adaptive immune system is composed of humoral (antigen-specific antibodies) and cellular immune arms (antigen-specific $CD4^+$ and $CD8^+$ T cells). During the first pathogen encounter, the adaptive immune responses get into effect relatively slowly as the responses are based on the expansion of limited antigen-specific B and T cells that are highly specific to their target antigens (Chaplin, 2010). Once activated, T cells will leave the lymphoid tissue and travel to infection sites to clear infected cells. On the other hand, activated B cells will differentiate into mature plasma cells to release high affinity antibodies into the blood and tissue fluids to neutralize the invading pathogens and aid to innate immune response, such as

complement activation and flagging the pathogens to the innate immune cells, such as NK cells and phagocytes, for destruction (Delves et al., 2000). Most importantly, during pathogen reencounter, the adaptive response is rapid and much stronger due to immunological memory, which forms the basis of modern vaccination (Krammer, 2019).

1.3.1 Humoral immunity to IAV

IAV infection induces virus-specific neutralising antibodies produced by B cells (Waffarn et al., 2011). The virus-specific antibodies largely direct toward IAV surface glycoproteins haemagglutinin (HA) and neuraminidase (NA) and have been shown to be protective (McKinstry et al., 2013; Treanor, 2004).

1.3.1.1 B cells and anti-IAV immunity

B cells are developed in the bone marrow, then differentiate into mature B cells in the secondary lymphoid organs such as spleen and lymph nodes, where they encounter antigen and become fully activated (Bertrand et al., 2000; Yuseff et al., 2013). B cells are well known as the precursors of antibody-secreting cells (Burnet, 1976), which play a significant role in protection against influenza infection (Gerhard et al., 1997; Simmons et al., 2007). It has been demonstrated that B cell-mediated immunity is an essential part of immune response not only to influenza virus infection but also the influenza virus vaccines. There are multiple ways B cells respond to IAV infection (Waffarn et al., 2011). First, B cells produce IAV-specific Immunoglobulin M (IgM), which are generally of lower affinity and the response does not require T cell help (Baumgarth et al., 1999; Baumgarth et al., 2000). Second, IAV antigen recognised by IgM on B cell can be endocytosed, further processed and re-expressed on the MHC-II molecule of the B cell to activate $CD4^+$ T cells. The activated $CD4^+$ T cells can then help such B cell to mature into high-affinity antibody-secreting cells. This is known as T cell-dependent B cell responses (Chaplin, 2010; Parkin et al., 2001). Lack of $CD4^+$ T cell help leads to a significant reduction of humoral response after IAV infection (Mozdzanowska et al., 2005).

1.3.2 Cellular immunity to IAV

IAV infection also stimulates cellular immunity characterised by the activation and proliferation of effector T lymphocytes (Butcher et al., 1996; Sun et al., 2013). There are two major types of T lymphocytes, which can simply be differentiated by the expression of surface markers as the helper T cells bearing CD4 co-receptor and cytotoxic T cells bearing CD8 co-receptor (Delves et al., 2000). $CD4^+$ T cells play "help" role in a range of immune responses, such as helping B cells to mature and produce high-affinity and class-switched antibodies; helping $CD8^+$ T cells to form memory cells and their subsequent antigen-specific expansion (Sun et al., 2013); inducing some innate cell differentiation, such as macrophages (Zhu et al., 2008) and maintaining immune homeostasis (Peterson, 2012; Stockinger et al., 2004). $CD8^+$ T cells are cytolytic, they are involved in viral clearance and cancer elimination (Hamada et al., 2013). $CD8^+$ and $CD4^+$ T cells work together to ensure effective immune surveillance (Ostroumov et al., 2018).

1.3.2.1 $CD4^+$ T cells and anti-IAV immunity

$CD4^+$ T cells are a group of cells with different functions and can be subdivided into four subsets according to their cytokine production (Zhu et al., 2008). These populations are Th1, Th2 (Mosmann et al., 1986), Th17 (Harrington et al., 2005; Park et al., 2005), and regulatory T cells (Tregs) (W. Chen et al., 2003; Sakaguchi et al., 2011; Zhu et al., 2008). $CD4^+$ T cells are well-known in their roles of helping $CD8^+$ T cells and B cells (Mozdzanowska et al., 2005; Sun et al., 2013; Swain et al., 2012), however, they also play direct roles against IAV infection (Swain et al., 2012) that is independent of their helper capacity. For example, Teijaro *et al.* demonstrated that both HA-specific and polyclonal IAV-specific mouse memory $CD4^+$ T cells provided direct protection against IAV infection, resulting in enhanced lung viral clearance, recovery from sublethal and lethal virus challenge in the absence of $CD8^+$ T cells, B cells, or other lymphocytes (Teijaro et al., 2010). In addition, a recent study, using 41 healthy volunteers inoculated with IAV intranasally, observed that the pre-existing $CD4^+$ T cell response, but not $CD8^+$ T cell responses, correlated with lower virus shedding and less severe illness

(Wilkinson et al., 2012). As this thesis is concentrated on characterising human IAV-specific $CD8^+$ T cell responses to novel IAV epitopes, the detailed function of $CD4^+$ T cell response to IAV will not be further discussed except for those specifically mentioned in the discussion.

1.3.2.2 $CD8^+$ T cell and anti-IAV immunity

$CD8^+$ T cells play an influential role in controlling and eradicating virus during IAV infection (McMichael et al., 1983). Naïve $CD8^+$ T cells emigrate from thymus before travelling to secondary lymphoid tissues such as lymph nodes and spleen (Butcher et al., 1996), where they wait for activation by DCs (Banchereau et al., 1998; Steinman, 2012). Naïve $CD8^+$ T cells are activated once they recognise virus peptides associated with MHC-I, in the presence of co-stimulation, on antigen-presenting cells, usually lymph node resident DCs (Butcher et al., 1996). Upon activation, they proliferate and differentiate into virus-specific $CD8^+$ T cells , which are capable of producing various proinflammatory cytokines, such as interferon-gamma (IFN-γ), interleukin (IL)-2, and tumour necrosis factor alpha (TNF-α), and chemokines, such as CCL3, CCL4, CCL5, CCL9 and CCL10. These molecules can either directly impede viral function or recruit other immune cells to assist with virus elimination (Garcia-Hernandez Mde et al., 2010; Hamada et al., 2013). In addition, La Gruta *et al.* described a hierarchical cytokine expression for IAV-specific $CD8^+$ T cells, demonstrating all IL-2 and TNF-α producing $CD8^+$ T cells are also capable of producing IFN-γ, but not vice versa (La Gruta et al., 2004). Hence, the production of IFN-γ is used as the readout cytokine for assessing antigen-specific $CD8^+$ T cell response after IAV infection in this thesis to avoid underestimation.

A few studies demonstrated that transferred IAV-specific $CD8^+$ T cells in mice confer powerful viral clearance and reduced mortality after IAV infection (Taylor et al., 1986; Wells et al., 1981; Yap & Ada, 1978; Yap, Ada, et al., 1978). In addition, mice lacking $CD8^+$ T cells showed delayed IAV clearance and increased mortality after IAV challenge (Bender et al., 1992). The early murine studies provided a basic understanding of how $CD8^+$ T cells eliminate IAV infection. It has been

demonstrated that IAV-specific $CD8^+$ T cells mainly respond to conserved internal IAV proteins such as Nucleoprotein (NP) and Matrix protein 1 (M1) rather than surface proteins HA and NA (E. Grant et al., 2013; Wu et al., 2011). Therefore, $CD8^+$ T cell displayed a commanding role in recognising different IAV strains (Gras et al., 2010; Lee et al., 2008). A more recent study provided evidence that human $CD8^+$ T cells showed cross-protection against influenza A, B and C viruses (Koutsakos et al., 2019). Additionally, memory $CD8^+$ T cells showed protective immunity against pandemic strains, such as 2009 H1N1 (Gras et al., 2010; Greenbaum et al., 2009) and decreased disease severity induced by newly emerged H7N9 (Z. Wang et al., 2015). Hence, IAV-specific $CD8^+$ T cells become a promising research target for better understanding and designing future universal IAV vaccines.

1.4 IAV infection

Last year marked the centenary of the 1918 Influenza pandemic. One hundred years on, IAV infection remains a tough public health problem. It remains one of the most contagious acute respiratory infectious disease that causes profound morbidity and mortality worldwide (Short et al., 2018). Influenza epidemics can often be deadly to individuals in the elderly, infants, Indigenous populations, as well as immune compromised groups such as pregnant women and those with serious medical conditions (Bishop et al., 2009). According to the World Health Organization (WHO), seasonal influenza epidemics cause approximately 3-5 million severe cases and nearly 290,000-650,000 deaths worldwide annually (https://www.who.int/en/news-room/fact-sheets/detail/influenza-(seasonal)). The 1918 H1N1 influenza pandemic caused approximately 50 million deaths worldwide (Martini et al., 2019; Saunders-Hastings et al., 2016). Except for the most devastating 1918 H1N1 Influenza pandemic, three other Influenza pandemics occurred in the past 100 years. The 1957, 1968 and 2009 pandemics caused by IAV H2N2, H3N2 and H1N1, respectively (Krammer et al., 2018). In 2009, a novel swine-origin IAV (H1N1) rapidly circulated globally and resulted in the first influenza pandemic in the 21st century (Bautista et al., 2010; Echevarria-Zuno et al., 2009). From April 12, 2009 to April 10, 2010, there were approximately 60.8 million

illnesses, 274,304 hospitalisations, and 12,469 deaths caused by the 2009 Influenza pandemics in the United States (Shrestha et al., 2011). Thus, an effective method of preventing influenza epidemics and influenza-related diseases is urgently needed, especially for people in the specific groups with compromised immune functions.

1.4.1 IAV and its genome

Influenza virus belongs to the Orthomyxoviridae family; there are three types of influenza viruses, Influenza A virus (IAV), Influenza B virus (IBV), Influenza C virus (ICV) (Krammer et al., 2018). Among them, IAV is considered to be the most common circulating virus and has been the most studied. Previous studies reported that IBV infection could also dominate an influenza season and cause severe influenza-related diseases (Koutsakos et al., 2016); whereas ICV only causes disease in children (Matsuzaki et al., 2006). As this thesis concentrates on IAV-specific $CD8^+$ T cell immunity, the IBV and ICV will not be further reviewed.

In brief, IAV is an enveloped, negatively-sensed, single-stranded RNA virus with eight gene segments encoding 12 proteins with known functions (Wise et al., 2009). There are up to 5 other IAV proteins identified, however their specific biological functions remain unclear (Muramoto et al., 2013; Selman et al., 2012; Wise et al., 2009; Wise et al., 2012). For the specific purpose of this thesis, only the 11-known functional IAV proteins are investigated in this study (excluding PA-x). Additionally, there is standardized nomenclature used for describing IAVs. For example, in the name of A/Beijing/262/1995(H1N1): A, virus type (A, B, C); Beijing, the geographic origin of the virus isolation; 262, the strain number of the isolate; 1995, the year of isolation; H1N1, the hemagglutinin and neuraminidase subtypes.

The genome of IAV was sequenced during the 1970s (Palese et al., 1976). After genetic screening, it was believed that eight IAV RNA segments encoded ten virus proteins (Figure 1.1). They are the polymerase basic proteins 1 (PB1) and 2 (PB2), the polymerase acidic protein (PA), nucleoprotein (NP), hemagglutinin (HA), neuraminidase (NA), matrix proteins 1 (M1) and 2 (M2), and non-structural protein

1 (NS1) and 2 (NS2) (Vasin et al., 2014). In 2001, the 11th IAV protein was identified by Chen and colleagues, it is a small pro-apoptotic mitochondrial protein translated from the +1-reading frame of PB1 and named as PB1-F2 (W. Chen et al., 2001). More recently, one more novel IAV protein which modulates the host response to infection from the +1 ribosomal frameshifting of the IAV segment 3 was found and called PA-x (Jagger et al., 2012). In addition, five IAV partial, in-frame translation products were recently identified: PB1-N40 (Wise et al., 2009), PA-N155 and PA-N182 (Muramoto et al., 2013), M42 (Wise et al., 2012), NS3 (Selman et al., 2012), however, their biological function are not clearly demonstrated.

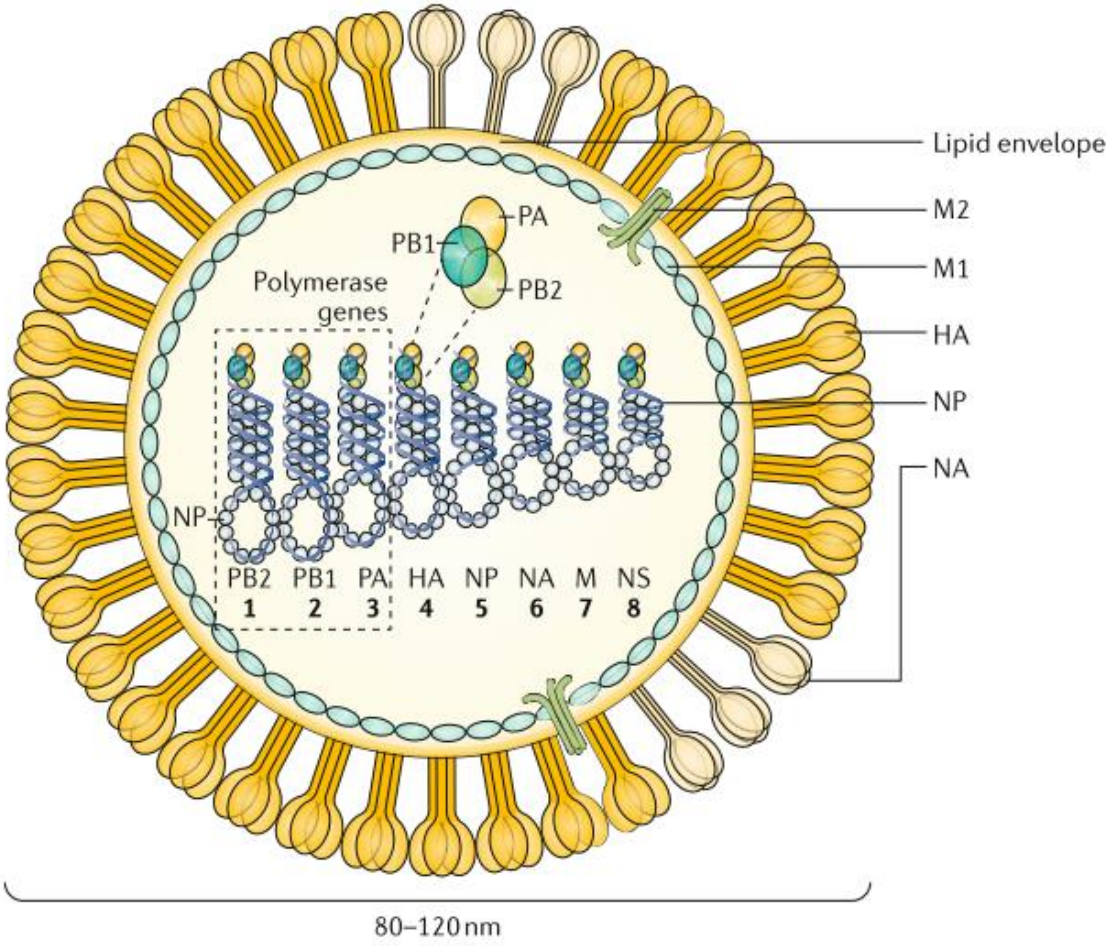

Figure 1.1. The structure of IAV particle

IAV is a negative-sense RNA virus with eight gene segments encoding 12 IAV proteins with known biological function. Three gene segments encode proteins which form the virus polymerase complex: the segment 1 encodes the polymerase basic protein 2 (PB2); the segment 2 encodes the polymerase basic protein 1 PB1 and also a small pro-apoptotic mitochondrial protein which is translated by the +1 reading frame of PB1 and named PB1-F2 (W. Chen et al., 2001); the segment 3 encodes the polymerase acidic protein (PA), and more recently, +1 ribosomal frameshifting product of the segment 3 was found and named as PA-x (Jagger et al., 2012). The segments 4 and 6 encode the surface glycoproteins haemagglutinin (HA) and neuraminidase (NA), respectively. The segment 5 encodes the nucleoprotein (NP) which binds to the viral RNA. The segment 7 encodes the matrix proteins M1 and M2. The segment 8 encodes two non-structural proteins NS1 and NS2. Schematic diagram adapted from (Krammer et al., 2018)

1.4.2 The limitations of current influenza vaccines

Currently, the most common and effective way of controlling IAV infection is IAV vaccines. They play an important role in reducing hospitalisation and morbidity rate with seasonal influenza epidemics. These IAV vaccines mainly target the surface IAV proteins HA and NA, eliciting humoral immune response by activating B cells to yield virus neutralising antibodies against predicted circulating IAV strains for the upcoming season (E. J. Grant et al., 2014; Wrammert et al., 2008). However, the surface proteins HA and NA are frequently mutated due to antigenic drift which is largely triggered by point mutations in the protein's coding gene segments (Grebe et al., 2008); and antigenic shift caused by genetic re-assortment of same gene segments when the host cells are simultaneously infected by two different IAV strains (Taubenberger et al., 2010). Therefore, if the predicted strain does not match the seasonal circulating IAV strains, the current antibody-based vaccines will not provide immune protection. Therefore, novel and more universal vaccines are urgently needed (Grebe et al., 2008). IAV-specific $CD8^+$ T cells typically recognise the conserved internal IAV proteins such as NP and M1 rather than the highly mutated surface proteins HA and NA (E. Grant et al., 2013; Wu et al., 2011). Hence, $CD8^+$ T cell-based vaccines have the potential to be cross-strain protective.

1.4.3 Indigenous Australian's response to IAV infection

Indigenous populations are more susceptible to severe influenza disease and have a high risk to develop influenza-related complications (La Ruche et al., 2009). Previous studies reported that up to 10-20% of Indigenous Australians died from the1918-19 influenza pandemic. Additionally, studies of 2009 H1N1 influenza pandemic (pH1N1) showed that remote-living Aboriginal and Torres Strait Islander people were particularly susceptible to pandemic IAV infection when compared to non-Indigenous groups (Chidgzey et al., 2015). More specifically, the higher pandemic attack and complication rates were associated with markedly higher hospitalisation, intensive care unit admission and death rate for Indigenous Australians during the 2009 pandemic period (Flint et al., 2010; Kelly et al., 2009). Several earlier studies indicated that Indigenous Australians have different HLA

molecules to those in the non-Indigenous populations (Lester et al., 1995; Lienert et al., 1995), suggesting that specific HLA molecules may have a connection with severe influenza disease. It has been subsequently demonstrated that individuals express HLA-A*24:02, HLA-A*01:01, HLA-A*68:01, HLA-B*15:01 showed more limited $CD8^+$ T cell response during IAV infection (Quinones-Parra et al., 2014). Among all, HLA-A*24:02 allele is highly expressed in Indigenous populations and was also shown to be associated with pH1N1 influenza-induced mortality (Clemens et al., 2016; Hertz et al., 2013). However, few studies have been conducted to identify $CD8^+$ T cell epitopes presented by HLAs related to Indigenous Australian populations. Hence, it is of great importance to further investigate the fine immune response in association with host factors, such as HLA alleles to better understand severe IAV infection in Indigenous groups.

1.5 Antigen recognition by $CD8^+$ T cells

1.5.1 The major histocompatibility complex class I (MHC-I) molecules

MHC molecules are the targets of antibodies and $CD8^+$ T cells during rejection of organ transplants (Bach et al., 1976). The main function of MHC-I molecules is to induce tolerance to self-antigens in the thymus and enable immune surveillance by displaying foreign antigen-derived peptides to $CD8^+$ T cells. Mature $CD8^+$ T cells bearing unique T cell receptors can recognise MHC-I molecules associated with non-self-peptides (Robey et al., 1994). Normally, one $CD8^+$ T cell only interacts with a single foreign peptide bound to a particular MHC-I molecule, a phenomenon known as MHC restriction first demonstrated by Zinkernagel and Doherty in 1974 (Zinkernagel et al., 1974).

MHC-I molecules are expressed by almost all nucleated cells, they are type I transmembrane glycoproteins (Halenius et al., 2015) and comprised of two polypeptide chains: a heavy chain and a non-covalently attached β_2-microglobulin (β_2m) light chain (Figure 1.2) (Bjorkman et al., 1987b). The heavy chain is composed of a cytoplasmic tail, a transmembrane region and an extracellular

region (Klein et al., 2000; McCluskey et al., 1999). The extracellular part of the heavy chain folds into α1, α2, and α3 domains. The α1 and α2 domains form a peptide-binding groove that selects peptides of 8-12 amino acids in length and it is also the region that interacts with a specific T cell receptor on a $CD8^+$ T cell (Figure 1.2) (Bjorkman et al., 1987b; Hewitt, 2003; Rist et al., 2013). The MHC-I antigenic specificities are determined by the α1 and α2 domains as they contain variable amino acid sequence (Bjorkman et al., 1987a). β_2m has extensive contacts with all three domains of the heavy chain (Bjorkman et al., 1987a, 1987b). The α3 domain and β_2m are invariant and share primary structural homology with immunoglobulin constant domains (Orr et al., 1979).

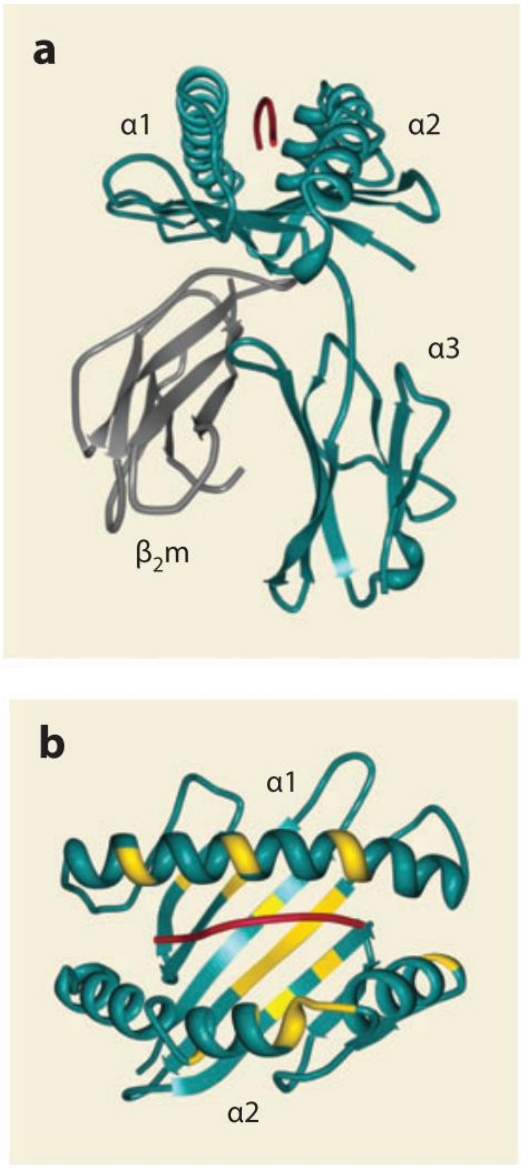

Figure 1.2. The structure of MHC-I molecule with a peptide ligand

The above figures show an HLA-A*2 complexed with $M1_{58-66}$ derived from IAV M1 protein. The structure of MHC-I composes of three domains (α1, α2 and α3, shown in teal) from the heavy chain and a non-covalently bound light chain β_2m (shown in grey). α1 and α2 domains form the top of the molecule with their helical sides facing away from the cell. These domains are distal to the cell membrane. They also form a peptide-binding cleft which binds the $M1_{58-66}$ peptide (shown in red) in both pictures. α3 and β_2m underneath the α1 and α2 domains are proximal to the cell membrane (Bjorkman et al., 1987b). Images adapted from (Blum et al., 2013).

1.5.2 The Human Leukocyte Antigen (*HLA*) and their polymorphisms

In humans, the MHC genes are known as the Human Leukocyte Antigens (*HLA*) and located on the short arm of chromosome 6. HLA class I (HLA-I) and class II (HLA-II) are both glycoproteins, which provide complementary functions in supporting peptide-binding and presenting them to T cells. Humans have three MHC-I gene loci encoding up to 6 class I molecules known as HLA-A, -B, -C; similarly, there are three MHC-II loci encoding up to 6 class II molecules, known as HLA-DR, -DQ, -DP (Blum et al., 2013). HLA genes are extremely polymorphic in human populations, resulting in thousands of individual HLA-I and HLA-II alleles. There are about 3,489 *HLA-A*, 4,356 *HLA-B* and 3,111 *HLA-C* alleles deposited in the Allele Frequency Net Database (Robinson et al., 2017). The polymorphisms lead to amino acid substitutions concentrated around the peptide-binding cleft of the α1 and α2 domains. The result is each *HLA* allele encodes an HLA that possesses almost unique peptide-binding characteristics (Bjorkman et al., 1987a; Sidney et al., 2008). Hence, HLA-I polymorphism directly impacts peptide selection.

1.5.3 MHC-I antigen processing and presentation pathway

Like all viruses, IAV replicates in the infected host cell. The MHC-I antigen presentation pathway plays a major role in alerting the host immune system of virus infection, which can be simply summarised as four main steps: a, peptide generation; b, peptide transportation; c, peptide loading and assembling with MHC-I molecules; d, antigen presentation (Figure 1.3) (Leone et al., 2013).

Early studies indicated that most MHC-I-associated peptides derive from proteasome degradation products of cytosolic (Bennink et al., 1982; Yewdell et al., 1988), nuclear (Gooding et al., 1983), and mitochondrial proteins (Udaka et al., 1993). Taking IAV infection as an example, viral proteins are degraded by proteasome into peptides ranging from 2 to 25 residues (Bell et al., 2009; Leone et al., 2013). These peptides are then translocated into the endoplasmic reticulum (ER) through the transporter associated with antigen processing

(TAP1+TAP2=TAPs) (York et al., 1996). Peptides transported into the ER via TAPs with suitable length are loaded onto nascent MHC-I molecules facilitated by the "peptide-loading complex" composed of ER resident chaperone proteins: Calnexin (Diedrich et al., 2001), Calreticulin (Sadasivan et al., 1996), ERp57 (Hughes et al., 1998), and Tapasin (Ortmann et al., 1997). Tapasin has been known as the first peptide editor that affect peptides loading onto MHC-I molecules (Howarth et al., 2004; Sadasivan et al., 1996). However, a recent study has reported that tapasin-related protein, named TAPBPR, function as a second peptide editor (Hermann et al., 2015; Ilca et al., 2018; Morozov et al., 2016); the crystal structure of a TAPBPR-MHC-I complex was also reported (Jiang et al., 2017). Although TAPBPR is not part of the peptide-loading complex, it works together with tapasin to ensure that peptides of best affinity and length are assembled with MHC-I molecules (Boyle et al., 2013). As MHC-I peptide-binding cleft usually accommodate 8-12 amino acid long peptides, loaded longer peptides with amino-terminal extensions are trimmed by an ER resident enzyme called endoplasmic reticulum aminopeptidase ERAP1 (Chang et al., 2005; Snyder et al., 1994) and ERAP2 (Saveanu et al., 2005). ERAP1 and ERAP2 act as a "molecular ruler" to trim the longer peptides (Chang et al., 2005; Saveanu et al., 2005). Once a peptide is stably bound to an MHC-I molecule and released from the peptide-loading complex, the peptide MHC-I (pMHC-I) complex leaves ER, travels through Golgi apparatus and migrates to plasma membrane awaiting antigen-specific $CD8^+$ T cell recognition.

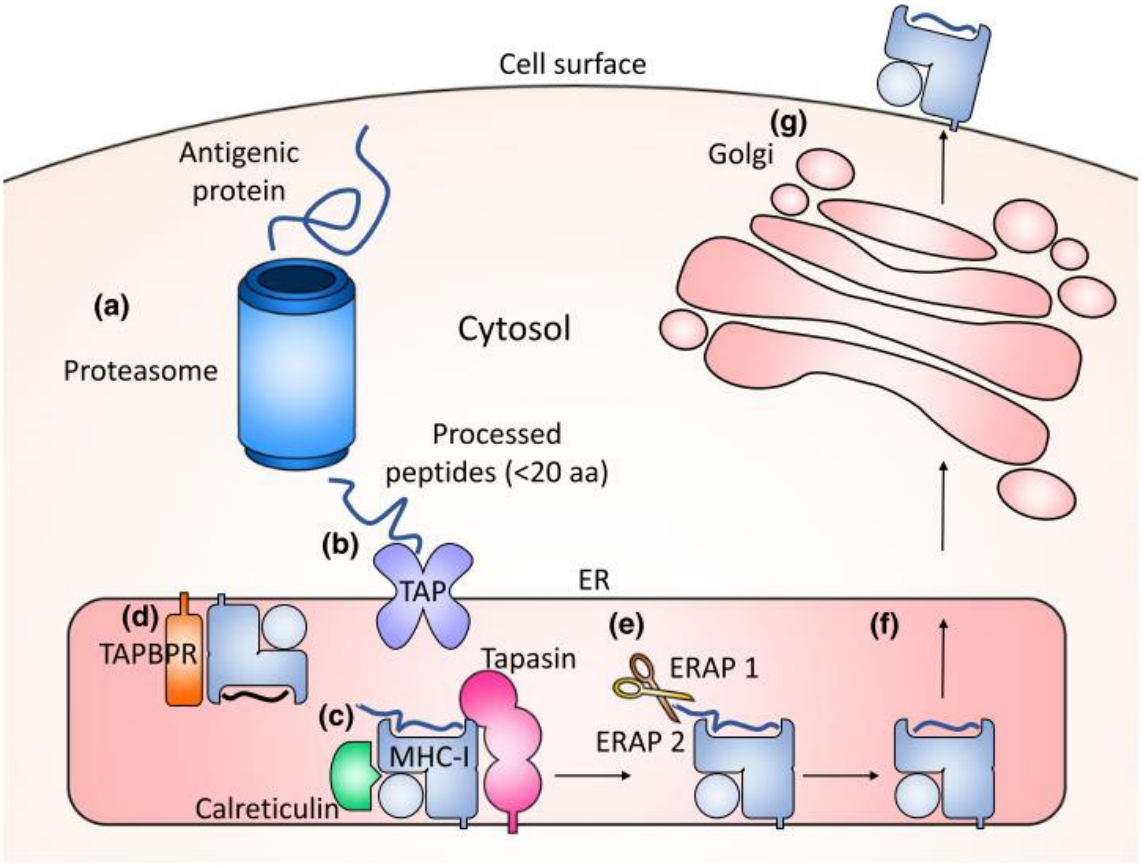

Figure 1.3. Illustrative overview of MHC-I antigen process and presentation pathway

The intracellular antigenic peptides presented by MHC-I molecules can be simply summarized as four steps. First, viral proteins go through proteasome-mediated degradation **(a)**; second, peptides are translocated into ER through TAPs **(b)** and assembled with MHC-I molecules by ER chaperones, a complex also called "peptide-loading complex" **(c)**; the already bound peptides can be edited by Tapasin and its homolog TAPBPR **(d)**; third, longer peptides can be trimmed by ERAP1 and ERAP2 **(e)**; last, the pMHC-I complex leaves ER, travels through Golgi and finally arrives to the cell surface, awaiting $CD8^+$ T cell recognition **(f-g)**. Schematic adapted from (Di Carluccio et al., 2018).

1.6 The T cell receptor

1.6.1 TCR gene rearrangement, complementarity-determining region, and repertoire diversity

$CD8^+$ T cells recognise virus pMHC-I on the surface of antigen presenting cells through their T cell receptors (TCRs) (Davis et al., 1988). TCRs (Figure 1.4) are membrane-bound heterodimers, α and β chain, each of which contains a variable (Vα and Vβ) and constant (Cα and Cβ) domains (Chothia et al., 1988). The V domain of the β chain is encoded by three gene segments: variable (V), diversity (D) and Junctional (J), while the V domain of α chains is encoded by V and J segments only (Chothia et al., 1988; Davis et al., 1988). The V gene segments encoded three regions of hypervariability, termed complementarity-determining regions (CDRs): CDR1, CDR2, and CDR3 (Chothia et al., 1988; Turner et al., 2006). The TCR diversity depends on not only the use of different CDR1 and CDR2 sequence but also the combinatorial and junctional variation in CDR3 (Pannetier et al., 1993).

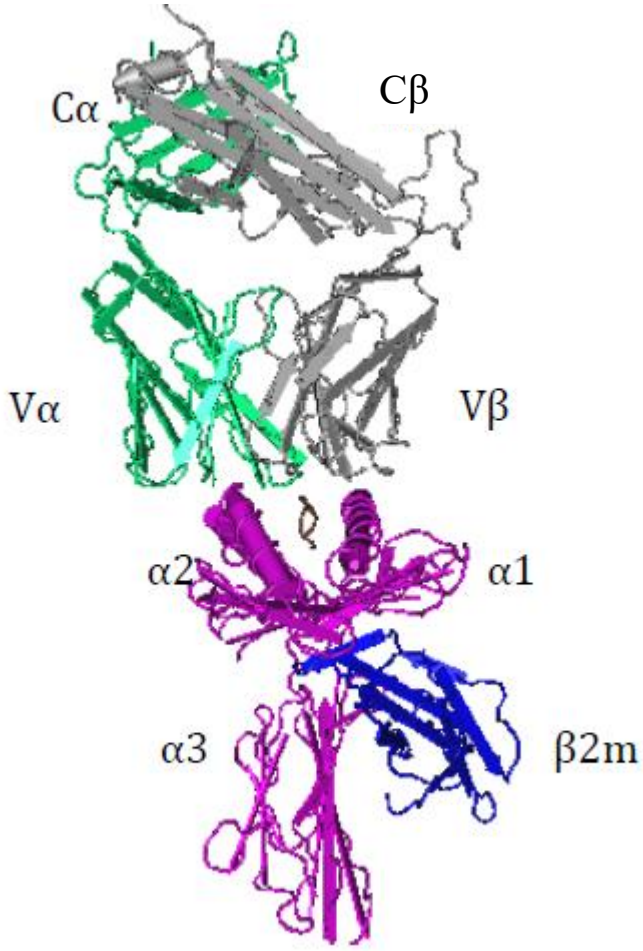

Figure 1.4. The structure of TCR interacts with a pMHC-I complex

The TCR heterodimer is consisted of two polypeptide chains, α and β chain, each of which contains a variable (Vα and Vβ) and a constant (Cα and Cβ) domain. The variable domains interact with the pMHC-I complex. Picture adapted from www.ncbi.nlm.nih.gov protein data bank and analysed using Cn3D version 4.3.

1.6.2 TCR and CD3 complex

The TCR-CD3 is a multi-subunit cell surface protein complex composed of an antigen-binding TCR αβ and CD3 complex (Wegener et al., 1992). More specifically, the TCR α and β subunits exist as a disulfide-linked heterodimer, possessing short cytosolic tails and clonally variable regions that determine its antigen specificity (Davis et al., 1988; Krogsgaard et al., 2005); the CD3 complex is formed by CD3δε and CD3γε heterodimers, and CD3ζζ homodimers (Clevers et al., 1988; Smith-Garvin et al., 2009). Unlike the TCR αβ chains, CD3 components possess large intracytoplasmic domains responsible for coupling antigen recognition to various signal transduction pathways (Wegener et al., 1992). CD3γ, δ and ε each possesses an intracellular immunoreceptor tyrosine-based activation motifs (ITAMs), while CD3ζ possesses three ITAMs in a tandem arrangement. Phosphorylation of these ITAMs leads to signal transduction and ultimately T cell activation (Kane et al., 2000; Kuhns et al., 2012). It has been demonstrated that CD3-γ phosphorylation mediates the downregulation of TCR/CD3 complex after T cell activation (Cantrell et al., 1985; Krangel, 1987)

1.6.3 CD3CD8 downregulation

CD8 is known as the coreceptor on cytotoxic T cells and associated with a cytoplasmic tyrosine kinase $P56^{lck}$ (lck) molecule (Veillette et al., 1988). It is a transmembrane glycoprotein which facilitates and amplifies pMHC-I triggered T cell activation (Bierer et al., 1989; G. F. Gao et al., 2000; Holler et al., 2003; Janeway, 1992). It binds to the α3 domain of the MHC-I that the TCR interacts with for optimal signal transduction during T cell activation (Janeway, 1992; Miceli & Parnes, 1991; Miceli, von Hoegen, et al., 1991; Salter et al., 1990). When CD8 molecule is blocked or in absence, such T cell activation is either blocked or requires longer TCR engagement time (Arcaro et al., 2001). Most importantly, CD8 engagement enhances and stabilises the interaction of TCR/pMHC-I with lower affinity (Laugel et al., 2007; Schott et al., 2002). As CD8 is typically expressed on cytotoxic T cells, it is commonly used as the marker to define cytotoxic T cells. Upon activation $CD8^{+}$

T cells not only down-regulate their TCR (CD3) complexes (Valitutti et al., 1995) but also its coreceptor CD8 (Xiao et al., 2007).

1.7 Immunodominance hierarchy

Following IAV infection, the viral proteins are processed through MHC-I antigen processing and presentation pathway and their peptides presented as pMHC-I complexes to the cell surface and recognised by anti-viral $CD8^+$ T cells. Immunodominance is a central feature of virus-specific T cell responses. In spite of thousands of peptides generated during IAV infection, only a small number of them are capable of eliciting a measurable $CD8^+$ T cell response; and often only a single or a couple of such epitopes stimulate an immunodominant T cell response. This phenomenon is termed as immunodominance (Yewdell et al., 1999). The epitopes that trigger significant anti-viral $CD8^+$ T cell responses are called immunodominant determinants; however, those stimulate much weaker responses are known as subdominant determinants (Yewdell et al., 1999).

1.7.1 Individual MHC-I affect immunodominance

Immunodominance has been studied for decades, however, the mechanisms are not fully understood. Most studies that investigated the underlying mechanisms of immunodominance often used syngeneic mouse models, such as the well-studied influenza infection model in the C57BL/6 and BALB/c mice (Belz et al., 2000; W. Chen et al., 2000), Lymphocytic choriomeningitis virus (LCMV) infected C57BL/6 and BALB/c mice (Oldstone et al., 1995), recombinant vaccinia virus (rVV) infected C57BL/6 mice (Tscharke et al., 2005), Herpes simplex virus (HSV) infected C57BL/6 mice (Wallace et al., 1999), and many others. In such studies, factors, such as peptide-binding ability to MHC, antigen-processing efficiency, and TCR repertoires are investigated (Belz et al., 2000; W. Chen et al., 2000; Oldstone et al., 1995; Tscharke et al., 2005; Wallace et al., 1999). Other factors influence immunodominance are also studied, including the ability of immunodominant $CD8^+$ T cells to actively suppress subdominant ones (Deng et al., 1997; Grufman et al., 1999; Zinkernagel et al., 1978). Importantly, few studies focused on MHC molecule's difference and its impact on immunodominance. In humans, HLA genes are extremely polymorphic, which means that they contain different alleles. Each allele is given a few unique sets of numbers separated by colons, for instance, like

HLA-A*02:01. It is well demonstrated that individual's HLA plays a major role in setting the immunodominance hierarchy. For example, the discovery of the immunodominant IAV epitope restricted to HLA-A*02:01 (Gotch et al., 1987); and similarly the Epstein-Barr Virus (EBV) epitope EBNA3A$_{325-333}$ presented by HLA-B*08:01 (Burrows et al., 1995). More strikingly, in human immunodeficiency virus (HIV) infected individuals who express HLA-B*57 or HLA-B*58:01, Gag$_{240-249}$ epitope is presented by these HLA alleles and stimulates an immunodominant CD8$^+$ T cell response, which not only protects the individuals but also forces the virus to mutate 242T→N resulting in a much-weakened virus. When this virus is passed to their newborn babies vertically, if the baby does not express HLA-B*57 or HLA-B*58:01 the virus mutates back to 242T (Leslie et al., 2004). Immunodominant CD8$^+$ T cell responses in humans have been also widely observed in other viral infections such as cytomegalovirus (CMV) and hepatitis B virus (HBV) (Elkington et al., 2003; Lacey et al., 2003; Malik et al., 2017; Schirmbeck et al., 2002)

1.7.2 HLA dependent immunodominance

As HLA molecules are highly polymorphic and few individuals share the same HLA alleles, the observed immunodominance in humans has been much less reproducible than those observed in the syngeneic murine systems. In the context of IAV, for example, through a systematic approach, our laboratory demonstrated that not all individuals expressing HLA-A*02:01 show immunodominant response to M1$_{58-66}$ (Wu et al., 2011). As this epitope is rarely mutated, the lack of immunodominant response to this epitope is likely the result of emerging novel immunodominant epitopes associated with other HLA molecules co-expressed with HLA-A*02:01 in these individuals (Wu et al., 2011). Moreover, in a group of HLA typed donors, Boon *et al.* demonstrated CD8$^+$ T cell responses to HLA-A*01:01 and HLA-B*08:01 were dominated by the response induced by HLA-A*02:01-, HLA-B*27:05- and HLA-B*35:01-restricted epitopes (Boon et al., 2004). Thus, if one individual expresses a set of HLA molecules that do not present any immunodominant CD8$^+$ T cell epitope from IAV, the prediction would be CD8$^+$ T cell responses in this individual will likely be broad and even to many determinants

during IAV infection and lack pronounced immunodominance. Such type of response has not been previously reported for $CD8^+$ T cells.

1.7.3 Broad-based polyclonal $CD8^+$ T cell responses

Chen *et al.* reported a broad-based IAV-specific $CD4^+$ T cell response from a healthy donor, in which no clear immunodominant response was observed (L. Chen et al., 2017). Following a systematic epitope discovery approach developed previously by our group (Wu et al., 2011), Chen *et al.* found that IAV-specific $CD4^+$ T cell responses focused on M1 and NP at the protein antigen level, however, at the peptide level, IAV-specific $CD4^+$ T cells responded to nine antigenic regions from M1 and NP. Of interest, not a significant immunodominant region can be detected from these nine antigenic regions (L. Chen et al., 2017). According to the literature search, no such phenomenon has been reported in antigen-specific $CD8^+$ T cell response to IAV infection. Hence, it would be interesting to investigate IAV-specific $CD8^+$ T cells to see whether such a broad-based response can also be observed.

1.8 Peptide-binding motifs and epitope prediction

Classically, HLA-I molecule has six pockets (A, B, C, D, E, F) distributed along the length of the peptide-binding cleft (Figure 1.5). Among these, there are generally two or less commonly three pockets that accommodate the side chains of selected amino acids, which are often termed anchor residues, as these residues are believed to play a more dominant role during HLA binding (Falk et al., 1991; Rammensee et al., 1999). For most of the HLA-I binding peptides, the two anchor residues can be found at P2 (pocket B) and C-terminus (pocket F) (Figure 1.5) (Falk et al., 1991; Falk et al., 1994). Pocket F often selects a bulky, hydrophobic or charged residue (Toes et al., 2001), while pocket B usually selects hydrophobic or charged residues, they are generally not as strict as for the F pocket anchor (Yewdell et al., 1999). These specific anchor requirements are often referred as “peptide-binding motifs”, which is available for many HLA molecules. Such motifs define certain peptide positions as primary and secondary anchors involved in HLA

binding. In some cases, such motifs also list the preferred and deleterious residues at these positions. Some motifs show more stringent peptide-binding requirements and, as a result, actually allow reasonably accurate peptide prediction (Ibe et al., 1996; Jardetzky et al., 1991). For example, HLA-B*44 molecules have a stringent binding motif requiring a Glutamate (E) in position two (P2) and a tyrosine (Y), or phenylalanine (F) and less often tryptophan (W) at the C-terminus (Luescher et al., 1996). Although many highly immunogenic peptides do not contain any typical MHC binding motif (E. Grant et al., 2013; Wu et al., 2011), peptide prediction through stringent binding motif enables time-saving identification of minimal antigenic peptides recognised by $CD8^+$ T cells (Rammensee et al., 1999).

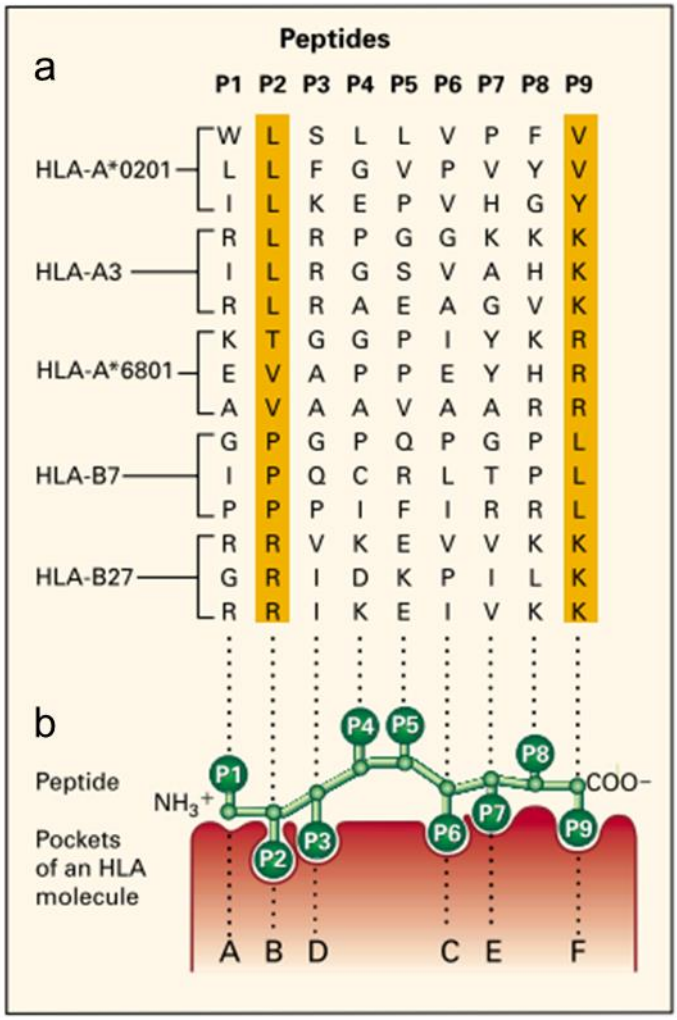

Figure 1.5. The interactions of HLA-I molecules and their bound peptides

(a) The upper panel shows some different HLA peptide-binding motifs; the anchor residues are yellow highlighted. **(b)** The lower panel displays the peptide-binding cleft of an HLA-I molecule, the amino acid side chains of the bound peptide from P1 to P9 are oriented either down into the HLA-I peptide-binding pockets or up. The six pockets (A to F) distributed along the length of the peptide-binding groove are also shown. Adapted from (Klein et al., 2000).

1.9 Antigenic peptide source

$CD8^+$ T cells recognise endogenously derived pMHC-I complexes on the surface of antigen-presenting cells. Interestingly, what are the major source antigens is still debated. Although most in the field believe peptides from previous functional proteins, the retirees, are the main source (Admon et al., 2003; Milner et al., 2006; Yewdell, 2001; Yewdell et al., 1988), some have shown that the main antigenic peptide sources are defective ribosomal products (DRiPs) (Anton et al., 2014; Princiotta et al., 2003; Schubert et al., 2000; Yewdell et al., 1996). Retirees are the matured proteins that no longer function as a result of age-associated or environmental stress-related damage (Goldberg et al., 1976; Yewdell et al., 2001). However, up to 30% of newly translated proteins are degraded as DRiPs before maturation (Yewdell et al., 1996). DRiPs are nascent peptides or proteins due to inevitable protein synthesis errors including alternative reading frame (ARF) translation (D. J. Zanker et al., 2019), ribosomal frameshifting (Bullock et al., 1996), downstream initiation on mRNA (Bullock et al., 1996), and other errors occurred during proteins synthesis and folding (Yewdell, 2011).

Epitopes derived from ARF translation have been reported in viruses (Bullock et al., 1996; Cardinaud et al., 2004), cancers (R. F. Wang et al., 1996) and autoimmune diseases (Saulquin et al., 2002), indicating that $CD8^+$ T cells surveil more comprehensive peptide repertoire than originally thought. Cardinaud *et al.* identified a panel of ARF encoded peptides (ARFP) with the *gag*, *pol*, and *env* genes, such as peptide Q9VF (QPRSDTHVF) derived from Gag-ARFP and restricted by HLA-B*07:02, recognised by $CD8^+$ T cells of HIV-infected patients (Cardinaud et al., 2004). Additionally, Wang and colleagues reported a novel human cancer antigenic peptide, MSLQRQFLR, derived from ARF translation of the gp75 gene (tyrosinase-related protein 1, also called gp75), which was recognised by melanoma-specific $CD8^+$ T cells (TIL586) (R. F. Wang et al., 1996). Epitopes encoded by ARFs reveal a novel mechanism for generating virus and cancer antigens, therefore, such responses should be taken into consideration in future vaccine design.

In the past, linear peptides were by far the most demonstrated source for $CD8^+$ T cell immune surveillance. Interestingly, it has become clear that $CD8^+$ T cells can also recognise peptide derived from protein splicing events (Hanada et al., 2004; Mannering et al., 2018; Vigneron et al., 2004). Moreover, a recent study argued that about one-third of the entire HLA-I immunopeptidome are likely composed of proteasome-generated spliced peptides (Liepe et al., 2016). However, it is not yet clear whether such spliced peptide mostly originates from “retired” functional proteins or DRiPs. Hence, the antigen peptide sources remain an interesting area for future investigation.

1.20 Peptide forms: linear, spliced and post-translationally modified

1.20.1 $CD8^+$ T cells recognise linear peptides

$CD8^+$ T cells recognise linear epitopes presented by HLA-I molecules on antigen-presenting cells. Synthetic peptides and phage peptide display libraries have been successfully used to discover many linear epitopes (Koivunen et al., 1999). For example, in 1986, the first human $CD8^+$ T cell epitope $NP_{335-349}$ restricted to HLA-B*37 was identified using short synthetic peptides (Townsend et al., 1986). Subsequently, Gotch *et al.* identified the second $CD8^+$ T cell epitope $M1_{58-66}$ from IAV M1 restricted to HLA-A*02 also using synthetic peptides (Gotch et al., 1987). Additionally, two recent studies using a systematic approach identified the most immunodominant IAV-specific $CD8^+$ T cell responses in health individuals either express or not express HLA-A*02:01 (E. Grant et al., 2013; Wu et al., 2011). This approach allowed for the isolation of immunodominant peptides to a single virus in people with vastly different HLA combinations.

1.20.2 $CD8^+$ T cells recognise spliced peptides

For a very long time, peptides recognised by $CD8^+$ T cells were believed to correspond exclusively to linear fragments of proteins. However, this notion was challenged by the observations in which $CD8^+$ T cells responded to peptides composed of two fragments originally distant in the parental protein (reviewed in (Mannering et al., 2018; Vigneron et al., 2018)). In 2004, Hanada *et al*. described the first $CD8^+$ T cell clone (C2) that recognised the fibroblast growth factor 5 (FGF-5) derived 9mer peptide generated by two non-contiguous segments of the parental protein. This 9mer peptide (NTYAS-PRFK) is formed by two determinant-forming fragments NTYAS and PRFK, which required the excision (splicing) of 40 amino acids in between (Hanada et al., 2004). Later, Vigneron *et al.* reported that a $CD8^+$ T cell clone (CTL 14) recognised a nonameric peptide derived from melanocytic glycoprotein $gp100^{PMEL17}$ presented by HLA-A*32. This peptide RTKQLYPEW was generated from a 13mer $gp100_{40-52}$ RTKAWNRQLYPEW by

removing four amino acids AWNR within the proteasome ($gp100_{43-46}$) (Vigneron et al., 2004). Interestingly, Warren *et al.* demonstrated that a $CD8^+$ T cell clone (DRN-7) recognised an HLA-A*03:01 restricted minor histocompatibility (H) antigen derived peptide SLPRGTSTPK from the SP110 protein by ligating two spliced peptide fragments in reverse order (Warren et al., 2006). Theoretically, peptide splicing could involve any proteasome-degraded fragment of any protein in a cell. However, the so far identified spliced peptides are limited to peptides of the same proteins (Michaux et al., 2014; Vigneron et al., 2004; Warren et al., 2006). Recently, Liepe *et al.* developed a custom peptide database and detected that the proteasome-generated spliced peptide pool could potentially represent about one-third of the diversity of the entire HLA-I ligands and one-fourth of the abundance of total HLA-I peptidomes (Liepe et al., 2016). Although two spliced peptides were recognised by $CD8^+$ T cells isolated from *Listeria* infected mice (Platteel et al., 2017), so far, no IAV-derived spliced peptide has been identified. Hence, it would be fascinating to see such observations holding true during Influenza virus infection.

1.20.3 $CD8^+$ T cells recognize post-translationally modified peptides

Common post-translational modifications (PTMs) are including glycosylation, phosphorylation, disulphide isomerisation, methylation etc. (Petersen et al., 2009). Both B cells and T cells were found to recognise PTMs derived epitopes, demonstrating that PTMs alter peptide repertoire and enhance the diversity of naturally presented peptide epitopes (Engelhard et al., 2006). PTM epitopes have been shown to be associated with infectious disease, autoimmunity and cancer (Anderton, 2004; Doyle et al., 2001). For example, sulfhydryl modification of cysteine residues significantly affected the immunogenicity and antigenicity of cysteine-containing peptides NP_{39-47} and $NP_{218-226}$ (W. Chen et al., 1999). Additionally, Mamula *et al.* described that T cells from mice immunized with the isoaspartyl form of snRNP D peptide derived from human systemic lupus erythematosus (SLE) triggered robust B and T cell responses, however, no immune response was detected when immunization of mice with the aspartyl form

of the same peptide (Mamula et al., 1999). Collectively, PTMs lead to the change of peptide repertoire and antigenicity of the unmodified peptides.

1.21 Aims of this thesis

Establishing antigen-specific $CD8^+$ T cell lines or clones *in vitro* has become increasingly important to better understand T cell biology and to conduct T cell-based immunotherapy. However, successfully establishing such T cell cultures is largely an empirical and lab-based experience. The main struggle of culturing such T cell is the result of inadequate antigen-specific T cell precursors and overwhelming nonspecific T cell expansion during the early culture stage. Although in most of the cases some antigen-specific T cells are detected, these T cells eventually vanish during repeated antigen re-stimulation. Even though there are several $CD8^+$ T cell culture methods published previously (Jackson et al., 2004; D. Zanker et al., 2013), it is still hard to find any robust $CD8^+$ T cell enrichment methods, especially for enriching antigen-specific T cells with a minimal number.

Prior to this study, our group has developed a systematic approach for identifying immunodominant $CD8^+$ and $CD4^+$ T cell response to IAV in healthy individuals (L. Chen et al., 2014; Wu et al., 2011). Using this approach, it is possible to discover many IAV immunodominant T cell epitopes efficiently, including those without any typical HLA-binding motif. Our lab have also reported broad-based $CD4^+$ T cell responses to IAV in a healthy donor without typical immunodominance hierarchy (L. Chen et al., 2017). I then invesigated whether such broad-based IAV-specific $CD8^+$ T cell responses could also be observed in some individuals for their IAV-specific $CD8^+$ T cells? Hence, the specific goal of this study was to characterise novel $CD8^+$ T cell responses to IAV in a donor with broad-based IAV-specific $CD8^+$ T cell responses.

To achieve the above-mentioned goal, I have the following specific aims:

1.21.1 Establishing optimal $CD8^+$ T cell enrichment method (Chapter 3)

In anticipating relatively small $CD8^+$ T cell responses in individuals with broad-based IAV-specific responses, I wanted to develop a method to enrich antigen specific $CD8^+$ T cells based on the phenomenon that activated $CD8^+$ T cells would

downregulate their TCR/CD3 complex and its co-receptor CD8. First, the kinetics and best antigen stimulation strength were optimised to induce the most suitable CD3 and CD8 downregulation after $CD8^+$ T cell activation. Second, the sensitivity of this method was assessed using low percentage antigen-specific T cell cultures. Third, a T cell cloning assay was conducted to evaluate the sorted $CD3^{low}CD8^{low}$ T cells for their expansion capacity. Fourth, the method was used to enrich multiple small IAV-specific $CD8^+$ T cell populations simultaneously from a polyclonal $CD8^+$ T cell culture. Last, $CD8^+$ T cells with less dramatic CD3 and CD8 downregulation were also enriched by this method.

1.21.2 Identification of novel IAV-specific $CD8^+$ T cell epitopes from a healthy donor with broad-based $CD8^+$ T cell responses (Chapter 4)

First of all, according to the investigation conducted in our laboratory in the past ten years, a healthy donor with potentially broad-based $CD8^+$ T cell response to IAV is selected and confirmed by a polyclonal $CD8^+$ T cell culture. Second, the small IAV-specific T cell populations will be enriched using the method developed in Chapter 3, and antigenic proteins and their specific antigenic epitopes and HLA restrictions will be delineated. Next, bioinformatics analysis is performed to reveal the conservancy of the novel epitopes sequences among the IAV strains circulated in Australia in the past 25 years. Finally, quantitatively antigen presentation assessments will be conducted for these novel epitopes to better understand the underlying mechanism of such an immune response.

1.21.3 Exploring the $CD8^+$ T cell responses to epitopes encoded by alternative reading frame (Chapter 5)

In Chapter 4, I observed that some IAV-specific $CD8^+$ T cells failed to recognise any of the NP or NS1 18mer overlapping peptides, although capable of recognising the APCs infected by rVV-NP and rVV-NS1, respectively. These results indicate that these $CD8^+$ T cells might respond to DRiP peptides encoded by ARFs, spliced peptides or peptides with post-translational modification. I aim to confirm the above

observation and unveil the mechanisms. Firstly, the predicted ARF peptides were then be screened as potential epitopes by incubating with NP and NS1-specific $CD8^+$ T cells and looking for reactivity. Next, if the outcome of the above-proposed screen is positive, minimal ARF epitopes will be confirmed using end-truncated and end-extended peptide sets; if the outcome is negative, peptide-extraction and HPLC fractionation will be employed to isolate the right antigenic peptides by Mass Spectrometry. Finally, confirming the positive peptide response through newly synthesised peptides. If both approaches fail to identify the novel $CD8^+$ T cell epitopes, I will turn to spliced epitope or epitope post-translational modification.

Chapter 2: Materials and methods

2.1 Materials

2.1.1 Cell lines

2.1.1.1 Peripheral Blood Mononuclear Cells (PBMCs):

Buffy coats from healthy blood donors were obtained from the Australian Red Cross under the agreement of 12-07VIC-17. PBMCs were isolated by Ficoll-Hypaque gradient and stored in liquid nitrogen for future use. HLA typing was performed by the Victorian Transplantation and Immunogenetics Service (VTIS, Melbourne, VIC, Australia). The healthy donor's PBMC sample used in this thesis (**Chapter 4**) is named as A_2^-20091201.

2.1.1.2 Antigen Presenting Cells (APCs)

Autologous B lymphocyte cell lines (BLCLs) were established from donor PBMCs via standard EBV transformation as formerly described (Wu et al., 2011). The other BLCLs were made available from the VTIS and Dr. Nicole Mifsud (Monash University, Melbourne, VIC, Australia). The HLA-A, -B and -C alleles were typed through PCR by VTIS.

Table 2.1. Cell lines

Cell	Description	Culture medium
Autologous BLCLs	Autologous BLCLs were made from donor PBMCs via a standard EBV transformation. Autologous BLCL used in this study expressing HLA-A*24:02, HLA-A*33:03, HLA-B*44:03, HLA-B*46:01, HLA-Cw*01:02, HLA-Cw*07:01	RF-10
C1R-B*44:03	C1R cell line expressing HLA-B*44:03	RF-10
C1R-A*33:03	C1R cell line expressing HLA-A*33:03	RF-10
9002	BLCL expressing HLA-A*24:02, HLA-B*14:02, HLA-Cw*02:02, HLA-Cw*06:02	RF-10
9004	BLCL expressing HLA-A*02:01, HLA-B*27:05, HLA-Cw*01:02	RF-10
9022	BLCL expressing HLA-A*01:01, HLA-B*08:01, HLA-Cw*07:01	RF-10

2.1.2 Viruses

The Mount Sinai strain of PR8 (A/Puerto Rico/8/1934 H1N1) was prepared as previously described (Wu et al., 2011), then aliquoted and stored at -80^{o}C until use. Recombinant vaccinia viruses (rVVs) encoding individual IAV proteins (all of the PR8 strain origin) were kind gifts from Drs. Jonathan Yewdell and Jack Bennink (NIH, Bethesda, MD, USA). rVVs were propagated in TK^{-} cell line and were stored at -80^{o}C until use.

Table 2.2. Viruses

Virus	Description
PR8	Influenza A virus (A/Puerto Rico/8/1934(H1N1)).
rVV-CR19	rVV vector
rVV-HA	rVV encoding the haemagglutinin (HA) protein from IAV.
rVV-NA	rVV encoding the neuraminidase (NA) protein from IAV.
rVV-M1	rVV encoding the matrix 1 (M1) protein from IAV.
rVV-M2	rVV encoding the matrix 2 (M2) protein from IAV.
rVV-NS1	rVV encoding the non-structural 1 (NS1) protein from IAV.
rVV-NS2	rVV encoding the non-structural 2 (NS2) protein from IAV.
rVV-NP	rVV encoding the nucleoprotein (NP) protein from IAV.
rVV-PB1	rVV encoding the basic polymerase 1 (PB1) protein from IAV.
rVV-PB2	rVV encoding the basic polymerase 2 (PB2) protein from IAV.
rVV-PB1F2	rVV encoding the +1 open reading frame PB1 (PB1F2) protein from IAV.
rVV-PA	rVV encoding the acidic polymerase (PA) protein from IAV.
rVV-1/3 NP	rVV encoding the 1/3 length (NP 1-168) of NP protein from IAV.
rVV-2/3 NP	rVV encoding the 2/3 length (NP 147-315) of NP protein from IAV.
rVV-3/3 NP	rVV encoding the 3/3 length (NP 298-496) of NP protein from IAV.

2.1.3 Synthetic peptides

All the peptides were synthesised by Mimotopes (Clayton, VIC, Australia), dissolved in Dimethyl Sulfoxide (DMSO) and stored in -20^{o}C until use. M1, M2, NP, NS1, PB1, PB2, NA, HA and PA overlapping 18mer peptides were synthesised as pin peptides with six amino acid shifts.

Table 2.3. 18mer overlapping peptides

18mer overlapping peptides	Description
NP 18mer peptides	IAV-NP overlapping 18mer peptides
NA 18mer peptides	IAV-NA overlapping 18mer peptides
NS1 18mer peptides	IAV-NS1 overlapping 18mer peptides
HA 18mer peptides	IAV-HA overlapping 18mer peptides
PB1 18mer peptides	IAV-PB1 overlapping 18mer peptides
PB2 18mer peptides	IAV-PB2 overlapping 18mer peptides
PA 18mer peptides	IAV-PA overlapping 18mer peptides
M1 18mer peptides	IAV-M1 overlapping 18mer peptides
M2 18mer peptides	IAV-M2 overlapping 18mer peptides

Table 2.4. Short peptides

Peptide	Sequence
M1 58–66	GILGFVFTL
NP 172–181	LPRRSGAAGA
NP 44–52	CTELKLSDY
M1 124-134	LASCMGLIYNR
M1 125-134	ASCMGLIYNR
M1 124-133	LASCMGLIYN
M2 7-15	VETPIRNEW
M2 8-15	ETPIRNEW
M2 7-14	VETPIRNE
NA 337-346	RYGNGVWIGR
NA 338-346	YGNGVWIGR
NA 337-345	RYGNGVWIG
NA 337-347	RYGNGVWIGRT
NA 336-346	YRYGNGVWIGR
NP 319-330	NENPAHKSQLVW
NP 320-330	ENPAHKSQLVW
NP 319-329	NENPAHKSQLV
HA 445-453	LENERTLDF
HA 446-453	ENERTLDF
HA 445-452	LENERTLD
PB2 39-49	QEKNPALRMKW
PB2 40-49	EKNPALRMKW
PB2 39-48	QEKNPALRMK
PB1 498-509	RYGFVANFSMEL
PB1 499-509	YGFVANFSMEL
PB1 498-508	RYGFVANFSME
NP-ARF 14-24	QELLMKECATF
NP-ARF 19-29	KECATFSKGNF
NP-ARF 17-24	KEKYPCFY
NP-ARF 3-12	KEGTIGLAAF
NP-ARF 40-51	AESTILSIVKLF
NP-ARF 32-41	DEFSHPLSVY
NS1-ARF 8-16	AESGRPSLY
Melan A 26–35	EAAGIGILTV

2.1.4 Antibodies

Table 2.5. Antibodies

Antibody-(conjugate)	Clone	Supplier
anti-human CD3-e450	UCHT1	eBioscience, USA
anti-human CD3-FITC	UCHT1	Invitrogen, USA
anti-human CD4-PE	RPA-T4	eBioscience, USA
anti-human CD8-APC	RPA-T8	BD biosciences, USA
anti-human IFN-γ	4S. B3	Invitrogen, USA

2.1.5 Media and solutions

RF-10 medium: RPMI-1640 supplemented with 10% FCS, 50µM 2-Mercaptoethanol (2-ME), 2mM L-glutamine and antibodies (penicillin 100U/mL and streptomycin 100µg/mL).

T cell culture medium: RF-10 medium supplemented with Sodium Pyruvate (1x), Non-essential amino acid (1x) and 20 IU/mL or 40 IU/mL human recombinant interleukin 2 (hrIL-2). Unless otherwise specified, in this thesis, T cell culture medium containing 20IU/mL hrIL-2 was used for culturing all the primary $CD8^+$ T cells, while the hrIL-2 concentration was increased to 40IU/mL for culturing all the restimulated $CD8^+$ T cell lines.

Acidic medium: RPMI-1640 supplemented with 1M Hydrochloric acid (HCL), pH adjusted to 6.8.
0.1% TFA/H_2O: 0.1% trifluoroacetic acid (TFA) in H_2O.
10mg/mL BFA: 10mg Brefeldin A (BFA) in Methanol.
0.2% Saponin: 0.2% saponin in PBS.
1% PHA: 1% Phytohemagglutinin (PHA) in PBS.
0.1% BSA/PBS: 0.1% bovine serum albumin (BSA) in PBS.
Sorting buffer: 5% FCS and 0.5µM EDTA in PBS.

2.1.6 Equipment, reagents, and materials

Table 2.6. Equipment and Reagents

Reagent	Distributor
1100 RP-HPLC	Agilent, USA
2-Mercaptoethanol	Gibco, Australia
Brefeldin A	Sigma-Aldrich, USA
Dimethyl sulphoxide (DMSO)	Sigma-Aldrich, USA
FACSAriaIII flow cytometer	BD Biosciences
FACSCanto II flow cytometer	BD Biosciences
Fetal Calf Serum (FCS)	Hyclone, South Logan, Utah
GlutaMax™ -1 (L-Glutamine 100x)	Gibco, USA
Lymphoprep™ (Ficoll-Paque)	Stemcell™, Canada
Paraformaldehyde 16% solution	Electron Microscopy Sciences, USA
Pen/Strep (Penicillin, Streptomycin 100x)	Gibco, USA
Pipette tips filtered	Stemcell™, Canada
Pipette tips unfiltered	Stemcell™, Canada
Polymyxin B sulphate	Lonza, Switzerland
Recombinant human IL-2	Peprotech, USA
RPMI-1640	Gibco, USA
Saponin	Sigma-Aldrich, USA
Tissue culture flasks T25 ml	Corning, USA
Tissue culture flasks T75 ml	Corning, USA
Tissue culture flasks T175 ml	Corning, USA
Tissue culture plates (6 wells-flat bottom)	Corning, USA
Tissue culture plates (12 wells-flat bottom)	Corning, USA
Tissue culture plates (24 wells-flat bottom)	Corning, USA
Tissue culture plates (48 wells-flat bottom)	Corning, USA
Tissue culture plates (96 wells-flat bottom)	Corning, USA
Tissue culture plates (96 wells-U bottom)	Corning, USA
Tris(2-Carboxyethyl)-Phosphine (TCEP)	Pierce, USA
Trypan Blue	Sigma-Aldrich, USA
10ml tube	Sarstedt, Germany
15ml tube	Greiner, Austria
50ml tube	Greiner, Austria

2.2 General Methods

2.2.1 Cell culture

Unless otherwise stated, all the cell lines were maintained in the RF-10 medium. Cells were passaged and the culture medium was changed according to the culture medium's colour (suspension cells) or when cells became around 80% confluence (adherent cells). Cells were used for experiments during the exponential growth phase.

2.2.2 Cell counting

Cell numbers were counted by Trypan Blue staining. In brief, cell suspensions were diluted 1:1 with Trypan Blue and well mixed, then counted using an inverted light microscope and a haemocytometer.

2.2.3 APCs infections

2.2.3.1 IAV infection

APCs were counted and washed with 10mL acidic medium twice. Cell pellets were resuspended in 200µL of acidic medium containing PR8 virus at 10 plaque-forming units (PFU) per cell. Cells were then incubated in a 37^{o}C water-bath for 1 hour and were gently shaken every 15 minutes. After the first hour incubation, cells were then topped up with 2mL fresh RF-10 and transferred to a 37^{o}C CO_2 incubator for another 4-hour incubation.

Virus calculation example:

When $1x10^6$ cells are infected at multiplicities of infection (MOI) of 10, $1x10^7$ PFU of IAV is used. As PR8 (AF44 batch) has a titre of $7.07x10^8$ PFU/mL, therefore $1x10^7 \div 7.07x10^8 \approx$ 14µL is required. Thus, 14µL virus with 86µL PBS and 100µL

acidic medium were added to a 10mL tube. Unless otherwise notified, APCs were infected at MOI of 10 in this thesis.

2.2.3.2 rVV infection

APCs were washed with 0.1% BSA/PBS twice then re-suspended in the same buffer and infected with rVV encoding individual IAV proteins at MOI of 10. Cells were then incubated in a 37ºC water-bath for 1 hour and were gently vortexed every 15 minutes. After the first hour infection, cells were topped up with 2mL fresh RF-10 and incubated in a 37ºC CO_2 incubator for further 16 hours.

2.3 Specialised techniques

2.3.1 Primary antigen-specific $CD8^+$ T cell culture

For establishing primary antigen-specific $CD8^+$ T cell lines, 1×10^6 PBMCs were resuspended in 200µL acidic medium and infected with PR8 at an MOI of 10 for 1 hour in a 37ºC water-bath. After 1 hour infection, 2mL of RF-10 was added to cells and incubated for another 4 hours in a 37ºC CO_2 incubator. The infected PBMCs served as APCs and subsequently co-cultured with 9×10^6 PMBCs (responders) for two weeks in T cell culture medium contains 20IU/mL of hrIL-2.

2.3.2 Antigen-specific $CD8^+$ T cells re-stimulation

2.3.2.1 $CD8^+$ T cell re-stimulation by IAV infected APCs

BLCLs were infected with PR8 overnight (16 hours). The infected BLCLs were then irradiated for 100 Grey before being used as stimulators and co-cultured with T cells (as responders) in T cell culture medium contains 40IU/mL hrIL-2. The ratio of T cell and APCs is generally 10:1.

2.3.2.2 $CD8^+$ T cell re-stimulation by peptide-pulsed APCs

BLCLs were resuspended in 200µL RF-10 and pulsed with 10^{-7}M peptides for 1 hour in a 37ºC water-bath. The peptide-pulsed BLCLs were then irradiated for 100 Grey before co-cultured with the responder T cells in T cell culture medium contains 40IU/mL IL-2. Again, the ratio of T cell and APCs is 10:1.

2.3.3 Systemic approach for identifying novel IAV epitopes

For identifying immunodominant $CD8^+$ T cell responses during IAV infection, our laboratory had created a detailed systematic experimental approach (Wu et al., 2011). A similar approach has been used in this thesis to discover a broad-based $CD8^+$ T cell response to IAV. The procedure of the systemic approach was also well described in Figure 4.1 of Chapter 4.

2.3.3.1 rVV infection for identifying protein-specific $CD8^+$ T cells

The primary polyclonal IAV-specific $CD8^+$ T cell culture was established according to section 2.3.1. APCs were infected with a panel of individual IAV protein encoding rVVs (rVV-HA, rVV-NA, rVV-NP, rVV-NS1, rVV-NS2, rVV-M1, rVV-M2, rVV-PB1, rVV-PB2, rVV-PB1F2, rVV-PA) and empty vector rVV-CR19. For identifying the specific antigenic protein, IAV-specific $CD8^+$ T cells were tested with the above rVV infected APCs.

2.3.3.2 Identification of novel IAV-specific $CD8^+$ T cell epitopes by 18mer peptide mapping

Once the specific antigenic proteins were identified, polyclonal $CD8^+$ T cells were directly used to determine the particular peptide regions by screening a whole set of synthetic IAV-protein derived 18mer overlapping peptides with six amino acid shifts.

2.3.3.3 Identification of minimal epitope within the 18mer peptide's region

After identifying the specific 18mer antigenic regions, $CD8^+$ T cells were used to work out the HLA restriction. They were also used to screen either overlapping 13mer peptides (with two amino acid shifts) or the predicted minimal epitope sequences based on peptide-binding motifs and their restricting HLAs.

2.3.3.4 HLA restriction assay

BLCLs with partial donor HLA match were pulsed with 10^{-6}M of relevant peptides for 1 hour at room temperature. Later, cells were extensively washed to remove free peptides and used as APCs in a co-culture with antigen-specific $CD8^+$ T cells for 4 hours in the presence of 10µL/mL BFA. HLA-restriction was assessed by ICS for production of IFN-γ.

2.3.4 $CD8^+$ T cell enrichment

2.3.4.1 Antigen-specific $CD8^+$ T cell enrichment via CD3CD8 downregulation sorting

The details of CD3CD8 downregulation guided sorting were described in **Chapter 3** (Huang et al., 2019). In short, APCs were pulsed with 10^{-7}M peptides for 1 hour then incubated with the antigen-specific $CD8^+$ T cells for 4 hours in the presence of 10µL/mL BFA. For cysteine-containing peptides, APCs were pulsed with peptides in the presence of 500µM Tris(2-Carboxyethyl)-Phosphine (TCEP) before being incubated with antigen-specific $CD8^+$ T cells. Additionally, the same T cells incubated with the same cells without peptide pulsing were used as a negative control to guide $CD3^{low}CD8^{low}$ population gating. After 4 hour incubation, the cells were stained with anti-CD3 (e450) and anti-CD8 (APC) for 30 minutes at 4 °C; washed and resuspended in FACS sorting buffer and sorted for $CD3^{low}CD8^{low}$ (downregulated) population on a FACS Aria III.

2.3.4.2 $CD8^+$ T cell re-stimulation after CD3CD8 downregulation sorting enrichment

Low purity $CD8^+$ T cells were enriched via CD3CD8 downregulation guided sorting and maintained in the T cell culture medium for about two weeks. T cell re-stimulation was generally performed on day 16 after the previous stimulation (sorting) or when cells had reduced in size and stop further proliferation. Re-stimulation of such T cell lines is as described in section 2.3.2. In a nutshell, BLCLs were infected with PR8 or pulsed with the specific peptides, then irradiated for 100 Grey before being used to stimulate their specific $CD8^+$ T cell lines.

2.3.5 HPLC fractionation of synthetic peptides

10µL synthetic peptide was diluted into 190µL 0.1% TFA/H_2O, well mixed, then injected into HPLC sampler and ran for 60 minutes (detail shown in table 2.7). HPLC fractions were collected into 96 well format cluster tube plates every 0.1 minutes between 10 and 39 minutes. 5µL collected fractions were pulsed onto APCs for 1 hour at room temperature in serum-free medium to avoid peptide degradation. Antigen-specific $CD8^+$ T cells were then used to screen the fraction-pulsed APCs via a standard ICS, and data were analysed by flow cytometry.

Table 2.7. HPLC fractionation

Column	Delta Pak 5µm, C18 (150 x 3.9mm, Waters) with guard column
Mobile phase	Gradient: Solution A, 0.1% TFA in H_2O (99.9%) Solution B, 0.1% TFA in Acetonitrile (99.9%)
Flow rate	0.5mL/minute
Detector/wavelength	UV (210nm)
Injection volume	200 µL
Run time	60 minutes

2.4 Experimental assays

2.4.1 Flow cytometric and CytoFlex analysis

In most cases, flow cytometry antibody staining for extracellular markers was performed using approximately 1.2~2 x 10^5 cells in a U-bottom 96 well plate. Cells were pelleted by centrifugation (1500rpm, 5 minutes) and washed with PBS before being stained with antibodies for 30 minutes at 4^{o}C in the dark. Cells were washed with PBS after each step, resuspended in 100-200µL PBS and finally analysed by flow cytometry.

2.4.2 Cell sorting

Monoclonal antibody (mAb) staining for cell surface markers was generally conducted using 2~3 x 10^6 cells in a 5mL sorting tube following the procedure described in section 2.4.1. After the final centrifugation, cells were filtered through 0.2µM filter and resuspended with sorting buffer at 5 x 10^6 cells/mL. The different population of cells were sorted on a FACS Aria III. The cells of interest were sorted either into tubes or plates on ice. After sorting, cells were pelleted and resuspended in RF-10 or T cell culture medium.

2.4.3 Intracellular cytokine staining (ICS)

ICS is a method based on flow cytometry to detect the intracellular cytokines (Figure 2.1) (Zelnickova et al., 2007). In this assay, Brefeldin A (BFA) is used to block secretory and membrane-bound proteins from leaving the ER (Doms et al., 1989). The details of interferon-gamma (IFN-γ) ICS was described previously (D. Zanker et al., 2013). In brief, antigen-specific $CD8^+$ T cells were stimulated with PR8/rVV-infected or peptide-pulsed APCs in a U-bottom 96-well plate in the presence of 10µg/mL BFA for 4 hours. During the 4 hours incubation, antigen-specific T cells were activated and the activation-induced cytokine IFN-γ production were then accumulated in the ER. Samples were subsequently harvested and stained for surface markers with anti-CD3 (e450), anti-CD8 (APC) for 30 minutes at 4^{o}C, then fixed with 1% Paraformaldehyde (PFA) for 20 minutes at room temperature. Finally, cells were permeabilised with 0.2% Saponin and intracellularly stained with anti-IFN-γ mAb (PE-cy7) overnight at 4^{o}C. Samples were finally washed with PBS and re-suspended in a FACS tube and analysed on a BD FACS Canto II machine. All the FACS data were analysed by FlowJo software (Tree Star Inc, Ashland, USA).

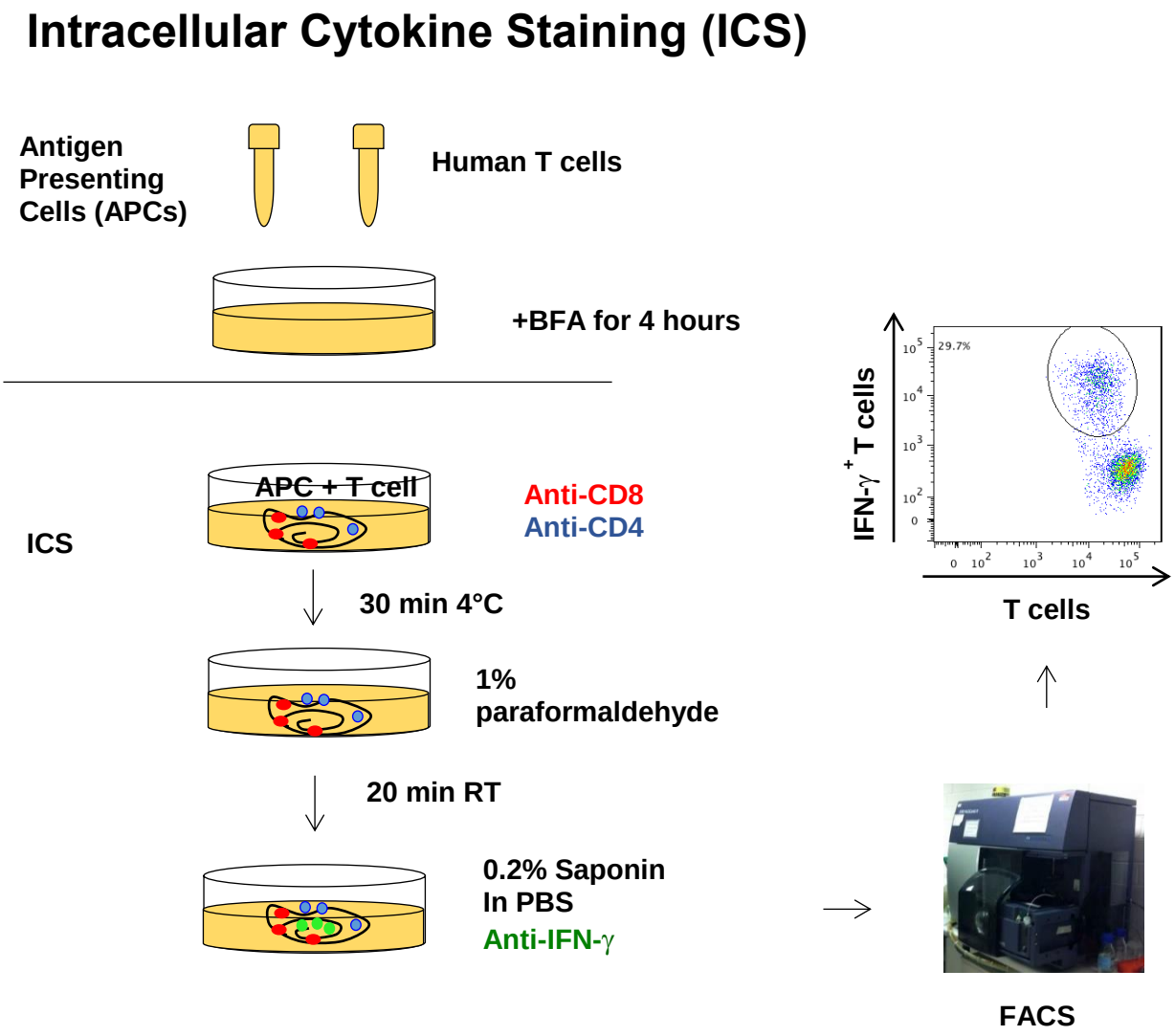

Figure 2.1. A brief overview of ICS procedure

Antigen-specific $CD8^+$ T cells and APCs were incubated in a U-bottom 96-well plate in the presence of 10µg/mL BFA for 4 hours, followed by cell surface marker then intracellular cytokine staining. Samples were acquired on a BD FACS canto II machine and data were analysed by FlowJo software.

2.4.4 Peptide titration analysis

To quantitatively assess the avidity of antigen-specific $CD8^+$ T cells, cognate peptide titration analysis was performed in this study. The working peptide concentration of 10^{-3}M was serially diluted to 10^{-5}M, 10^{-6}M, 10^{-7}M, 10^{-8}M, 10^{-9}M in RF-10 medium. APCs were firstly pulsed with the diluted peptides and washed before being mixed with antigen-specific $CD8^+$ T cells in the presence of 10µg/mL BFA. APCs and T cells were incubated for 4 hours and analysed via a standard ICS for IFN-γ production.

2.4.5 Antigen presentation kinetics analysis

Antigen presentation kinetics assay, also known as BFA kinetics assay, is a highly sensitive assay based on ICS for IFN-γ production. It quantitatively evaluates the pMHC-I presentation to antigen-specific $CD8^+$ T cells (Pang et al., 2006). In this assay, further antigen presentation from virus-infected APCs was stopped by BFA addition. Therefore, T cell activation dependents on the already presented surface pMHC-I at the time of BFA addition.

Briefly, autologous BLCLs were initially infected with rVV-NP, rVV-NS1, rVV-PB1, rVV-PB2, rVV-M1, rVV-M1, rVV-M2, rVV-PA, or rVV-CR19 (empty vector) for 1 hour. The antigen presentation by the infected BLCLs was then blocked by the addition of BFA at various time points (0h, 0.5h, 1h, 2h, 4h, 6h, 8h) after the initial 1-hour infection. The antigen-specific $CD8^+$ T cells were added and incubated with the infected APCs to evaluate the antigen-presentation at that particular time point. Following addition of T cells and BFA, cells were incubated at 37°C for a further 4 hours, after the 4-hour incubation, each time point sample was harvested into a 0.6mL Eppendorf tube and stored at 4°C to synchronize ICS analysis. Samples were analysed on a BD FACS Canto II machine and FlowJo software.

2.4.6 TCEP reduction of cysteine disulfide modification

Cysteine-containing peptides could either form dimer peptides through a disulfide bond between the two peptides or form cysteinylated peptide in the culture medium containing free cysteine (W. Chen et al., 1999). Therefore, cysteine-containing peptides were treated with 500μM TCEP in cysteine free DMEM for 1 hour at room temperature before use to reduce dimmer peptides. Alternatively, APCs and T cells were incubated in the presence of 500μM TCEP in the experimental system to both reduce dimmer peptides and prevent cysteinylation.

Chapter 3: Establishing a robust human antigen-specific $CD8^+$ T cells enrichment method based on activation-induced CD3CD8 downregulation

3.1 Preface

$CD8^+$ T cells play vital roles in the elimination of viruses and tumours. Cultured $CD8^+$ T cells *in vitro* have been employed as an essential tool for understanding T cell biology and have also been used for immunotherapy. However, establishing $CD8^+$ T cell lines or clones remains a challenge in many laboratories, especially for expanding rare antigen-specific $CD8^+$ T cells. The major obstacle in creating such T cell cultures is that limited antigen-specific $CD8^+$ T cell precursors are usually overwhelmed by nonspecific cell expansion in the early culture stage. Hence, the key factor for solving this problem is to isolate or enrich the antigen-specific $CD8^+$ T cell as early as possible to avoid being overgrown by irrelevant T cell populations. In this chapter, I describe a novel FACS-based sorting method for enriching antigen-specific $CD8^+$ T cells based on activation-induced T cell receptor (CD3 complex) and its co-receptor (CD8) downregulation. This method enables the enrichment of single specificity or multiple specificity $CD8^+$ T cell populations simultaneously. The specific details of this approach are described comprehensively in this chapter.

Following is my manuscript: **Huang, M**.; Zhang, J.; Chen, W. FACS isolation of low percentage human antigen-specific $CD8^+$ T cells based on activation-induced CD3 and CD8 downregulation. *Journal of Immunological Methods*. 472 (2019) 35-43
Supplemental information can be located online at
doi.org/10.1016/j.jim.2019.06.013

3.2 Published paper

Journal of Immunological Methods 472 (2019) 35–43

Contents lists available at ScienceDirect

Journal of Immunological Methods

journal homepage: www.elsevier.com/locate/jim

Research paper

FACS isolation of low percentage human antigen-specific CD8$^+$ T cells based on activation-induced CD3 and CD8 downregulation

Miaojuan Huang[a], Jian Zhang[b], Weisan Chen[a,*]

[a] La Trobe Institute for Molecular Science, School of Molecular Science, La Trobe University, Bundoora, VIC, Australia
[b] Department of Oncology, Zhujiang Hospital, Southern Medical University, 253 Industrial Avenue, Guangdong, People's Republic of China

ARTICLE INFO

Keywords:
CD8$^+$ T cell
CD3 and CD8 downregulation

ABSTRACT

As T cell activation leads to downregulation of T cell receptor (TCR) and coreceptor CD8, we developed a novel FACS-based sorting method to enrich activated antigen-specific CD8$^+$ T cells. Using multiple established or low percentage T cell cultures, with either single antigen specificity or multiple influenza A virus antigen specificities, we have optimized the sorting method for T cell activation time and stimulating antigen dose. We have also sorted various numbers of antigen-specific CD8$^+$ T cells into 96-well plates to demonstrate these T cells are capable of expanding into nearly pure CD8$^+$ T cell lines. Our approach has the advantage of sorting antigen-specific T cells without knowing their specific antigenic epitopes or restricting HLA. We believe this method can be very helpful for successfully establishing CD8$^+$ T cell lines for various purpose, including immunotherapy.

1. Introduction

CD8$^+$ cytotoxic T lymphocytes (CTLs) play key roles in viral clearance and tumor surveillance. CD8$^+$ T cells recognize specific peptide-MHC class I complexes (pMHC-I) on the surface of antigen presenting cells (APCs) with T cell receptors (TCRs). The TCR-CD3 is a multi-subunit cell surface protein complex composed of an antigen-binding TCR disulfide-linked αβ heterodimer and CD3 complex (Davis and Bjorkman, 1988; Wegener et al., 1992; Krogsgaard et al., 2005); the CD3 complex is formed by CD3δε and CD3γε heterodimers, and CD3ζζ homodimers (Clevers et al., 1988; Smith-Garvin et al., 2009). Unlike the TCR αβ chains, CD3 components possess large intracytoplasmic domains responsible for coupling antigen recognition to various signal transduction pathways (Wegener et al., 1992). CD3γ, δ and ε each possesses an intracellular immunoreceptor tyrosine-based activation motifs (ITAM), while CD3ζ possesses three ITAMs in a tandem arrangement. Phosphorylation of these ITAMs leads to signal transduction and ultimately T cell activation (Kane et al., 2000; Kuhns and Davis, 2012). It has been demonstrated that CD3-γ phosphorylation mediates the downregulation of TCR/CD3 complex after T cell activation (Cantrell et al., 1985; Krangel, 1987; Valitutti et al., 1995).

CD8 is known as the coreceptor on cytotoxic T cells. It is a transmembrane glycoprotein which facilitates and amplifies pMHC-I triggered T cell activation (Bierer et al., 1989; Janeway, 1992; Gao and Jakobsen, 2000; Holler and Kranz, 2003). It binds to the α3 domain of the MHC that the TCR interacts with for optimal signal transduction during T cell activation (Salter et al., 1990; Janeway Jr., 1992). When CD8 molecule is blocked or in absence, such T cell activation is either blocked or requires longer TCR engagement time (Arcaro et al., 2001). Most importantly, CD8 engagement enhances and stabilizes the interaction of TCR/pMHC-I with lower affinity (Schott and Ploegh, 2002; Laugel et al., 2007). Upon activation CD8$^+$ T cells not only downregulate their TCR (CD3) complexes (Valitutti et al., 1995) but also its coreceptor CD8 (Xiao et al., 2007).

Establishing CD8$^+$ T cell lines or clones *in vitro* has been an important technique and has played very important role in understanding T cell biology and, more recently, T cell-based immunotherapy. For instance, *in vitro* propagated CD8$^+$ T cells have been used as essential tools for discovering CD8$^+$ T cell epitopes and studying the mechanisms of immunodominance hierarchies during virus infection (Wu et al., 2011; Grant et al., 2013; Clemens et al., 2016) and they have been used to treat cancer patients in adoptive cell therapy (Rosenberg et al., 2004). They can also be used to study mechanisms and kinetics of antigen processing and presentation (Pang et al., 2006a). However, successfully establishing CD8$^+$ T cell cultures is still largely an empirical and lab-based phenomenon. The major difficulty of such T cell cultures is that limited antigen-specific CD8$^+$ T cell precursors are often overwhelmed by the nonspecific proliferation of T cells with irrelevant specificities during early culture stage. It is often the case that although some antigen-specific T cells are detected in many primary cultures,

* Corresponding author.
E-mail address: weisan.chen@latrobe.edu.au (W. Chen).

https://doi.org/10.1016/j.jim.2019.06.013
Received 15 April 2019; Received in revised form 11 June 2019
Available online 12 June 2019

these T cells are eventually lost during the next round of antigen re-stimulation. Hence, the key solution for successful *in vitro* $CD8^+$ T cell expansion is to isolate or enrich these antigen-specific $CD8^+$ T cells as early as possible to avoid being over grown by irrelevant T cell populations.

Our group evaluated T cell culturing conditions previously including culture sera, cytokines and feeder cells and developed a robust human T cell culture method for monitoring both antigen-specific $CD4^+$ and $CD8^+$ T cells during short-term cultures (Jackson et al., 2004). We also optimized culture conditions for establishing murine $CD8^+$ T cells (Zanker et al., 2013). In this study, we successfully established a method to enrich antigen-specific $CD8^+$ T cell during primary T cell culture stage to dramatically boost antigen-specific T cell purity and enhance the success rate of $CD8^+$ T cell cultures with minimal knowledge of T cell epitope and its HLA restriction. Our novel approach is based on the phenomenon that upon activation $CD8^+$ T cells down-regulate their TCR (CD3) complexes and its coreceptor CD8. Therefore, antigen-specific $CD8^+$ T cells can be detected and sorted as a $CD3^{low}CD8^{low}$ population by fluorescence activated cell sorting (FACS). These features were utilized by our group to reveal low frequency antigen-specific human $CD4^+$ Tregs previously (Ebert et al., 2012). Using this approach, we successfully enriched human antigen-specific $CD8^+$ T cell populations, sometimes < 1% of total $CD8^+$ T cells.

2. Materials and methods

2.1. Human Peripheral Blood Mononuclear cells (PBMCs)

PBMCs of healthy donors used in this study were obtained from Australian Red Cross Blood Service (ARCBS) in Melbourne under the agreement 12-07VIC-17. PBMCs were isolated from blood buffy coats using Ficoll-Hypaque gradient centrifugation, then resuspended in FCS (Hyclone, South Logan, Utah) containing 10% dimethyl sulfoxide (DMSO) and stored in liquid nitrogen until use.

2.2. Culture medium, synthetic peptides and antibodies

Unless otherwise stated, antigen presenting cells (APCs) were cultured in RF-10 (RPMI 1640 supplemented with 10% FCS (Hyclone), 50 μM 2-ME, 2 mM L-glutamine and antibodies (penicillin 100 U/mL and streptomycin 100 μg/mL) (all from Gibco, NY, USA)). Peptides used in this study were synthesized by Mimotopes (Clayton, Victoria, Australia). Influenza A virus (IAV) peptides $M1_{58-66}$ (GILGFVFTL), $NP_{172-181}$ (LPRRSGAAGA), NP_{44-52} (CTELKLSDY), and a melanoma peptide Melan A_{26-35} (EAAGIGILTV) were synthesized as crude, desalted peptides with a purity > 75%. Peptides were reconstituted to a concentration of 1 mM in DMSO. APC-labelled anti-CD8 was purchased from BD Biosciences, e450-labelled anti-CD3 was purchased from eBioscience (San Diego, CA, USA). FITC-labelled anti-CD3 and PE-cy7 labelled anti-IFNγ were purchased from Invitrogen (San Diego, CA, USA).

2.3. Viruses and antigen presenting cell

The influenza A virus strain A/Puerto Rico/8/1934 H1N1 (PR8) was propagated in 10 days old embryonated chicken eggs. Two days after infection, the allantoic fluids were collected, aliquoted and stored at −80 °C freezer until use. Recombinant vaccinia viruses (rVV) encoding individual IAV proteins HA, NA, NP, NS1, NS2, M1, M2, PB1, PB2, PB1F2, PA, and empty vector rVV-CR19 were kind gifts from Drs Jonathan Yewdell and Jack Bennink (National Institutes of Health, Bethesda, MD). Autologous B lymphocyte cell line (BLCL) was made from donor PBMCs using EBV transformation (Wu et al., 2011) and cultured in RF-10.

2.4. Generation of poly-specificity or single peptide-specific $CD8^+$ T cell lines in vitro

For generating poly-specificity $CD8^+$ T cell lines, 1×10^6 PBMCs were resuspended in 200 μL acidic RPMI-1640 (pH adjusted to 6.8) and infected with PR8 at a MOI of 10 for 1 h in a 37 °C water bath. Later, 2 mL of prewarmed RF-10 was added to the cells and incubated for a further 4 h. Cells were pelleted and subsequently co-cultured with 9×10^6 PBMCs for 12–15 days in RF-10 contains 20 IU/mL of human recombinant interleukin 2 (hrIL-2) (Peprotech Inc., Rocky Hill, NJ, USA). For generating peptide-specific $CD8^+$ T cell lines, 1×10^6 PBMCs were resuspended in 200 μL RF-10 and pulsed with 10^{-7} M peptides for 1 h in a 37 °C water bath. Next, the peptide pulsed PBMCs were washed and co-cultured with 9×10^6 PBMCs for 12–15 days in RF-10 contains 20 IU/mL of hrIL-2 (Jackson et al., 2004; Wu et al., 2011; Grant et al., 2013). Unless otherwise stated, $CD8^+$ T cells were cultured with RF-10 supplemented with Sodium Pyruvate (1×) and Non-essential amino acid (1×) (Gibco, NY, USA).

2.5. Intracellular cytokine staining (ICS) and antigen presentation kinetic assay

The IFN-γ ICS assay was performed as previously described (Wu et al., 2011). For antigen presentation kinetic assay, the detailed method was previously published (Pang et al., 2006b). Briefly, the antigen-presentation of PR8-infected autologous BLCLs was blocked by addition of BFA (Sigma-Aldrich, St Louis, USA) at different time points, peptide-specific $CD8^+$ T cells were added for 4 h to assess the antigen-presentation at that time point; the T cells were then harvested and synchronized on ice before being stained together in a standard ICS. Samples were analyzed using BD FACS Canto II machine (BD Biosciences) and FlowJo software (Tree Star Inc., Ashland, USA).

2.6. Antigen-specific $CD8^+$ T cell enrichment by sorting the $CD3^{low}CD8^{low}$ population

Autologous BLCLs were pulsed with 10^{-7} M peptides for 1 h then cocultured with the $CD8^+$ T cells in the presence of BFA for 4 h. In addition, same T cells cocultured with un-pulsed BLCLs served as a negative control and were used to guide $CD3^{low}CD8^{low}$ population gating. In cysteine-containing peptide, for example NP_{44-52}, BLCLs were pulsed with NP_{44-52} in the presence of 500 μM TCEP (tris(2-carboxyethyl)phosphine, Pierce™), washed out excess peptides, then incubated with NP_{44-52}-specific $CD8^+$ T cells again in the presence of 500 μM TCEP and BFA for 4 h. After 4 h activation, the cells were stained with anti-CD3 (e450) and anti-CD8 (APC) for 30mins at 4 °C; washed and resuspended in sorting buffer (5% FCS, 0.5 μM EDTA in PBS) and sorted for $CD3^{low}CD8^{low}$ (downregulated) population using a FACS ARIA III (BD Biosciences).

For T cell cloning, the $CD3^{low}CD8^{low}$ population were sorted and various cell numbers (1 cell/well, 3 cells/well, 10 cells/well, 100 cells/well, 1000 cells/well, 5000 cells/well, 10,000 cells/well) were directly deposited into U-bottom 96 wells containing 3×10^5 irradiated allogeneic PBMC feeder cells (1:1:1 mixed feeders from 3 different donors' PBMC) in RF-5 (RPMI-1640 supplemented with 5% pooled human AB sera, L-glutamine, 2-ME, Non-essential amino acids, Sodium pyruvate, antibiotics, 300 IU/mL hrIL-2 and 1 μg/mL phytohaemagglutinin (PHA, Invitrogen, San Diego, USA,) (Potter and Moore, 1975). Sorted cells were cultured in the central wells of the plate to avoid medium evaporation. Only the central 60 wells from each 96-well plate were used to culture the sorted $CD8^+$ T cells. The outer wells of 96 well plates were filled up with sterile PBS to act as a buffer zone to minimized medium evaporation over long periods of incubation. Half medium was replaced with fresh one 24 h after sorting to reduce PHA concentration. The cells were checked every second day and medium changed as required. Growing wells were first split in 2 × 96-well before being

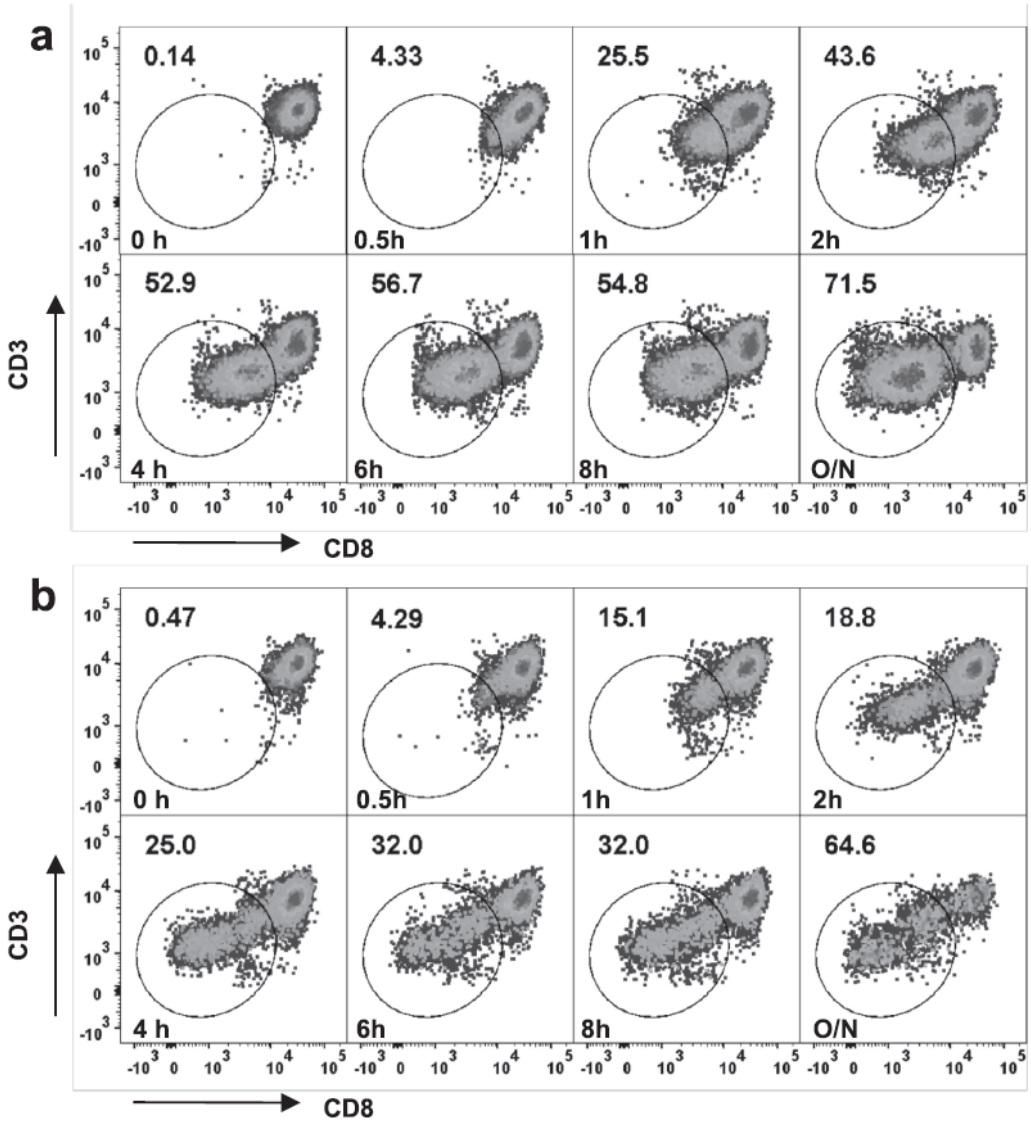

Fig. 1. 4-h activation provides optimal CD3CD8 downregulation peptide-specific $CD8^+$ T cell lines.
T cells were activated by $M1_{58-66}$ or $NP_{172-181}$ peptide; at different time points (0 h, 0.5 h, 1 h, 2 h, 4 h, 6 h, 8 h, and 16 h) the T cell activation-induced CD3CD8 downregulation was assessed by flow cytometry. **a)** the kinetic of CD3CD8 downregulation in $M1_{58-66}$ specific $CD8^+$ T cells; **b)** CD3CD8 downregulation kinetics of $NP_{172-181}$-specific $CD8^+$ T cells. Data shown are representative of two independent experiments.

transferred into 48-well plate when cell numbers reached to about 2 million per well.

3. Results

3.1. CD3 and CD8 are quickly down-regulated on antigen-specific $CD8^+$ T cells after activation

To simplify the method development process, two $CD8^+$ T cell lines specific to influenza A virus Matrix 1 protein ($M1_{58-66}$ restricted to HLA-A*02:01) and Nuclear Protein ($NP_{172-181}$ restricted to HLA-A*55:01) (Grant et al., 2013) were initially established. We first investigated the kinetics of TCR and CD8 downregulation. The two $CD8^+$ T cell lines were activated by 10^{-6} M peptide-pulsed APC and their activation-induced TCR and CD8 downregulation, at various time points (0 h, 0.5 h, 1 h, 2 h, 4 h, 6 h, 8 h, and 16 h) were monitored. As shown in Fig. 1, a population of the $M1_{58-66}$ specific T cells (25.5%) and the $NP_{172-181}$ specific line (15.1%) responded within an hour after stimulation.

The activation-induced TCR and CD8 downregulation gradually increased over time, peaking at 4 h after activation. Although the later time points, especially the overnight (16 h) point, showed even more significant downregulation, some T cells were clearly overstimulated and underwent apoptosis as previously reported (Alexander-Miller et al., 1998). We, therefore, concluded that a 4-h activation of these $CD8^+$ T cells provided optimal CD3 and CD8 downregulation.

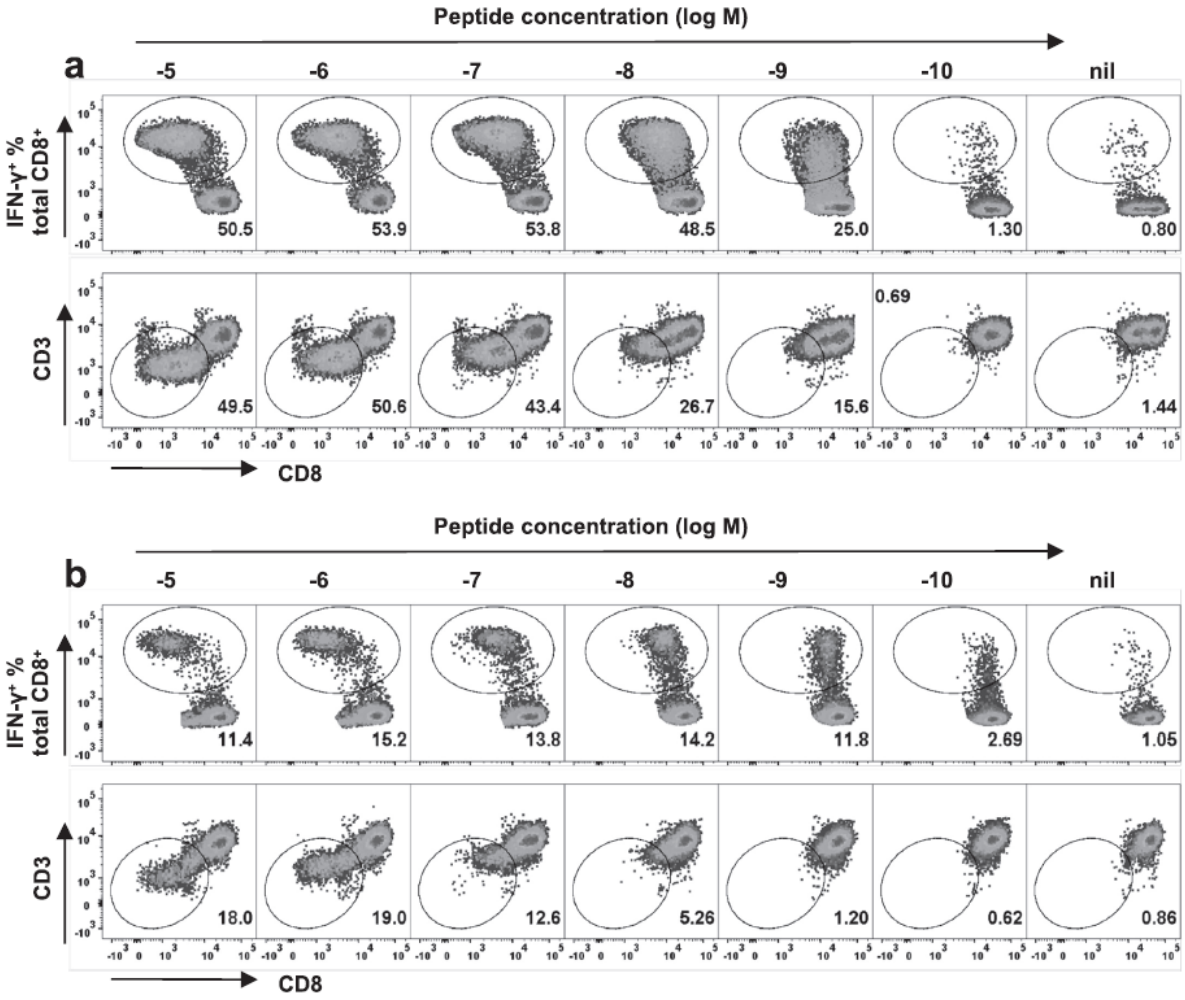

Fig. 2. 10^{-7} M peptides induce optimal CD3CD8 downregulation in antigen-specific $CD8^+$ T cells.
APCs were pulsed with serially diluted peptides for 1 h in complete medium then washed and incubated with T cells for assessing $M1_{58-66}$- and $NP_{172-181}$-specific $CD8^+$ T cell percentage at various peptide concentrations by a standard ICS. **a)** $M1_{58-66}$-specific T cell IFN-γ expression and CD3CD8 downregulation; **b)** $NP_{172-181}$-specific T cell IFN-γ response and CD3CD8 downregulation. Data shown are representative of two independent experiments.

3.2. Sub-micromolar antigen doses induce sufficient T cell activation-induced CD3CD8 downregulation

It is well established that over stimulating T cells could lead to T cell exhaustion (Wherry and Kurachi, 2015). To avoid T cell over-stimulation and yet to find out the optimal antigen dose range for activating $CD8^+$ T cells to sufficiently downregulate CD3 and CD8, we performed peptide titration experiments and monitored T cell lines' CD3 and CD8 downregulation stimulated by various peptide concentrations. Fig. 2 shows the two $CD8^+$ T cell lines' IFN-γ response and CD3CD8 downregulation at 4 h after stimulation by various peptide concentrations. It was obvious that IFN-γ response required less antigen stimulation than that required for CD3CD8 downregulation. For example, 10^{-8} M of $M1_{58-66}$ peptide activated almost all specific T cells (48.5%) to produce IFN-γ, but only about half of these cells (26.7%) showed obvious CD3 and CD8 downregulation (Fig. 2a). Such difference seemed to be T cell specificity dependent, because lower $NP_{172-181}$ peptide concentration was able to stimulate its specific T cells to produce IFN-γ (10^{-9} M activated 80%); while much higher $NP_{172-181}$ peptide concentration (10^{-7} M) was required to stimulate the same T cells to downregulate CD3 and CD8 (Fig. 2b). Taken together from these data, we concluded T cell stimulation with 10^{-7} M peptide should induce optimal CD3 and CD8 downregulation in antigen-specific $CD8^+$ T cells while avoiding significant T cell over stimulation.

3.3. Sorting $CD3^{low}CD8^{low}$ T cells after activation enriches antigen-specific $CD8^+$ T cells

Having worked out the optimal antigen dose (10^{-7} M) and stimulation time (4 h), we wanted to test the sensitivity of our T cell enriching approach. To achieve this, a T cell culture with relatively low antigen-specific T cell purity (around 2%) was activated and enriched by sorting $CD3^{low}CD8^{low}$ T cells. The sorting gate was set according to the control group that was cocultured with un-pulsed BLCLs. The gating example is shown in Fig. 3a. Only a $CD3^{high}CD8^{high}$ population can be observed from the un-stimulated group (Fig. 3a, upper panel); while a $CD3^{low}CD8^{low}$ subpopulation was obviously found in the stimulated group (Fig. 3a, lower panel). $M1_{58-66}$-specific $CD8^+$ T cells were sorted

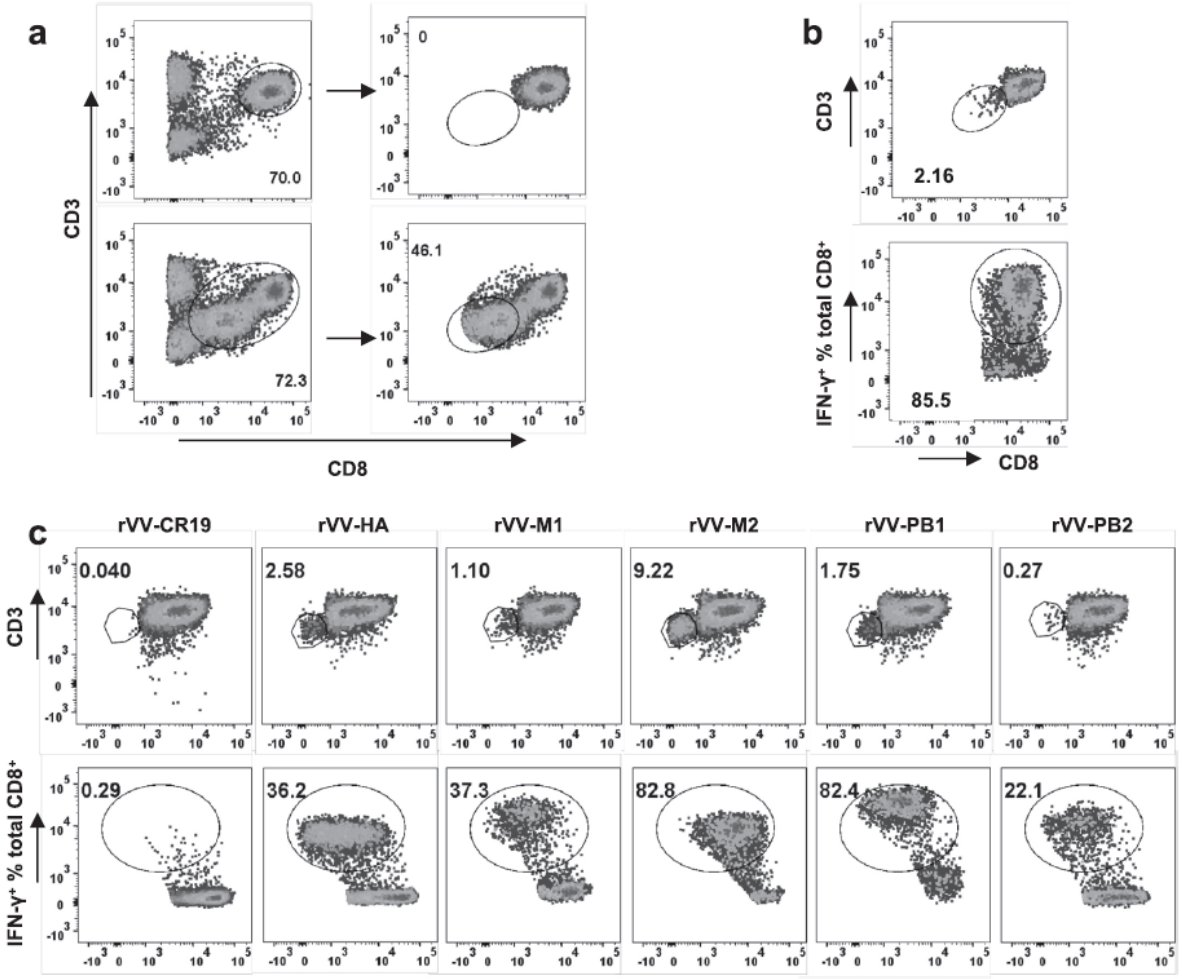

Fig. 3. Sorting $CD3^{low}CD8^{low}$ T cells after activation enriches peptide- or virus-specific $CD8^+$ T cells.
a) An example for gating CD3CD8 downregulated $M1_{58-66}$-specific T cells responding to peptide-pulsed or un-pulsed APCs. $CD8^+$ T cell culture was established as described in the M&M using PR8 infected PBMCs. $CD8^+$ T cells were stimulated with $M1_{58-66}$ peptide-pulsed (10^{-7} M) APCs for 4 h, stained with anti-CD3 and anti-CD8 and analyzed by flow cytometry. Gates were set according to T cell group co-cultured with un-pulsed BLCLs. First, gated on $CD8^+$ T cells then displayed as CD3 (Y-axis) and CD8 (X-axis). An oval gate was then applied to $CD3^{low}CD8^{low}$ population (Fig. 3a, right panel). **b)** BLCLs pulsed with $M1_{58-66}$ peptide (10^{-7} M) were used to stimulate low purity $M1_{58-66}$-specific $CD8^+$ T cells; then the $CD3^{low}CD8^{low}$ population was sorted and assessed by ICS. **c)** The rVV-infected BLCLs were used as APCs to stimulate a bulk IAV-specific $CD8^+$ T cell culture, then the $CD3^{low}CD8^{low}$ T cells were sorted and assessed by ICS. rVV-CR19 infected APCs served as a negative control.

and cultured in 48-well plate; an ICS was performed to assess the purity of antigen-specific $CD8^+$ T cells 72 h after sorting. As shown in Fig. 3b, T cells were enriched about 40 times (from 2.16% to 85.5%) after sorting $CD3^{low}CD8^{low}$ T cells. This result indicated that sorting CD3CD8 downregulated T cells after antigen stimulation could efficiently increase the purity of antigen-specific $CD8^+$ T cell population.

Generally, working out unknown antigenic epitopes is not only a time-consuming process it also often requires a large number of epitope-specific T cells to screen synthetic overlapping peptides. To achieve quality data, T cell lines with good purities are highly desired. However, it is often the case that lower purity T cell cultures are difficult to maintain for its specificity. As the above sorting was conducted using T cell lines with known peptide-specificities, we were curious to know whether our novel method would allow us to enrich $CD8^+$ T cells with unknown specificity.

We therefore established a bulk T cell culture using autologous BLCLs infected with IAV as stimulating APCs. 15 days later, $CD8^+$ T cells with various IAV specificities and purities (as a percentage of the total $CD8^+$ T cells in the culture) were expected. At this stage, autologous BLCLs were infected with recombinant vaccinia viruses (rVV) expressing individual IAV antigen, such as HA, M1, M2, PB1 or PB2, for 16 h, then used as APCs to stimulate each IAV antigen-specific T cell population in the bulk culture. 4 h later, activated T cells as a $CD3^{low}CD8^{low}$ population were sorted into 96-well plate. 72 h later the purities of sorted antigen-specific T cells were assessed by ICS. As shown in Fig. 3c, the M2-specific T cell population was 9.22% before sorting and it reached to 82.8% after sorting indicating nearly 10-fold enrichment; similarly, the T cell population specific to PB2 was 0.27% before sorting and it reached 22.1% after sorting, nearly 100-fold enrichment. Other T cell populations specific to HA, M1, and PB1 also

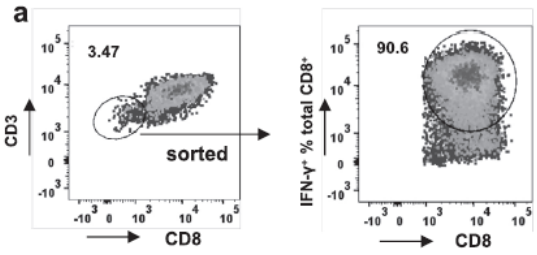

b

Cells/96-well plate	Cells expansion rate Average%(SD%)
1 cell	NA
3 Cells	12 (2)
10 Cells	19 (4)
100 Cells	32 (2)
1,000 Cells	90 (3)
5,000 Cells	100 (0)
10,000 Cells	100 (0)

Note: 1. only 60 wells are used per 96-well plate
2. Data are summarised from three independent experiments

Fig. 4. CD3CD8 downregulation-guided sorting show good $CD8^+$ T cell survival and expansion.
a) Activated $M1_{58–66}$-specific $CD8^+$ T cells were sorted into 96-well plate with ranged numbers including 1, 3, 10, 100, 1000, 5000, 10,000 cells per well; and each well contained 3×10^5 irradiated allogeneic feeder cells and was cultured in RF-5 containing 300UI/mL hrIL-2 and 1 μg/mL PHA. Cells were carefully maintained for two weeks and the specificities and purity were assessed by ICS at day 15 for IFN-γ production. NA represents not expanded wells after two week's culture. **b)** A summary of various cell numbers sorted based on CD3CD8 downregulation in three independent experiments.

reached 10–40-fold enrichment. Taken together, these results indicate that sorting according to antigen-specific CD3CD8 downregulation can efficiently enhance virus-specific $CD8^+$ T cell purity.

3.4. High purity $CD8^+$ T cell lines can be established from sorted $CD3^{low}CD8^{low}$ antigen-specific T cells

To further investigate the potential of this approach, various number of cells (1 cell/well, 3 cells/well, 10 cells/well, 100 cells/well, 1000 cells/well, 5000 cells/well, 10,000 cells/well) were sorted and deposited into U-bottom 96-well plate with 3×10^5 allogeneic feeder cells and cultured in RF-5. Two weeks later, an ICS was conducted to assess the purity of these T cells. All the expanded antigen specific T cells achieved 90% purity after CD3CD8 downregulation-guided sorting (Fig. 4a). However, no single T cell clone was successfully established from these experiments, although high purity T cell cultures (> 90%) were derived from 3 cells/well group. Fig. 4b summarises cell expansion results from the above-mentioned groups in three independent experiments. For example, from 3 cells/well group, an average of 12% wells expanded and became high purity T cell lines. However, in the 1000 cells/well group 90% expanded successfully. Furthermore, all the expanded wells eventually contained high purity T cell lines. Taken together, CD3CD8 downregulation-guided sorting was not only able to increase T cell purity but also has the potential to derive pure T cell line from very limited cell numbers (3 cells per well was demonstrated in these experiments).

3.5. CD3CD8 downregulation-guided sorting enriches multiple small antigen-specific $CD8^+$ T cell populations

To determine the reproducibility and sensitivity of this approach, a primary bulk T cell culture with multiple small IAV-specific $CD8^+$ T cell responses was established from a known donor according to our published method (Wu et al., 2011; Grant et al., 2013). The IAV specificity was then assessed using a panel of recombinant vaccinia viruses (rVV) encoding 11 individual IAV proteins (Chen et al., 2001). As shown in Fig. 5a, among all $CD8^+$ T cells only 2.85% IAV-specific $CD8^+$ T cells were identified by obvious CD3CD8 downregulation. Importantly, these IAV-specific T cells responded to 9 different IAV proteins (HA, M1, M2, NA, NP, NS1, PA, PB1, and PB2) and all the specific T cell populations were smaller than 1% of the total $CD8^+$ T cells (Fig. 5b). The IAV-specific T cells were then activated by IAV-infected BLCLs and about 1 million $CD3^{low}CD8^{low}$ cells were sorted into a well in a 48-well plate. These T cells formed clusters 24 h after sorting, suggesting that they were healthy and activated (Observed by phase contrast microscopy daily, data not shown). 72 h later, 10^4 cells were used to assess specificity and purity for each IAV antigen. The total IAV specific T cell purity increased from 2.85% to 45.8% (Fig. 5c). To further confirm the specificity of these $CD3^{low}CD8^{low}$ sorted cells, BLCLs were again infected with the rVV panel encoding 11 single IAV proteins and used to stimulate the enriched T cells in a standard ICS. As shown in Fig. 5d, specificities of every single protein were increased in the sorted $CD3^{low}CD8^{low}$ group, indicating that CD3CD8 downregulation-guided sorting was able to greatly enrich a low percentage, poly-specificity IAV-specific T cell population.

3.6. $CD8^+$ T cells that downregulate CD3CD8 less dramatically can also be enriched

Some T cells are very sensitive to antigen stimulation and subsequently show a dramatic CD3CD8 downregulation pattern after T cell activation, as shown above. However, some $CD8^+$ T cells may not downregulate their CD3 and CD8 so dramatically after antigen stimulation. We therefore sought to investigate whether our novel sorting method was also capable of enriching such $CD8^+$ T cells and, if so, whether similar purity could be achieved after a single sort. For example, it has been demonstrated that posttranslational modification of cysteine could affect immunogenicity and antigenicity of cysteine-containing peptides (Chen et al., 1999), leading to reduced T cell activation. We first selected a viral epitope that contains a cysteine in its first amino acid position (NP44–52 CTELKLSDY) (Wu et al., 2011) to test our novel enrichment method. As the peptide stock was dissolved in DMSO which is an oxidant, cysteines could easily be oxidized to form dimer peptides through disulfide bonds (Chen et al., 1999). $NP_{44–52}$-specific $CD8^+$ T cells were stimulated by peptide-pulsed APCs in the presence of 500 μM Tris(2-carboxyethyl)phosphine (TCEP) to reduce dimer peptide formation. As shown in Fig. 6a, $NP_{44–52}$-specific $CD8^+$ T cells failed to show dramatic CD3CD8 downregulation after activation. 2.43% of $NP_{44–52}$-specific $CD8^+$ T cells were detected and sorted according to the unstimulated group. Impressively, T cell purity increased by 10-fold assessed at 72 h after sorting.

We then investigated $MelanA_{26–35}$ specific $CD8^+$ T cells as this peptide binds HLA-A*02:01 weakly (Valmori et al., 1999). As shown in Fig. 6b, the CD3CD8 downregulation was rather subtle. Again, our sorting gates were set according to the unstimulated group, only 1.2% antigen-specific $CD3^{low}CD8^{low}$ T cells were detected and then sorted. Interestingly, an ICS assay conducted 72 h after the sorting again indicated a 10-fold enrichment was acheived for this $MelanA_{26–35}$-specific $CD8^+$ T cells. Taken together, the above results indicate that CD3CD8 downregulation-guided sorting is able to enrich antigen-specific $CD8^+$ T cells that show much less dramatic CD3CD8 downregulation and also capable of purifying activated $CD8^+$ T cells specific to a cysteine-containing peptide or a peptide with weak HLA-binding ability.

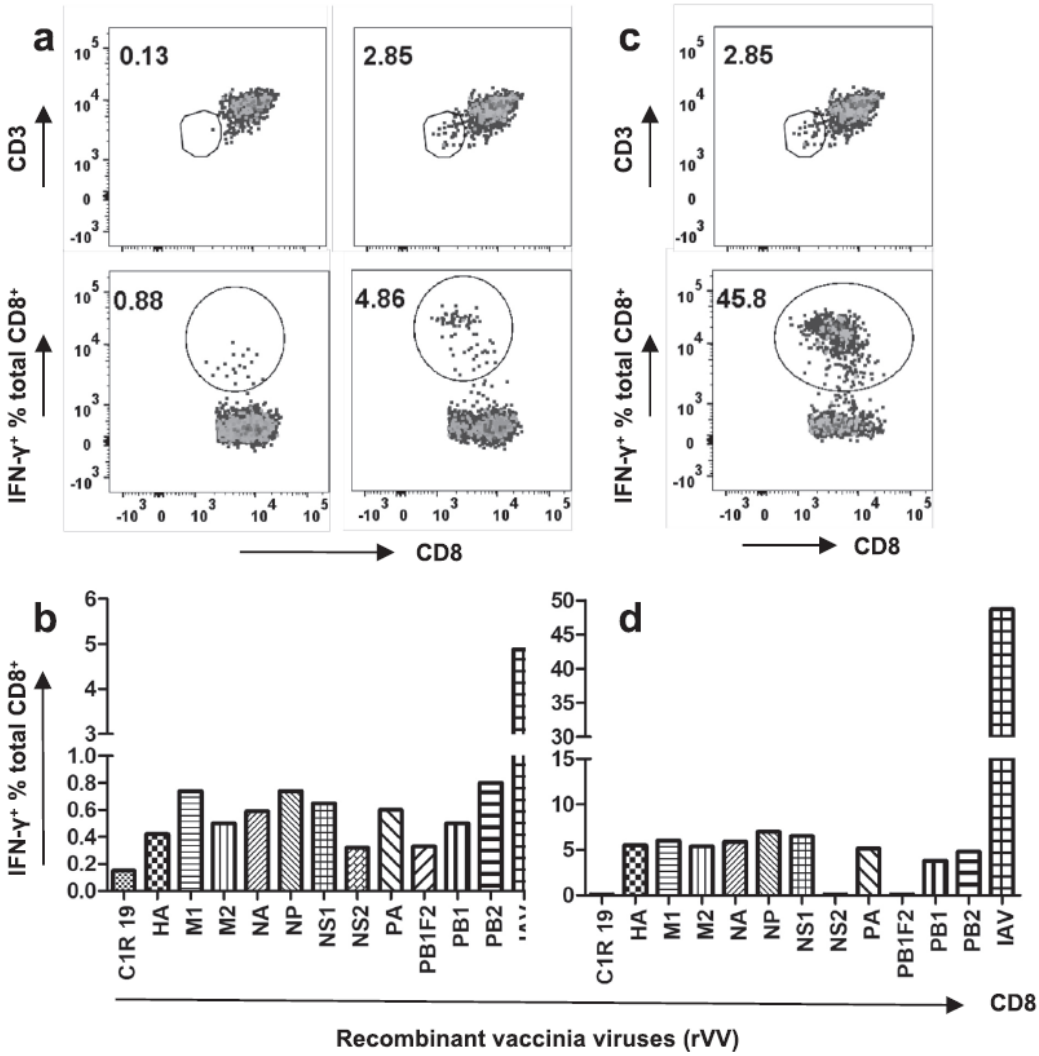

Fig. 5. Multiple small IAV-specific CD8$^+$T cell specificities were simultaneously enriched by CD3CD8 downregulation-guided sorting.
Primary T cell culture was established using IAV PR8-infected PBMC as described in the method. **a-b)** After 2 weeks' culture, IAV-specific CD8$^+$ T cell responses were assessed by their reactivity to the 11 individual IAV proteins expressed by rVV infected autologous BLCLs in an ICS assay. The IAV infected BLCLs served as a positive control and the rVV-CR19 vector infected BLCLs served as a negative control (Fig. 5b). TCR and CD8 were also stained and gated the CD3^{low}CD8^{low} population according to the unstimulated group (Fig. 5a, upper left panel). **c-d)** CD3^{low}CD8^{low} population was sorted and cultured for 3 days before being assessed for the overall IAV response and responses to the individual IAV antigens by ICS for IFN-γ as described above.

4. Discussion and conclusion

In this study, we have established and optimized a novel method for enriching antigen-specific CD8$^+$ T cells. We have demonstrated that using CD3CD8 downregulation-guided sorting can greatly enrich antigen-specific CD8$^+$ T cells. We have successfully employed this method first to enrich established immunodominant CD8$^+$ T cell line (Fig. 3b), later single IAV protein-specific T cells (Fig. 3c); and finally, a poly-specificity, low purity IAV-specific bulk CD8$^+$ T cell population. We have further demonstrated that enriched CD8$^+$ T cell populations using this method maintained broad T cell specificities (Fig. 5) and they are capable of expansion from very low numbers.

This method could potentially be widely applicable to any antigen-specific CD8$^+$ T cell enrichment, especially at the early stage of T cell culture which is the most problematic time for most, if not all T cell cultures in worldwide laboratories. Comparing to the mostly utilized tetramer-guided antigen-specific T cell sorting, our novel antigen-specific T cell enriching method has the following major advantages: first, our novel approach enriches any antigen-specific CD8$^+$ T cells without the need to know HLA restriction or minimum epitope sequence, as both are critical for the tetramer-guided T cell sorting (Altman et al., 1996; Sims et al., 2010; Hunsucker et al., 2015). In this regard, our approach should be more convenient with much wider application; second, tetramers are expensive to make, and they often have limited shelve life. So, our approach will be cheaper and always ready to run; and finally, tetramer-guided sorting is mostly only applicable to individual T cell population specific for a single pMHC. However, our approach, as demonstrated in this study, is able to enrich many antigen-

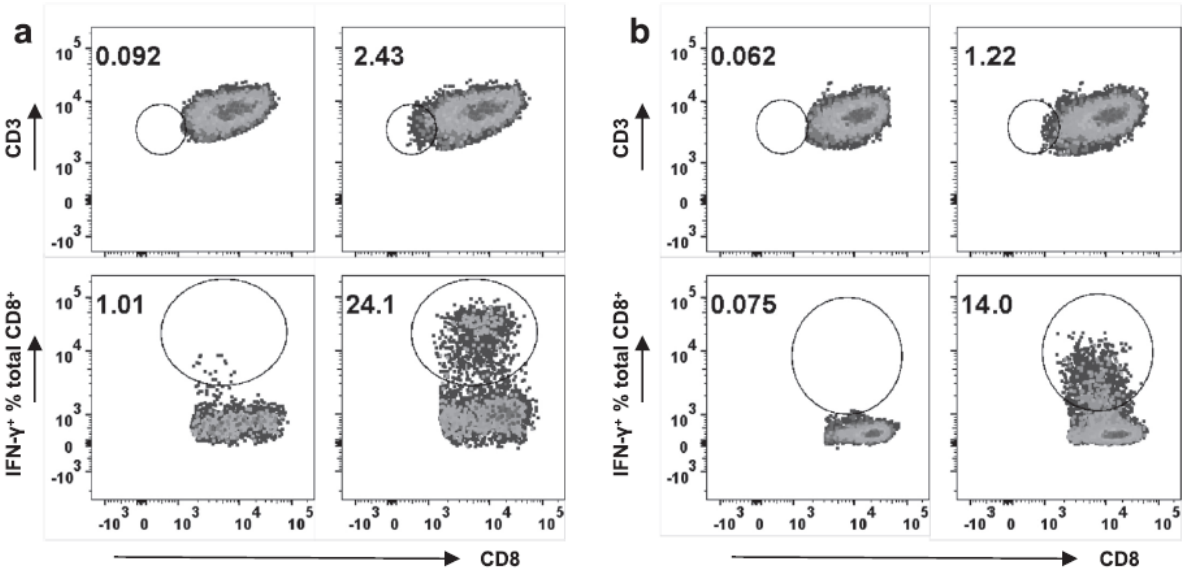

Fig. 6. CD3CD8 downregulation-guided sorting can enrich $CD8^+$ T cells with limited CD3CD8 downregulation after antigen activation.
a) Autologous BLCLs were pulsed with cysteine-containing $NP_{44–52}$ (CTELKLSDY HLA-A*01:01) then incubated with $NP_{44–52}$-specific $CD8^+$ T cells in the presence of TCEP. After activation a small population of $CD3^{low}CD8^{low}$ T cells were sorted and assessed for IFN-γ production as described in the method. **b)** Melan $A_{26–35}$ specific $CD8^+$ T cells were stimulated by peptide-pulsed HLA-A*02:01$^+$ BLCLs. T cell activation induced $CD3^{low}CD8^{low}$ T cells were sorted and assessed *via* ICS.

specific T cell populations by a single run, which may allow our method be used for antigen discovery in potentially complicated epitope discovery experiments or quick assessments to rank major T cell response to a particular antigen or pathogen.

In this study, we have not performed a side-by-side comparison study with tetramer-guided sorting. As a result, we are not sure about which method is more sensitive and/or more accurate. However, several studies have reported that pMHC tetramer staining fail to detect fully functional T cells as the TCR-affinity threshold for tetramer staining is higher than that required for T cell activation (Derby et al., 2001; Dolton et al., 2014). Furthermore, a more recent study has demonstrated that standard pMHC tetramer staining fail to detect relevant functional T cell clonotypes and underestimated antigen-reactive T cell populations (Rius et al., 2018) stressing the importance of using optimized protocols for T cell study.

Although we trialled T cell cloning using this novel method, we failed to acquire any antigen-specific T cell clone originated from single cell culture. Judging from the results we have so far, especially those from 3 cells per well cultures, we have every reason to believe this approach should be suitable for T cell cloning. We believe it is likely a cell culture related issue rather than a sorting related one, which is also reflected by a relatively low success rate of 3 cells/well group. If it was a sorting related issue, for example, cell damage during activation and/or sorting, we would have expected the same negative outcome from 3 cells/well, or even higher number wells. The second possibility could be a low rate related issue as we only trialled 60 culture for each cell number although three trials were conducted. It might be possible that should we have trialled a few hundred each time, we would have had a few clones successfully.

During this study, we observed that a T cell line did not show any CD3CD8 downregulation after being stimulated by 10^{-7}M peptide. This was a long-term cultured $CD8^+$ T cell line and had been stimulated for > 10 times and cultured for 6 months continuously. We then increased the stimulating peptide concentration to 10^{-6}M or 10^{-5}M, also enhanced T cell activation time to 6–8 h. After such activation, a small portion of $CD3^{low}CD8^{low}$ T cells could be detected in the 10^{-5}M peptide stimulated group. We also observed that after CD3CD8 downregulation-guided sorting, EBV-specific $CD8^+$ T cells were dramatically enriched. This could be due to the fact that autologous BLCL line was used as APCs. Hence, the best approach to reduce such unwanted response is to avoid using autologous BLCL. Instead, using an APC that shares only the peptide presenting HLA allele(s). For example, T2 cell line expresses HLA-A*02:01 can be used to replace HLA-A*02:01 positive autologous BLCLs. By doing this, all the EBV-specific $CD8^+$ T cells restricted to other HLA alleles, rather than HLA-A*02:01 will be avoided.

In conclusion, we have developed a novel method which utilizes the basic T cell property of CD3CD8 downregulation after antigen-triggered activation to enrich antigen-specific T cells. We have shown that this method can be utilized to enrich various T cell populations with known HLA-restrictions and peptide specificities. We have also shown that such a method can be used to enrich T cell populations with diverse specificities, unknown HLA restriction and unknown epitope sequence. Most importantly, we expect this method to be used to enrich low antigen-specific T cell populations at early, not yet established T cell culture stage, at which culture failure seems inevitable, to go on to establish relatively high purity T cell lines, or even clones without the need for tetramers or even the critical information relating to HLA restriction and T cell fine epitope sequence. As once a T cell line, or a clone is established, all this information can be easily derived. We also hope this approach may contribute to future T cell immunotherapy.

Acknowledgements

This project was partly supported by the National Health and Medical Research Council Program grant 567122 and NHMRC Senior Research Fellowship 603104 to WC.

References

Alexander-Miller, M.A., Derby, M.A., Sarin, A., Henkart, P.A., Berzofsky, J.A., 1998. Supraoptimal peptide-major histocompatibility complex causes a decrease in bcl-2 levels and allows tumor necrosis factor alpha receptor II-mediated apoptosis of

cytotoxic T lymphocytes. J. Exp. Med. 188, 1391–1399.
Altman, J.D., Moss, P.A., Goulder, P.J., Barouch, D.H., McHeyzer-Williams, M.G., Bell, J.I., McMichael, A.J., Davis, M.M., 1996. Phenotypic analysis of antigen-specific T lymphocytes. Science (New York, N.Y.) 274, 94–96.
Arcaro, A., Gregoire, C., Bakker, T.R., Baldi, L., Jordan, M., Goffin, L., Boucheron, N., Wurm, F., van der Merwe, P.A., Malissen, B., Luescher, I.F., 2001. CD8beta endows CD8 with efficient coreceptor function by coupling T cell receptor/CD3 to raft-associated CD8/p56(lck) complexes. J. Exp. Med. 194, 1485–1495.
Bierer, B.E., Sleckman, B.P., Ratnofsky, S.E., Burakoff, S.J., 1989. The biologic roles of CD2, CD4, and CD8 in T-cell activation. Annu. Rev. Immunol. 7, 579–599.
Cantrell, D.A., Davies, A.A., Crumpton, M.J., 1985. Activators of protein kinase C down-regulate and phosphorylate the T3/T-cell antigen receptor complex of human T lymphocytes. Proc. Natl. Acad. Sci. U. S. A. 82, 8158–8162.
Chen, W., Yewdell, J.W., Levine, R.L., Bennink, J.R., 1999. Modification of cysteine residues in vitro and in vivo affects the immunogenicity and antigenicity of major histocompatibility complex class I-restricted viral determinants. J. Exp. Med. 189, 1757–1764.
Chen, W., Calvo, P.A., Malide, D., Gibbs, J., Schubert, U., Bacik, I., Basta, S., O'Neill, R., Schickli, J., Palese, P., Henklein, P., Bennink, J.R., Yewdell, J.W., 2001. A novel influenza a virus mitochondrial protein that induces cell death. Nat. Med. 7, 1306–1312.
Clemens, E.B., Grant, E.J., Wang, Z., Gras, S., Tipping, P., Rossjohn, J., Miller, A., Tong, S.Y., Kedzierska, K., 2016. Towards identification of immune and genetic correlates of severe influenza disease in indigenous Australians. Immunol. Cell Biol. 94, 367–377.
Clevers, H., Alarcon, B., Wileman, T., Terhorst, C., 1988. The T cell receptor/CD3 complex: a dynamic protein ensemble. Annu. Rev. Immunol. 6, 629–662.
Davis, M.M., Bjorkman, P.J., 1988. T-cell antigen receptor genes and T-cell recognition. Nature 334, 395–402.
Derby, M.A., Wang, J., Margulies, D.H., Berzofsky, J.A., 2001. Two intermediate-avidity cytotoxic T lymphocyte clones with a disparity between functional avidity and MHC tetramer staining. Int. Immunol. 13, 817–824.
Dolton, G., Lissina, A., Skowera, A., Ladell, K., Tungatt, K., Jones, E., Kronenberg-Versteeg, D., Akpovwa, H., Pentier, J.M., Holland, C.J., Godkin, A.J., Cole, D.K., Neller, M.A., Miles, J.J., Price, D.A., Peakman, M., Sewell, A.K., 2014. Comparison of peptide-major histocompatibility complex tetramers and dextramers for the identification of antigen-specific T cells. Clin. Exp. Immunol. 177, 47–63.
Ebert, L.M., MacRaild, S.E., Davis, I.D., Cebon, J., Chen, W., 2012. A novel method for detecting antigen-specific human regulatory T cells. J. Immunol. Methods 377, 56–61.
Gao, G.F., Jakobsen, B.K., 2000. Molecular interactions of coreceptor CD8 and MHC class I: the molecular basis for functional coordination with the T-cell receptor. Immunol. Today 21, 630–636.
Grant, E., Wu, C., Chan, K.F., Eckle, S., Bharadwaj, M., Zou, Q.M., Kedzierska, K., Chen, W., 2013. Nucleoprotein of influenza a virus is a major target of immunodominant CD8+ T-cell responses. Immunol. Cell Biol. 91, 184–194.
Holler, P.D., Kranz, D.M., 2003. Quantitative analysis of the contribution of TCR/pepMHC affinity and CD8 to T cell activation. Immunity 18, 255–264.
Hunsucker, S.A., McGary, C.S., Vincent, B.G., Enyenihi, A.A., Waugh, J.P., McKinnon, K.P., Bixby, L.M., Ropp, P.A., Coghill, J.M., Wood, W.A., Gabriel, D.A., Sarantopoulos, S., Shea, T.C., Serody, J.S., Alatrash, G., Rodriguez-Cruz, T., Lizee, G., Buntzman, A.S., Frelinger, J.A., Glish, G.L., Armistead, P.M., 2015. Peptide/MHC tetramer-based sorting of CD8(+) T cells to a leukemia antigen yields clonotypes drawn nonspecifically from an underlying restricted repertoire. Cancer immunology research 3, 228–235.
Jackson, H.M., Dimopoulos, N., Chen, Q., Luke, T., Yee Tai, T., Maraskovsky, E., Old, L.J., Davis, I.D., Cebon, J., Chen, W., 2004. A robust human T-cell culture method suitable for monitoring CD8+ and CD4+ T-cell responses from cancer clinical trial samples. J. Immunol. Methods 291, 51–62.
Janeway Jr., C.A., 1992. The T cell receptor as a multicomponent signalling machine: CD4/CD8 coreceptors and CD45 in T cell activation. Annu. Rev. Immunol. 10, 645–674.
Kane, L.P., Lin, J., Weiss, A., 2000. Signal transduction by the TCR for antigen. Curr. Opin. Immunol. 12, 242–249.
Krangel, M.S., 1987. Endocytosis and recycling of the T3-T cell receptor complex. The role of T3 phosphorylation. J. Exp. Med. 165, 1141–1159.
Krogsgaard, M., Li, Q.J., Sumen, C., Huppa, J.B., Huse, M., Davis, M.M., 2005. Agonist/endogenous peptide-MHC heterodimers drive T cell activation and sensitivity. Nature 434, 238–243.
Kuhns, M.S., Davis, M.M., 2012. TCR signaling emerges from the sum of many parts. Front. Immunol. 3, 159.
Laugel, B., van den Berg, H.A., Gostick, E., Cole, D.K., Wooldridge, L., Boulter, J., Milicic, A., Price, D.A., Sewell, A.K., 2007. Different T cell receptor affinity thresholds and CD8 coreceptor dependence govern cytotoxic T lymphocyte activation and tetramer binding properties. J. Biol. Chem. 282, 23799–23810.
Pang, K.C., Sanders, M.T., Monaco, J.J., Doherty, P.C., Turner, S.J., Chen, W., 2006a. Immunoproteasome subunit deficiencies impact differentially on two immunodominant influenza virus-specific CD8 + T cell responses. Journal of immunology (Baltimore, Md. : 1950) 177, 7680–7688.
Pang, K.C., Wei, J.Q., Chen, W., 2006b. Dynamic quantification of MHC class I-peptide presentation to CD8+ T cells via intracellular cytokine staining. J. Immunol. Methods 311, 12–18.
Potter, M.R., Moore, M., 1975. PHA stimulation of separated human lymphocyte populations. Clin. Exp. Immunol. 21, 456–467.
Rius, C., Attaf, M., Tungatt, K., Bianchi, V., Legut, M., Bovay, A., Donia, M., Thor Straten, P., Peakman, M., Svane, I.M., Ott, S., Connor, T., Szomolay, B., Dolton, G., Sewell, A.K., 2018. Peptide-MHC class I tetramers can fail to detect relevant functional T cell Clonotypes and underestimate antigen-reactive T cell populations. Journal of immunology (Baltimore, Md. : 1950) 200, 2263–2279.
Rosenberg, S.A., Yang, J.C., Restifo, N.P., 2004. Cancer immunotherapy: moving beyond current vaccines. Nat. Med. 10, 909–915.
Salter, R.D., Benjamin, R.J., Wesley, P.K., Buxton, S.E., Garrett, T.P., Clayberger, C., Krensky, A.M., Norment, A.M., Littman, D.R., Parham, P., 1990. A binding site for the T-cell co-receptor CD8 on the alpha 3 domain of HLA-A2. Nature 345, 41–46.
Schott, E., Ploegh, H.L., 2002. Mouse MHC class I tetramers that are unable to bind to CD8 reveal the need for CD8 engagement in order to activate naive CD8 T cells. Eur. J. Immunol. 32, 3425–3434.
Sims, S., Willberg, C., Klenerman, P., 2010. MHC-peptide tetramers for the analysis of antigen-specific T cells. Expert review of vaccines 9, 765–774.
Smith-Garvin, J.E., Koretzky, G.A., Jordan, M.S., 2009. T cell activation. Annu. Rev. Immunol. 27, 591–619.
Valitutti, S., Muller, S., Cella, M., Padovan, E., Lanzavecchia, A., 1995. Serial triggering of many T-cell receptors by a few peptide-MHC complexes. Nature 375, 148–151.
Valmori, D., Fonteneau, J.F., Valitutti, S., Gervois, N., Dunbar, R., Lienard, D., Rimoldi, D., Cerundolo, V., Jotereau, F., Cerottini, J.C., Speiser, D.E., Romero, P., 1999. Optimal activation of tumor-reactive T cells by selected antigenic peptide analogues. Int. Immunol. 11, 1971–1980.
Wegener, A.M., Letourneur, F., Hoeveler, A., Brocker, T., Luton, F., Malissen, B., 1992. The T cell receptor/CD3 complex is composed of at least two autonomous transduction modules. Cell 68, 83–95.
Wherry, E.J., Kurachi, M., 2015. Molecular and cellular insights into T cell exhaustion. Nat. Rev. Immunol. 15, 486–499.
Wu, C., Zanker, D., Valkenburg, S., Tan, B., Kedzierska, K., Zou, Q.M., Doherty, P.C., Chen, W., 2011. Systematic identification of immunodominant CD8+ T-cell responses to influenza a virus in HLA-A2 individuals. Proc. Natl. Acad. Sci. U. S. A. 108, 9178–9183.
Xiao, Z., Mescher, M.F., Jameson, S.C., 2007. Detuning CD8 T cells: down-regulation of CD8 expression, tetramer binding, and response during CTL activation. J. Exp. Med. 204, 2667–2677.
Zanker, D., Xiao, K., Oveissi, S., Guillaume, P., Luescher, I.F., Chen, W., 2013. An optimized method for establishing high purity murine CD8+ T cell cultures. J. Immunol. Methods 387, 173–180.

Chapter 4: Identification of novel IAV-specific $CD8^+$ T cell epitopes from a healthy donor with broad-based $CD8^+$ T cell responses

4.1 Introduction

IAV infection causes significant morbidity and mortality worldwide (Krammer et al., 2018). The 1918 Spanish influenza pandemic resulted in over 50 million people deaths worldwide, making it one of the deadliest plagues ever experienced in human history (Ahmed et al., 2007). Data from the WHO has reported that annual IAV epidemics are responsible for 3-5 million severe infections and more than 500,000 deaths worldwide https://www.who.int/en/news-room/fact-sheets/detail/influenza-(seasonal). IAV vaccines are widely available; however, their efficacy in elderly and young are still debated (E. J. Grant et al., 2014). As these vaccines are designed to stimulate neutralising antibodies to the surface proteins HA and NA (Grebe et al., 2008), which mutate frequently, the vaccine requires to be updated annually (Krammer et al., 2018). Moreover, antibody-based IAV vaccines often showed little effect on newly-emerged IAV strains (E. J. Grant et al., 2014), such as the avian-origin H7N9 IAV emerged in China during 2013 (Gao et al., 2013). Hence, more effective vaccines with broader strain coverage are urgently required.

$CD8^+$ T cells play an essential role in controlling virulent IAV infections (Bender et al., 1992). They eliminate virus-infected cells efficiently by producing antiviral cytokines and other cytolytic molecules (Doherty et al., 1996). IAV -specific $CD8^+$ T cells are mainly directed against the relatively conserved internal viral proteins, like NP. Our previous studies have demonstrated that NP is the major target of immunodominant IAV-specific $CD8^+$ T cells in both HLA-A*02:01 positive and negative donors (E. Grant et al., 2013; Wu et al., 2011). In addition, IAV-specific $CD8^+$ T cells were also associated with enhanced recovery from novel IAV infection. For example, Wang and colleagues reported that early H7N9 specific $CD8^+$ T cell response was contributed to shorter-term hospitalisation, while patients who had late recruitment of $CD8^+$ T cell responses were most likely to develop severe complications and discharge delays (Z. Wang et al., 2015). Furthermore, virus-specific $CD8^+$ T cells induced after infection with seasonal circulating IAV display considerable cross-reactivity with 2009 pandemic influenza A (H1N1) virus (Gras et al., 2010; Hillaire et al., 2013), and other more virulent strains like H7N9 (van de

Sandt et al., 2014) and H5N1 (Kreijtz et al., 2008). Hence, such cross-reactive $CD8^+$ T cells in the human populations could provide cross-strain protection and dampen the impact of a pandemic outbreak caused by newly-emerged IAV strains.

$CD8^+$ T cells recognise viral derived peptides bound to MHC-I molecules (Davis et al., 1988). Some viruses encode many proteins and many peptides could potentially be presented to $CD8^+$ T cells. However, it is often observed that only a small fraction of such viral peptides is recognised by virus-specific $CD8^+$ T cells with a measurable response. Among these, often a couple of responses are much bigger than the rest, a phenomenon known as immunodominance (Yewdell et al., 1999), and the peptides stimulate major responses are termed immunodominant determinants and the others called subdominant determinants (Sercarz et al., 1993; Yewdell et al., 1999).

Most studies that investigated the underlying mechanisms of immunodominance often used syngeneic mouse models, such as the well-studied influenza infection model in the C57BL/6 and BALB/c mice (Belz et al., 2000; W. Chen et al., 2000), LCMV infected C57BL/6 and BALB/c mice (Oldstone et al., 1995), rVV-infected C57BL/6 mice (Tscharke et al., 2005), HSV-infected C57BL/6 mice (Wallace et al., 1999), and many others. In such studies, factors, such as peptide-binding ability to MHC, antigen-processing efficiency, and TCR repertoires are investigated (Belz et al., 2000; W. Chen et al., 2000; Oldstone et al., 1995; Tscharke et al., 2005; Wallace et al., 1999). Importantly, few studies focused on MHC allelic difference and its impact on immunodominance. It is well demonstrated that individual's HLA plays a significant role in setting the immunodominance hierarchy. For example, in HIV-infected individuals who express HLA-B*57 or *58:01 present the immunodominant $Gag_{240\text{-}249}$ (TSTLQEQIAW) epitope to $CD8^+$ T cells, which protects the individuals by forcing the virus to mutate 242T→N resulting in a weakened virus. When this virus is passed to their newborn babies vertically, if the baby does not express HLA-B*57 or *58:01 the virus mutates back to 242T (Leslie et al., 2004). Immunodominant $CD8^+$ T cell responses in humans have been also widely observed in other viral infections such as CMV and HBV (Elkington et al., 2003; Lacey et al., 2003; Malik et al., 2017; Schirmbeck et al., 2002)

HLA is extremely polymorphic and most of the polymorphism is concentrated on the peptide-binding cleft (Bjorkman et al., 1987a; Sidney et al., 2008). There are generally two pockets exist in the peptide-binding groove that accommodate the side chains of selected amino acids, which are often termed anchor residues (Falk et al., 1991). This specific peptide preference is often referred as “peptide-binding motif” that allows reasonably accurate peptide prediction for many HLA alleles (Ibe et al., 1996; Jardetzky et al., 1991). For example, HLA-B*44 molecules have a stringent binding motif requiring a Glutamate (E) in position two (P2) and a tyrosine (Y), or phenylalanine (F) and less often tryptophan (W) at the C-terminus (Luescher et al., 1996). Similar to HLA-B*44:03, HLA-A*33:03 also has relatively stringent peptide-binding motifs. Although it tolerates Alanine (A), Isoleucine (I), Leucine (L), Phenylalanine (F), Tyrosine (Y) or Valine (V) at P2, it requires almost exceptionally an Arginine (R) at the C-terminus (Takiguchi et al., 2000). HLA-A*24:02 peptide-binding motifs prefer a Tyrosine (Y) at P2 and a phenylalanine (F) or Leucine (L) at the C-terminus (Kubo et al., 1994). Such stringent binding motifs enhance the accuracy of peptide prediction and enable easy and time-saving identification of potential antigenic peptides recognised by $CD8^+$ T cells (Ibe et al., 1996; Jardetzky et al., 1991; Rammensee et al., 1999).

As mentioned above HLA molecules are highly polymorphic and few individuals share the same HLA alleles, the observed immunodominance in humans has been much less reproducible than those observed in the syngeneic murine systems. For instance, through a systematic approach, our laboratory demonstrated that not all individuals expressing HLA-A*02:01 show immunodominant response to $M1_{58\text{-}66}$ (Wu et al., 2011). As this epitope is rarely mutated, the lack of immunodominant response to this epitope is likely the result of emerging novel immunodominant epitopes associated with other HLA molecules co-expressed with HLA-A*02:01 in these individuals (Wu et al., 2011). Thus, if one individual expresses a set of HLA molecules that do not present any immunodominant $CD8^+$ T cell epitope from IAV, the prediction would be that T cell responses in this individual will likely be broad and even to many subdominant determinants and lack pronounced immunodominance during IAV infection. Such type of response has not been previously reported for $CD8^+$ T cells.

Our laboratory reported such an IAV-specific $CD4^+$ T cell response previously as no clear immunodominant response was detected among all the antigenic regions from NP and M1 (L. Chen et al., 2017). In this study, I report broad-based IAV-specific $CD8^+$ T cell responses to various IAV antigens from a healthy donor. I found $CD8^+$ T cell responses to nine IAV proteins, including the previously shown dominant $CD8^+$ T cell target antigens M1 and NP in most healthy individuals (Wu et al., 2011). Interestingly, most of these $CD8^+$ T cell responses specific to the epitopes from the nine IAV proteins showed similar intensity. I believe that an in-depth understanding of such $CD8^+$ T cell responses could help vaccines design.

4.2 Results

4.2.1 A systematic approach for identifying IAV-specific CD8$^+$ T cell responses

A two-step systematic approach (E. Grant et al., 2013; Wu et al., 2011) was created to i) identify the viral proteins that stimulated CD8$^+$ T cell responses (Figure 4.1a), and then to, ii) determine minimum antigenic peptide sequences and their HLA restrictions (Figure 4.1b). To achieve this, IAV-specific polyclonal CD8$^+$ T cell lines were established by infecting 10% of autologous PBMCs, as the infected PBMCs serving as APCs would be able to stimulate all IAV-specific memory CD8$^+$ T cells among these PBMCs. Two weeks later, CD8$^+$ T cell' specificities were assessed by infected autologous BLCLs with a panel of 11 rVVs encoding individual IAV proteins followed by synthetic overlapping 18mer peptides via ICS for IFN-γ production. Once the specific antigenic regions were identified, the minimal epitope sequences were determined using either overlapping 13mer peptides or other shorter predicted peptides within the active 18mer sequence. Partially HLA-matched cell lines were used to determine these epitopes' HLA-restriction.

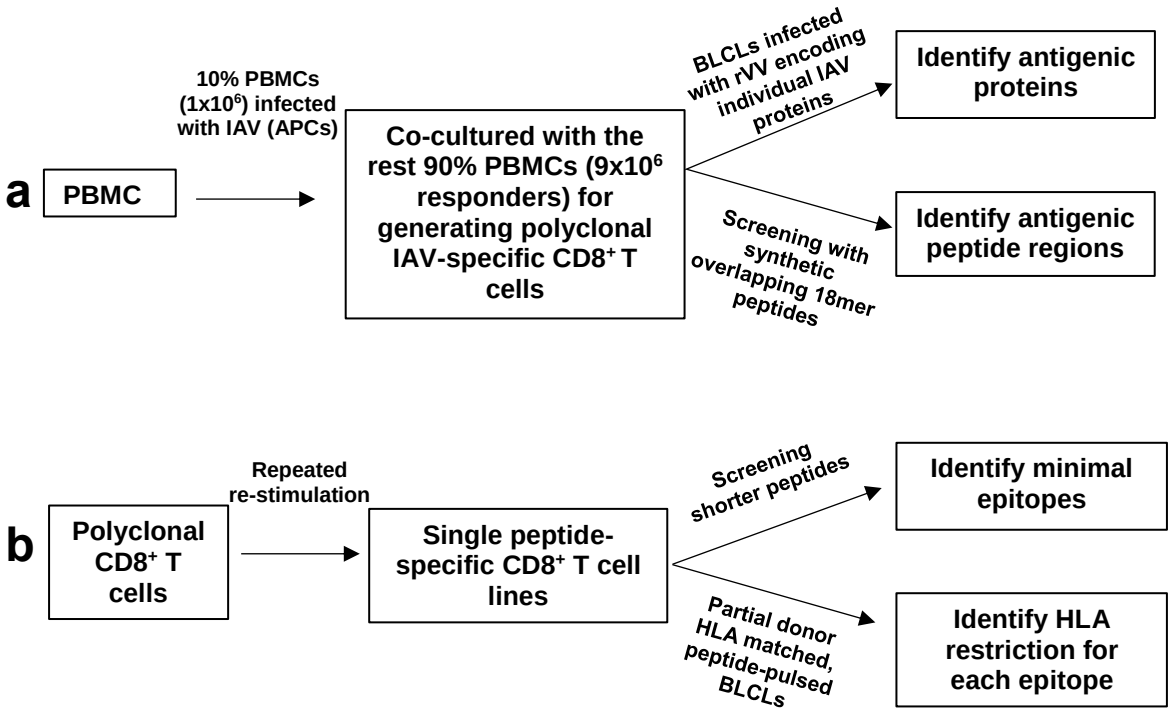

Figure 4.1. A systematic approach for identifying IAV-specific CD8$^+$ T cell responses

(a), Establishing polyclonal IAV-specific CD8$^+$ T cells. After about two weeks' culture, CD8$^+$ T cells were screened by a panel of individual IAV protein-encoding rVV to identify specific antigenic proteins. After knowing the specific antigenic proteins, CD8$^+$ T cells were screened with synthetic overlapping 18mer peptides to determine the specific antigenic peptide regions within the protein.

(b), Generating individual peptide-specific CD8$^+$ T cell lines by using individual peptide-pulsed APCs, irradiated, co-cultured with polyclonal IAV-specific T cells or T cells were isolated and enriched via CD3CD8 downregulation-guided sorting. Two weeks later, CD8$^+$ T cells were tested with shorter peptides to assess the core sequence and HLA restriction of the particular peptide.

4.2.2 Broad-based IAV-specific $CD8^+$ T cell responses to multiple IAV proteins

To identify a donor with broad-based $CD8^+$ T cell responses to IAV antigens, PBMC samples from multiple donors were screened. Polyclonal IAV-specific $CD8^+$ T cell cultures were established and screened as described in Figure 4.1a. Briefly, $1x10^6$ PBMCs were infected as APCs and co-cultured with the rest $9x10^6$ uninfected PBMCs (responders). After about 15 days' culture, the polyclonal T cells were used to screen rVV encoding individual IAV proteins. One of the screen results showed broad T cell responses to nine IAV proteins (PA, NA, HA, M1, M2, NP, NS1, PB1, PB2) except PB1F2 and NS2 (Figure 4.2). Although NP was demonstrated to be the most dominant antigen in most healthy donors (E. Grant et al., 2013; Wu et al., 2011), that is not the case in this individual as most T cell responses specific to the nine IAV proteins showed similar intensity. To further investigate this broad-based $CD8^+$ T cell response, the IAV-specific T cells were enriched via the novel CD3CD8 downregulation-guided sorting in Chapter 3 (Huang et al., 2019)

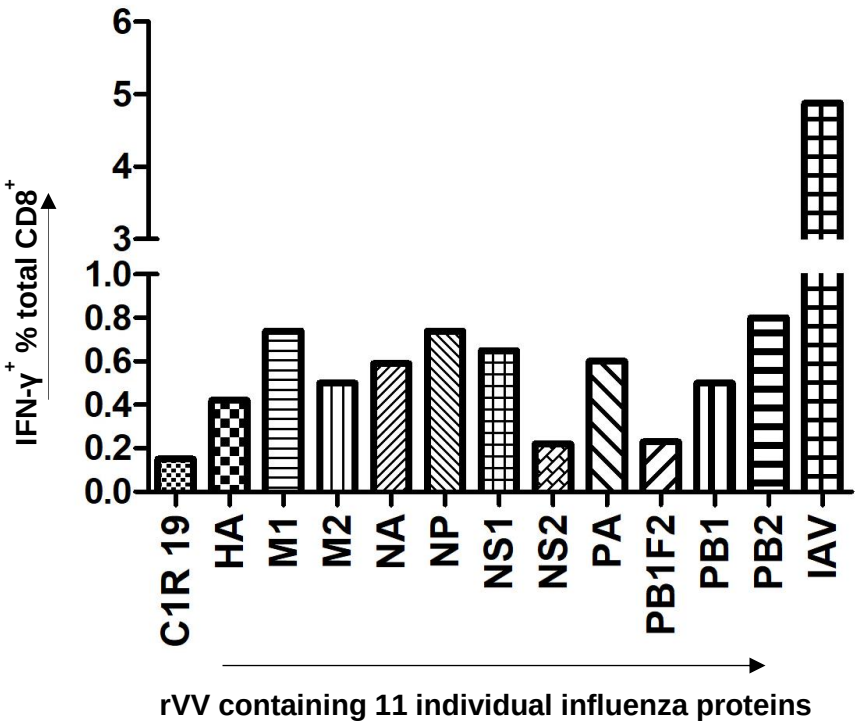

Figure 4.2. Broad-based CD8$^+$ T cell responses to multiple IAV proteins

Autologous BLCLs were infected with rVVs encoding individual IAV proteins for 16 hours before being used as APCs to assess CD8$^+$ T cell responses via a standard ICS for IFN-γ production.

4.2.3 Characterising antigenic peptide regions in multiple IAV proteins

Following the identification of broad-based $CD8^+$ T cell responses at IAV protein level, a whole set of synthetic 18mer overlapping peptides from these proteins were screened by the bulk T cell line used in Figure 4.2 to further identify antigenic regions in each protein. Because this was a polyclonal, low purity IAV-specific bulk $CD8^+$ T cell line, a quick assessment of 18mer peptides was performed to avoid losing any protein specificity during antigen re-stimulated T cell expansion. The polyclonal $CD8^+$ T cell line was subsequently enriched by CD3CD8 downregulation guided sorting (Huang et al., 2019); the enriched $CD8^+$ T cell lines were tested again with the whole set of synthetic 18mer peptides to further confirm the results obtained from the bulk T cell line used in Figure 4.2. As shown in Figure 4.3 (results derived from the enriched $CD8^+$ T cell line), the antigenic regions from the above-mentioned nine IAV proteins were revealed by synthetic 18mer overlapping peptide screen: they are M2 7-24, M1 121-138, NP 313-330, NS1 193-210, PB1 493-510, PB2 37-54, HA 439-456, NA 331-348, PA 121-138. Interestingly, only one antigenic region in each IAV protein was recognised by the specific $CD8^+$ T cells except for NS1, in which I failed to detect a clear antigenic peptide region.

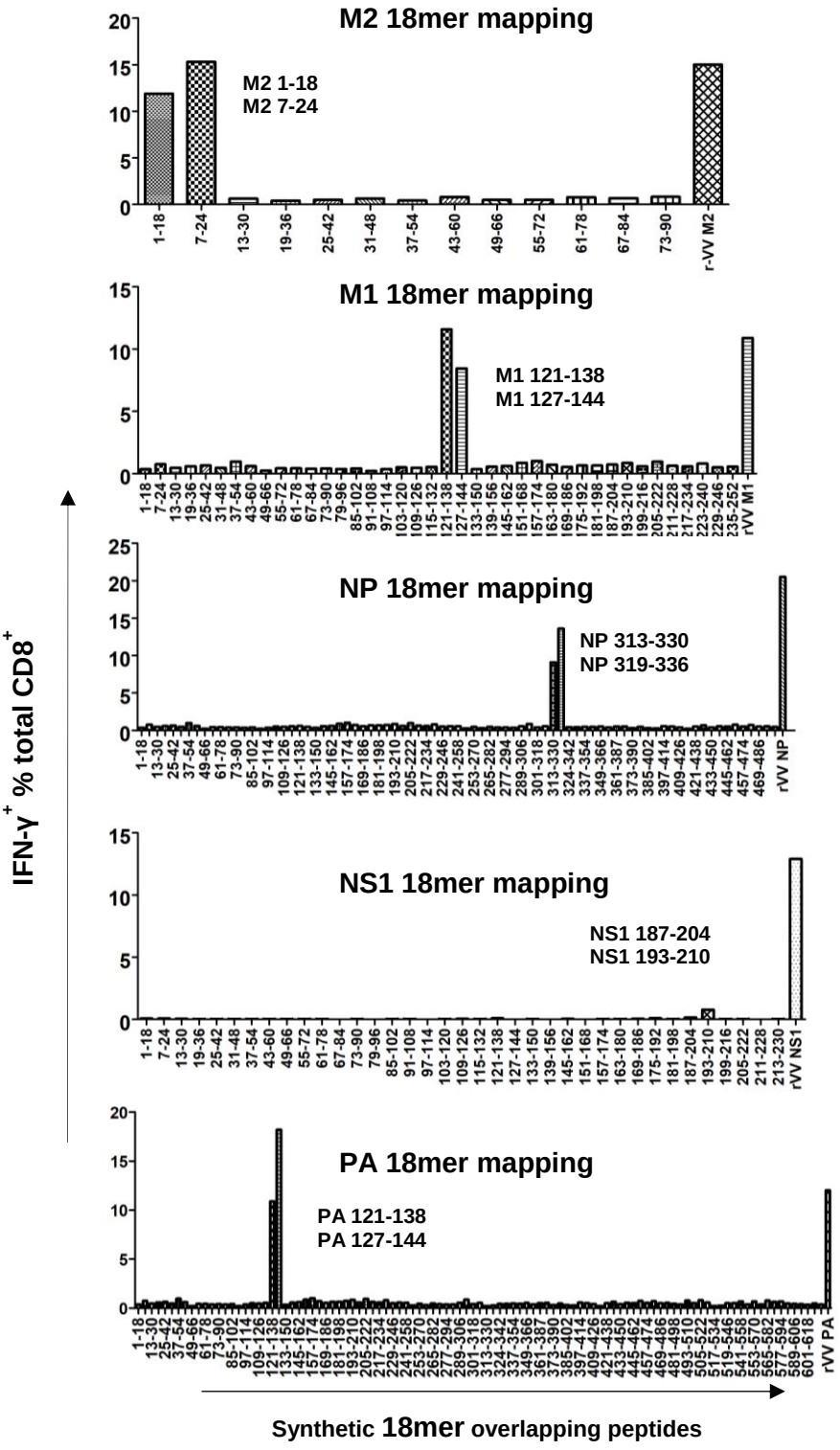
M2 18mer mapping
M2 1-18
M2 7-24
M1 18mer mapping
M1 121-138
M1 127-144
NP 18mer mapping
NP 313-330
NP 319-336
NS1 18mer mapping
NS1 187-204
NS1 193-210
PA 18mer mapping
PA 121-138
PA 127-144
IFN-γ+ % total CD8+
Synthetic 18mer overlapping peptides

Figure 4.3 (continued)

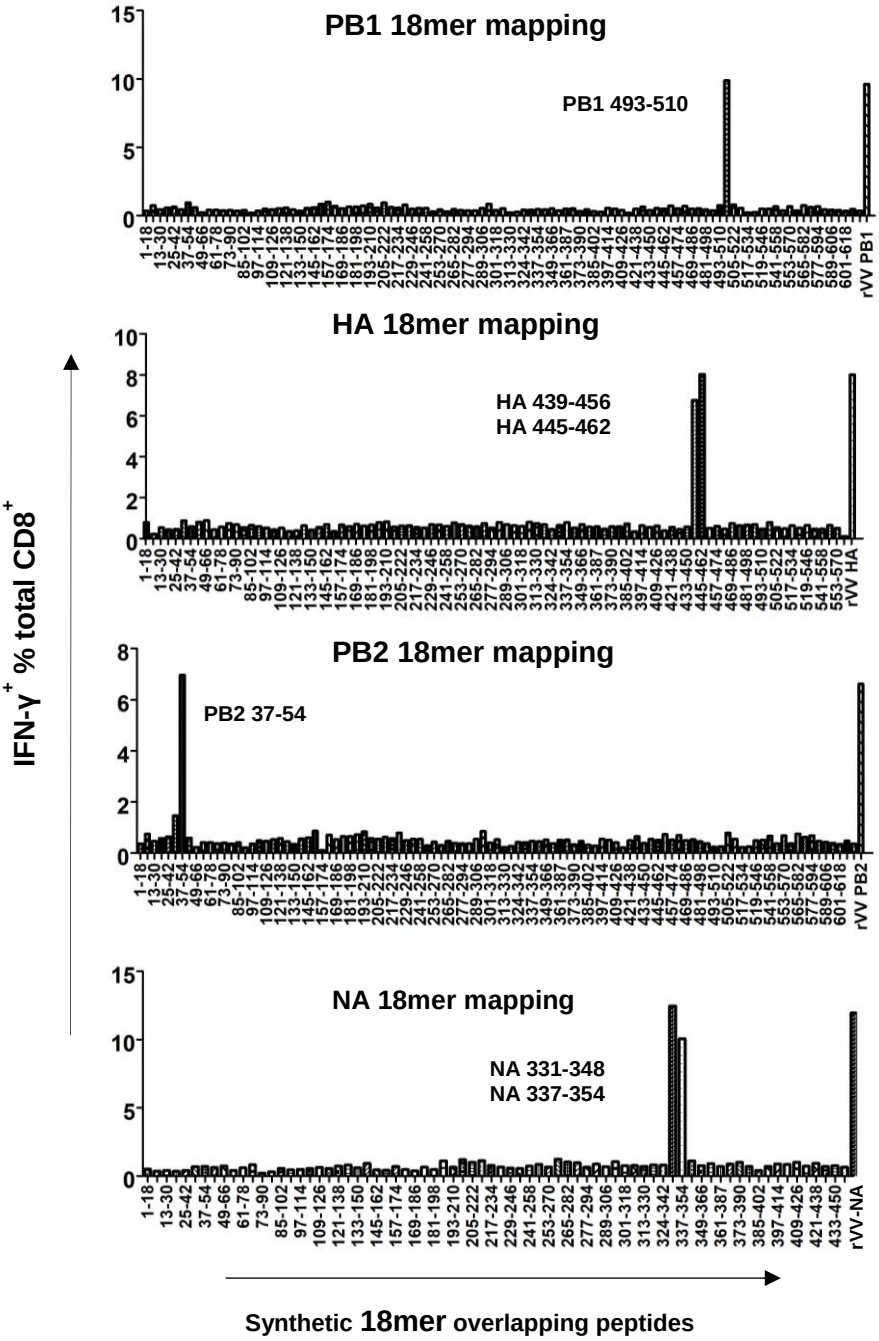

Figure 4.3. Identification of specific antigenic regions using synthetic 18mer overlapping peptides

The $CD8^+$ T cell responses of individual IAV proteins were assessed with 18mer overlapping peptides covering the full-sequences of M2, M1, NP, NS1, PB1, PB2, HA, NA, and PA in a standard ICS assay. In the same experiment, APCs infected by each rVV encoding individual IAV proteins were used as positive controls shown at the far right in each graph.

4.2.4 Minimal epitopes of differing lengths are presented by three HLA alleles

It has been demonstrated that MHC is one of the critical determining factors of the immunodominance (Burrows et al., 1995; Gotch et al., 1987) and the MHC-I peptide-binding groove can only accommodate peptide generally of 8-12 amino acid in length (Blum et al., 2013; Rist et al., 2013). Therefore, minimal epitope sequences and their HLA restrictions were investigated for better understanding such a broad-based $CD8^+$ T cell responses. First, single peptide-specific $CD8^+$ T cell lines were generated either by 18mer peptide stimulation as demonstrated in Figure 4.1b or by enriching and isolating through the novel CD3CD8 downregulation-guide sorting (Huang et al., 2019). All the newly identified 18mer peptides were shown to be restricted by HLA-A*33:03, or HLA-A*24:02, or HLA-B*44:03 (Appendix Figure 4.1) and interestingly, not a single peptide was shown to be restricted to HLA-B*46:01 expressed also by this donor. As all three HLA molecules have stringent peptide-binding motifs (Kubo et al., 1994; Luescher et al., 1996; Takiguchi et al., 2000), for example, HLA-B*44 molecules requiring a Glutamate (E) in position two (P2) and a tyrosine (Y), or phenylalanine (F) and less often tryptophan (W) at the C-terminus (Luescher et al., 1996), shorter peptides within the 18mer region of interest were predicted according to the peptide-binding motifs and screened by single peptide-specific $CD8^+$ T cell lines.

4.2.4.1 Identifying the core sequences of the epitopes presented by HLA-B*44:03

4.2.4.1.1 HA-specific $CD8^+$ T cell minimal epitope

For HA-specific $CD8^+$ T cells, HA 439-456 (AELLVL**LENERTLDFHDS**) and HA 445-462 (**LENERTLDFHDS**NVKNLY) peptides revealed a positive $CD8^+$ T cell response among all the 18mer peptides (Figure 4.3). Moreover, these two neighbouring peptides stimulated T cell activation to a similar degree, indicating that the minimal epitope was likely within the shared sequence HA 445-456 (**LENERTLDFHDS**). I then worked out these two positive peptides are restricted

by HLA-B*44:03 (Appendix Figure 4.1) using donor HLA-matched APCs from Table 4.1. As HLA-B*44:03 requires P2 and C-terminal anchor residues E and Y/F respectively, I predicted HA 445-453 **LENERTLDF** as the minimal epitope. The peptide and its single amino acid truncated versions were synthesised and tested in a peptide titration experiment. As shown in Figure 4.4 a-i, HA 445-453 peptide stimulated $CD8^+$ T cell response even at a concentration of 10^{-9}M. However, HA 446-453 was only able to stimulate a weaker T cell response at much higher peptide concentration (10^{-6}M) while HA 445-452 lost all the activity. Therefore $HA_{445-453}$ is the minimal epitope and its HLA-B*44:03 restriction was further confirmed (Figure 4.4 a-ii). According to Immune Epitope Database (IEDB) (www.immuneepitope.org) (unless otherwise noted, the last search time is 27th July 2019), HLA-B*44:03 restricted $HA_{445-453}$ is a novel epitope identified in this study.

4.2.4.1.2 M2-specific $CD8^+$ T cell minimal epitope

Similarly, the M2 specific $CD8^+$ T cells recognised both M2 1-18 (MSLLTE**VETPIRNEWGCR**) and M2 7-24 (**VETPIRNEWGCR**CNGSSD) to a similar degree (Figure 4.3) and showed HLA-B*44:03 restriction (Appendix Figure 4.1). I, therefore, predicted the minimal epitope as M2 7-15 (**VETPIRNEW)** within the shared M2 7-18 (**VETPIRNEWGCR**) region. Peptide titration experiments were performed for M2 7-15, M2 8-15 and M2 7-14 and very similar results were obstained (Figure 4.4 b-i) as those acquired above, and HLA-B*44:03 restriction was further confirmed (Figure 4.4 b-ii). According to IEDB, I concluded that $M2_{7-15}$ is a novel epitope identified in this study.

4.2.4.1.3 NP-specific $CD8^+$ T cell minimal epitope

In similar fashion, NP-specific $CD8^+$ T cells recognised 18mer peptides NP 313-330 (YSLIRP**NENPAHKSQLVW**) and NP 319-336 (**NENPAHKSQLVW**MACHSA) (Figure 4.3) and restricted by HLA-B*44:03 (Appendix Figure 4.1). I predicted NP 319-330 (**NENPAHKSQLVW**) as the minimal epitope, which was confirmed by the decreased and total loss of T cell activation capacity of the amino- and carboxyl-terminal single amino acid truncation peptides (Figure 4.4 c-i). This is a longer minimal epitope containing 12 amino acids, and HLA-B*44:03 restriction was again

confirmed (figure 4.4 c-ii). Thus, I concluded that $NP_{319-330}$ is the minimal epitope and it is also the longest HLA-B*44:03 restricted novel IAV epitope confirmed by IEDB.

4.2.4.1.4 PB2-specific $CD8^+$ T cell minimal epitope

The PB2-specific $CD8^+$ T cells (HLA-B*44:03 restricted, Appendix Figure 4.1) showed an interesting pattern of peptide recognition as they were slightly activated by PB2 31-48 (IKKYTSGR**QEKNPALRMK**) but well activated by PB2 37-54 (GR**QEKNPALRMKW**MMAMK) (Figure 4.3), indicating that PB2 37-54 must contain the minimal peptide sequence and PB2 31-48 likely misses a single C-terminal amino acid. PB2 39-49 (**QEKNPALRMKW**) was considered as the minimal epitope. This was confirmed by the loss of T cell activating capacity of the two peptides with a single amino acid truncation at either end of PB2 39-49 (Figure 4.4 d-i). The restricting HLA for $PB2_{39-49}$ was subsequently reconfirmed as HLA-B*44:03 (Figure 4.4 d-ii). Again, this is a novel peptide by comparing with those listed in the IEDB.

4.2.4.1.5 NS1-specific $CD8^+$ T cell minimal epitope

The NS1-specific $CD8^+$ T cells, although recognised rVV-NS1 infected APC (15% produced IFN-γ), they basically failed to recognise any NS1 18mers, except for very limited T cell activation induced by NS1 187-204 (WNDNTVRV**SETLQRFAW**R) and NS1 193-210 (RV**SETLQRFAW**RSSNENG) (<1%) (Figure 4.3) and restricted by HLA-B*44:03 (Appendix Figure 4.1). Although the NS1 18mer responses were very low, according to the FACS profiles I believed the NS1 18mer peptide-specific $CD8^+$ T cell response was real. Therefore, these $CD8^+$ T cells were specifically enriched by NS1 193-210 pulsed APCs through CD3CD8 downregulation guided-sorting. I then predicted NS1 195-203 (**SETLQRFAW**) as the minimal epitope. Indeed, T cell activation was significantly reduced when they were stimulated by peptides with a single amino acid truncation at either end of NS1 195-203 (Figure 4.4 e-i). I, therefore, concluded that $NS1_{195-203}$ is the minimal epitope and its MHC restriction was also reconfirmed as HLA-

B*44:03 (Figure 4.4 e-ii). Again, comparing to those listed in the IEDB, this epitope is undeniably a novel one.

4.2.4.2 Identifying the core sequences of the epitopes presented by HLA-A*33:03

Similar to HLA-B*44:03, HLA-A*33:03 also has relatively stringent peptide-binding motifs. Although it tolerates Alanine (A), Isoleucine (I), Leucine (L), Phenylalanine (F), Tyrosine (Y) or Valine (V) at P2, it requires almost exceptionally an Arginine (R) at the C-terminus (Takiguchi et al., 2000).

4.2.4.2.1 M1-specific $CD8^+$ T cell minimal epitope

The M1-specific $CD8^+$ T cells responded to M1 121-138 (AGA**LASCMGLIYNR**MGAV) and M1 127-144 (**CMGLIYNR**MGAVTTEVAF) 18mers (Figure 4.3) and the response was restricted by HLA-A*33:03 (Appendix Figure 4.1). As the two 18mer peptides only contained a single Arginine (R) at position 134, and as M1 127-144 still had some T cell activation capacity (Figure 4.3), likely due to week stimulation at high concentration, I predicted that the P2 residue as 125 A rather than 124 L or 123 A because 12mer and 13mer epitopes are rare. Again M1 124-134 (**LASCMGLIYNR**) and its single terminal truncation peptides were synthesised. As P4 is a cysteine, to avoid cysteinylation and peptide dimerization (W. Chen et al., 1999), I assessed these peptides in the presence of 500µM TCEP. As shown in Figure 4.4 f-i, both M1 124-134 and M1 125-134 were quite potent in the titration experiment, while M1 124-133 was no longer capable of T cell activation due to missing the C-terminal anchor residue Arginine. Judging from the titration curves, M1 124-134 is more potent than M1 125-134, therefore, I concluded that $M1_{124\text{-}134}$ is minimal epitope. HLA restriction of this minimal epitope was also reconfirmed by peptide-pulsed C1R-A*33:03 APCs (Figure 4.4 f-ii) and again this is a novel epitope.

4.2.4.2.2 NA-specific $CD8^+$ T cell minimal epitope

The NA-specific $CD8^+$ T cells (HLA-A*33:03 restricted, Appendix Figure 4.1) responded to two neighbouring 18mer peptides NA 331-348 (VKGFSY**RYGNGVWIGRTK**) and NA 337-354 (**RYGNGVWIGRTK**SHSSRH) (Figure 4.3) indicating that the minimal epitope should be within the shared region

NA 337-348 (**RYGNGVWIGRTK**). I, therefore, predicted NA 337-346 (**RYGNGVWIGR**) as the minimal epitope. This was confirmed by the peptide titration experiments showing reduced T cell activation capacity of the two peptides with a single amino acid truncation at either end of NA 337-346 (Figure 4.4 g-i). C1R-A*33:03 cell line was used to confirm the HLA-restriction of this newly identified minimal epitope $NA_{337-346}$ (Figure 4.4g-ii). Moreover, this is a novel sequence as it is not published previously by searching from IEDB website.

4.2.4.3 Identifying the core sequences of the epitopes presented by HLA-A*24:02

4.2.4.3.1 PB1-specific $CD8^+$ T cell minimal epitope

HLA-A*24:02 peptide-binding motifs prefer a Tyrosine (Y) at P2 and a phenylalanine (F) or Leucine (L) at the C-terminus (Kubo et al., 1994). According to PB1 18mer mapping result (Figure 4.3), PB1 specific $CD8^+$ T cells responded to PB1 493-510 (TSFFY**RYGFVANFSMELP**) only and the response was restricted by HLA-A*24:02 (Appendix Figure 4.1). Therefore, the minimal epitope was considered to be within PB1 498-510 (**RYGFVANFSMELP**). As HLA-A*24:02 C-terminus anchor can be either Leucine (L) or Phenylalanine (F), it was then possible that either PB1 498-505 (**RYGFVANF**) or PB1 498-509 (**RYGFVANFSMEL**) could be the minimal epitope. As PB1 498-505 has been published (J. Liu et al., 2012), I then test PB1 498-509 and the single amino acid truncated at either side PB1 499-509, PB1 498-508. To avoid unexpected peptide trimming by serum protease (Falo et al., 1992), peptide titrations were conducted in the presence and absence of FCS. As shown in Figure 4.4 h-i (in the presence of FCS), PB1 498-508 and 498-509 can be titrated to 10^{-9} M, the stimulation capacity was same with the previously published PB1 498-505 (Figure 4.4 h-i, shown in red). However, in the absence of FCS (Figure 4.4 i-i), PB1 498-505 is more potent than PB1 498-508 and PB1 498-509 in the titration experiment. Therefore, I conclude that the minimal epitope is the published $PB1_{498-505}$. The HLA restriction was also confirmed as HLA-A*24:02 (Figure 4.4 h-ii).

4.2.4.3.2 PA-specific $CD8^+$ T cell minimal epitope

The PA-specific $CD8^+$ T cells recognised two neighbouring overlapping 18mer peptides PA 121-138 (GVTRRE**VHIYYLEKANKI**) and PA 127-144 (**VHIYYLEKANKI**KSEKTH) to the same degree (Figure 4.3), indicating that the minimal epitope is located in the shared sequence PA 127-138 (**VHIYYLEKANKI)**. The response from 18mer peptide was confirmed as HLA-A*24:02 (Appendix Figure 4.1). Following the HLA-A*24:02 motifs, I predicted $PA_{130\text{-}138}$ (**YYLEKANKI**) as the minimal epitope and the response was further confirmed by IAV-specific $CD8^+$ T cells (data not shown), however, this epitope was previously identified (Alexander et al., 2010).

Table 4.1. HLA information of APCs

APCs	HLA-A	HLA-B	HLA-Cw
auto-BLCL	**24:02, 33:03**	**44:03, 46:01**	**01:02, 07:01**
9002	**24:02**	14:02	02:02, 08:02
C1R-B*44:03		**44:03**	
C1R-A*33:03	**33:03**		
9004	02:01	27:05	**01:02**
9022	01:01	08:01	**07:01**

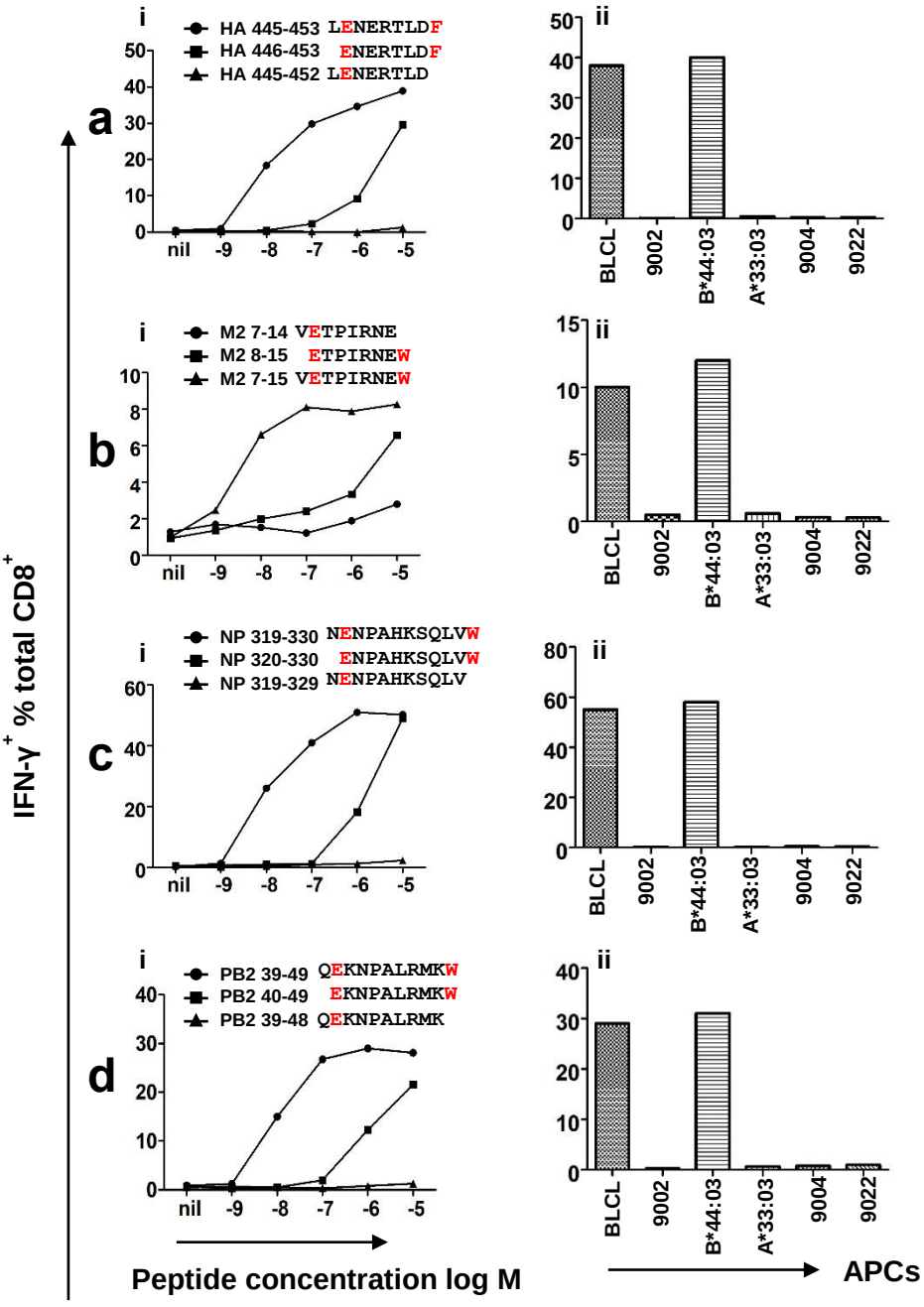
a
i
HA 445-453 LENERTLDF
HA 446-453 ENERTLDF
HA 445-452 LENERTLD
nil -9 -8 -7 -6 -5
ii
BLCL 9002 B*44:03 A*33:03 9004 9022
b
i
M2 7-14 VETPIRNE
M2 8-15 ETPIRNEW
M2 7-15 VETPIRNEW
nil -9 -8 -7 -6 -5
ii
BLCL 9002 B*44:03 A*33:03 9004 9022
c
i
NP 319-330 NENPAHKSQLVW
NP 320-330 ENPAHKSQLVW
NP 319-329 NENPAHKSQLV
nil -9 -8 -7 -6 -5
ii
BLCL 9002 B*44:03 A*33:03 9004 9022
d
i
PB2 39-49 QEKNPALRMKW
PB2 40-49 EKNPALRMKW
PB2 39-48 QEKNPALRMK
nil -9 -8 -7 -6 -5
ii
BLCL 9002 B*44:03 A*33:03 9004 9022
IFN-γ+ % total CD8+
Peptide concentration log M
APCs

Figure 4.4 (continued)

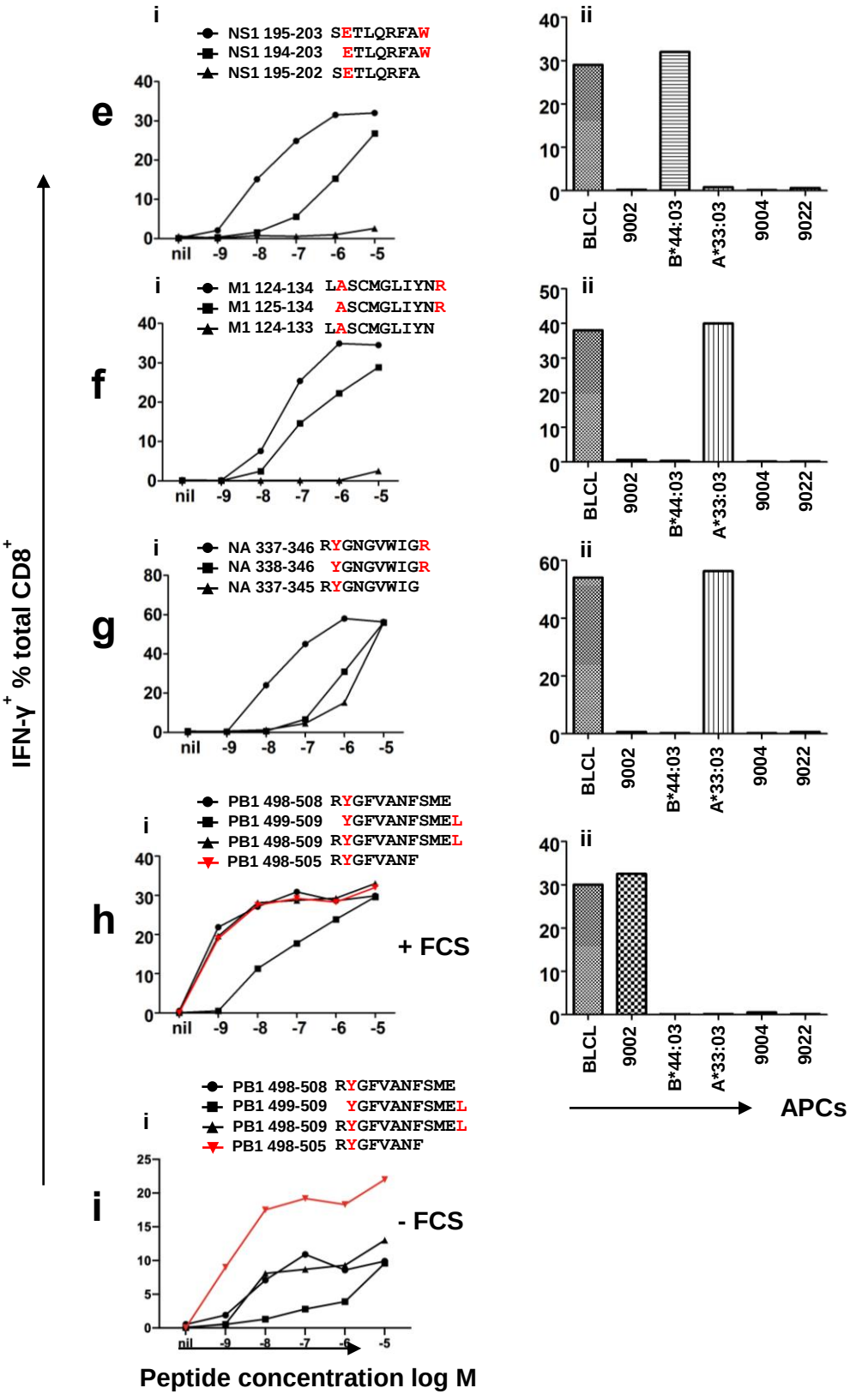

Figure 4.4. Minimal epitopes of differing lengths are presented by HLA-B*44:03, HLA-A*33:03 and HLA-A*24:02

Peptide-specific $CD8^+$ T cells were established as described in the legend to Figure 4.1b; **(a-i)**, various $CD8^+$ T cell specificities were assessed via standard ICS for the production of IFN-γ with different peptides and APCs. (i), peptide titrations of all the minimal peptides and their truncation peptides (ii) HLA restrictions of each minimal epitope are shown. **(h)**, peptide titration of PB1 minimal peptides in the presence of FCS (+ FCS); **(i)**, peptide titration of PB1 minimal peptides in the absence of FCS (- FCS).

4.2.5 Epitope conservancy among all the IAV strains circulated in Australia during 1994-2019 period

To analyse the conservancy of all the novel immunogenic epitopes discovered in this study, IAV protein sequences were aligned, and amino acid differences were scored for the IAV strains circulated in Australia during the 25 years between 1994-2019. As the PBMC sample used in this study was collected in 2009, it is better to have the conservation analysis cover the IAV strains circulated in Australia in a quarter-century. The information of circulated IAV strains (Table 4.3) was obtained from National Center for Biotechnology Information (NCBI) influenza virus resource database accessed on July 28, 2019. According to my analysis, three out of the seven novel IAV epitopes are 100% conserved in these viruses, including $NP_{319-330}$, $M1_{124-134}$ and $M2_{7-15}$ in both H1N1 and H3N2. For $NA_{337-346}$ and $PB2_{39-49}$ $CD8^+$ T cell epitopes, although amino acid differences are found, the HLA anchor residues of these three epitopes are still conserved (Table 4.2). Based on the above analysis, it is highly likely that most IAV-specific $CD8^+$ T cells studied here would be able to fully or partially recognise cells infected by these different IAV strains including the 2009 H1N1 pandemic strain. Taken together, my results revealed multiple novel $CD8^+$ T cell epitopes restricted to the individual's HLA-A and B molecules with 100% conserved epitope sequences.

Table 4.2. Conservancy of the novel epitope sequences among all the IAV strains circulated in Australia during 1994-2019

Peptide	Peptide sequence	Frequency (%) of peptide variants	
		H1N1	H3N2
NP$_{319-330}$	N**E**NPAHKSQLV**W**[a]	100.0	100.0
M1$_{124-134}$	L**A**SCMGLIYN**R**	100.0	100.0
M2$_{7-15}$	V**E**TPIRNE**W**	100.0	100.0
NA$_{337-346}$	R**Y**GNGVWIG**R**	87.5	0.0
	..*D*[b].....	12.5	100.0
PB2$_{39-49}$	Q**E**KNPALRMK**W**	0.0	0.0
	.....*S*.....	100.0	100.0
HA$_{445-453}$	L**E**NERTLD**F**	100.0	0.0
	...*QH*.*I*.*L*	0.0	100.0
NS1$_{195-203}$	S**E**TLQRFA**W**	75.0	0.0
	.*K*.....*S*.	12.5	0.0
	..*I*.....	12.5	0.0
	.*KN*.....	0.0	100.0

Note: Australian circulated H1N1 and H3N2 IAV strain full-length sequences for the studied proteins were downloaded from the NCBI influenza resource database (https://www.ncbi.nlm.nih.gov/genomes/FLU/Database/nph-select.cgi?go=database). Specific searching criteria for downloading were Country/region (Australia), Protein (NP/M1/M2/NA/PB2/HA/NS1), Subtype (H1N1/H3N2), Sequence Length (Full-length only), Collection data (from 1994 to 2019), identical sequences were represented by the oldest sequence in the group. [a] HLA anchor residues are shown in bold; [b] Variations from the PR8 strain sequences are shown in italics.

Table 4.3. All the IAV strains used for conservation analysis

H1N1	H3N2		
A/Cairns North/INS597/2010	A/Australia/18/2009	A/Perth/1055/2014	A/Sydney/852M/2002
A/Sydney/DD3-02/2009	A/Australia/NHRC0001/2003	A/Perth/113/2015	A/Sydney/329Q/2003
A/Victoria/2005/2009	A/Australia/NHRC0001/2005	A/Perth/153/2012	A/Sydney/419J/2004
A/Brisbane/59/2007	A/Brisbane/9/2006	A/Perth/16/2009	A/Sydney/348N/2006
A/New South Wales/18/1999(H1N1)	A/Brisbane/1/2012	A/Perth/164/2013	A/Sydney/257U/2009
A/South Australia/45/2000	A/Brisbane/1/2013	A/Perth/22/2016	A/Sydney/DD2-01/2010
A/Western Australia/18/2001	A/Brisbane/1/2017	A/Queensland/1/2000	A/Tasmania/60/2012
A/Brisbane/193/2004	A/Brisbane/10/2007	A/Queensland/11/2001	A/Tasmania/11/2014
A/South Australia/55/2005	A/Brisbane/100/2014	A/Queensland/21/2002	A/Tasmania/1005/2015
A/Western Australia/77/2005	A/Brisbane/1000/2015	A/Queensland/31/2003	A/Tasmania/1001/2016
A/Victoria/500/2006	A/Brisbane/1004/2016	A/Queensland/41/2004	A/Townsville/1004/2012
A/Brisbane/297/2006	A/Brisbane/11/2010	A/Queensland/51/2005	A/Townsville/10/2015
A/Perth/1/2007	A/Canberra/1001/2012	A/South Australia/1/2012	A/Townsville/1003/2016
A/Victoria/501/2007	A/Canberra/1001/2016	A/South Australia/1/2015	A/Victoria/75/1995
A/South Australia/423/2007	A/Canberra/113/2013	A/South Australia/1002/2014	A/Victoria/210/2009
A/Sydney/581/2007	A/Canberra/12/2015	A/South Australia/1007/2016	A/Victoria/361/2011
A/South Australia/2001/2009	A/Canberra/2/2014	A/South Australia/15/1994	A/Victoria/1002/2012
A/Brisbane/17/2009	A/Darwin/1000/2015	A/South Australia/15/2000	A/Victoria/504/2013
A/Australia/1/2009	A/Darwin/1001/2012	A/South Australia/18/2005	A/Victoria/1012/2014
A/swine/VIC/09-02767-01/2009	A/Darwin/1002/2016	A/South Australia/2/2013	A/Victoria/1000/2015
A/swine/QLD/09-02865-07/2009	A/Darwin/4/2005	A/Sydney/223G/2005	A/Victoria/109/2016
A/Sydney/DD3-37/2010	A/New South Wales/13/1999	A/Sydney/0017/2007	A/Western Australia/1/2000
A/North Fitzroy/INS463/2010	A/New South Wales/27/2000	A/Sydney/1001/2012	A/Western Australia/13/2001
A/Melbourne/INS467/2010	A/Newcastle/1/2013	A/Sydney/1014/2013	A/Western Australia/23/2002
A/Westmead/INS524/2010	A/Newcastle/1000/2016	A/Sydney/1004/2014	A/Western Australia/37/2003
A/Sydney/DD3-58/2011	A/Newcastle/1001/2015	A/Sydney/10/2015	A/Western Australia/51/2004
A/Westmead/INS3_659/2011	A/Newcastle/1016/2014	A/Sydney/101/2016	A/Western Australia/65/2005
A/Darlinghurst/INS3_645/2011	A/PERTH/1/2003	A/Sydney/5/1997	
A/Melbourne/INS3_670/2011	A/Perth/10/2010	A/Sydney/405A/2001	

Note: This table including all the IAV strains circulated in Australia during 1994-2019 period.

4.2.6 Quantitatively assess HLA-I peptide presentation to the antigen-specific CD8$^+$ T cells

It has been demonstrated that the speed of antigen processing and presentation influences the hierarchy of CD8$^+$ T cell response during virus infections (Akram et al., 2012; W. Chen et al., 2000; W. Chen et al., 2004; Tenzer et al., 2009). To further understand the basis of the broad-based IAV-specific CD8$^+$ T cell response observed in this study, I investigated the antigen presentation kinetics of the above T cell epitopes using a BFA kinetics assay as slow antigen presentation could potentially explain the observed overall small and lack of immunodominant responses in this individual. BFA blocks pMHC-I egressing of ER (Yewdell et al., 1989) therefore “freezes” pMHC-I complexes on the virus infected APC at the time of addition and allows the assessment of pMHC-I antigen presentation level at any time point after infection (Pang et al., 2006). This method also allows the comparison of different T cell populations engaging the same APC which presents various CD8$^+$ T cell epitopes simultaneously. Additionally, I included a most studied immunodominant epitope M1$_{58\text{-}66}$ as the “golden standard” to compare the antigen presentation kinetics of the novel epitopes investigated in this study.

The presentation kinetics results are separately shown by epitopes’ HLA restriction. For example, as shown in Figure 4.5, Figure 4.5a shows data for HLA-B*44:03 restricted epitopes. In this Figure, both M1$_{124\text{-}134}$ and NP$_{319\text{-}330}$ presentations were detected at 0.5 hour after infection, at that time presentation of M1$_{58\text{-}66}$ was barely detectable; M1$_{124\text{-}134}$ presentation rapidly reached a level that activated 50% of its antigen-specific T cells around 2 hours after rVV-M1 infection (Figure 4.5c); while M1$_{58\text{-}66}$ reached the same level 2 hours later and NP$_{319\text{-}330}$ reached the same level with a further 2 hour delay (Figure 4.5a). M2$_{7\text{-}15}$, NS1$_{195\text{-}203}$, PB2$_{39\text{-}49}$ and HA$_{445\text{-}453}$ showed similar slower presentation kinetics with detectable presentation at 2 hour and 50% presentation at around 6 hour after infection (Figure 4.5a).

Figure 4.5b shows data for HLA-A*24:02 restricted epitopes. It illustrates that PA$_{130\text{-}138}$ and PB1$_{498\text{-}505}$ presentations were detected at 2 hours and reached 50% saturating presentation at 4 hours. Figure 4.5c shows data for HLA-A*33:03

restricted epitopes. This figure displays that $NA_{337-346}$ presentation became detectable at 1 hour after infection and reached 50% saturating presentation at 4 hours. Taken together, these results indicate that antigen presentation did not seem to correlate the magnitude of $CD8^+$ T cell response to each epitope, albeit these responses were all assessed after *in vitro* T cell expansion by PR8-infected APCs after 16 hours infection.

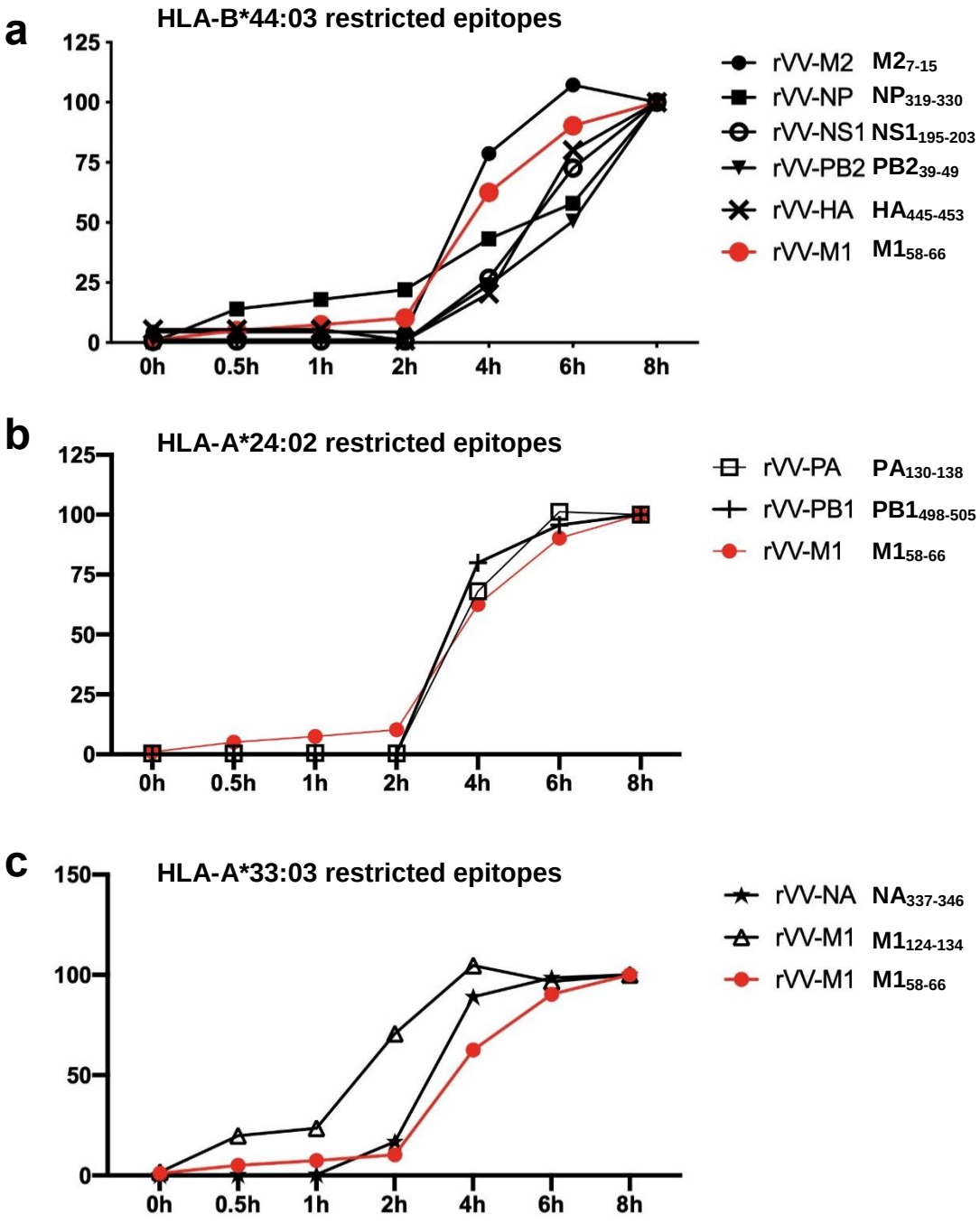
a
HLA-B*44:03 restricted epitopes
125
100
75
50
25
0
0h
0.5h
1h
2h
4h
6h
8h
rVV-M2 M2 7-15
rVV-NP NP 319-330
rVV-NS1 NS1 195-203
rVV-PB2 PB2 39-49
rVV-HA HA 445-453
rVV-M1 M1 58-66
b
HLA-A*24:02 restricted epitopes
125
100
75
50
25
0
0h
0.5h
1h
2h
4h
6h
8h
rVV-PA PA 130-138
rVV-PB1 PB1 498-505
rVV-M1 M1 58-66
c
HLA-A*33:03 restricted epitopes
150
100
50
0
0h
0.5h
1h
2h
4h
6h
8h
rVV-NA NA 337-346
rVV-M1 M1 124-134
rVV-M1 M1 58-66

Figure 4.5. Most novel CD8$^+$ T cell epitopes are presented with a fast kinetics
CD8$^+$ T cells were activated by rVVs infected BLCLs at various time points (0h, 0.5h, 2h, 4h, 6h, 8h) after the first-hour infection, then T cells and BFA were added to “freeze” and read out antigen presentation at that time point after rVVs infection. The antigen presentation, reflected by the amount of epitope-specific T cell activation was assessed for IFN-γ production by ICS as described in the method. **(a)**, HLA-B*44:03 restricted epitope presentation is compared to that of a well-studied immunodominant epitope $M1_{58-66}$ (shown in red). (**b)**, HLA-A*24:02 restricted epitope presentation is compared to that of a well-studied immunodominant epitope $M1_{58-66}$ (shown in red). (**c)**, HLA-A*33:03 restricted epitope presentation is compared to that of a well-studied immunodominant epitope $M1_{58-66}$ (shown in red). This experiment was performed and analysed together. For clarity, the results are displayed as three figure panels according to the HLA restriction of each epitope. Data shown are representative of two independent experiments.

4.3 Conclusion, Discussion and Future directions:

In this study, I report a broad-based $CD8^+$ T cell response, rather than one with a typical immunodominance hierarchy, in an IAV-experienced healthy individual. By using a systematic approach, I demonstrated that such $CD8^+$ T cell responses to nine IAV proteins (M1, M2, NP, NS1, PA, PB1, PB2, HA and NA) except for NS2 and PB1-F2 (Figure 4.2). I further identified the minimal epitope sequences of these responses (Figure 4.4). They are restricted to HLA-B*44:03, HLA-A*24:02 and HLA-A*33:03 and seven out of nine epitopes are novel ones ($NP_{319-330}$, $M1_{124-134}$, $M2_{7-15}$, $NA_{337-346}$, $PB2_{39-49}$, $HA_{445-453}$ and $NS1_{195-203}$). Most of these novel epitopes are highly conserved among strains of H1N1 and H3N2 once circulated in Australia. Similar to our previous observation on broad-based $CD4^+$ T cell responses to IAV, I conclude that such a phenomenon not only occur to $CD4^+$ T cell response but also $CD8^+$ T cell response.

Several HLA molecules such as HLA-A*02:01, HLA-A*03:01, HLA-B*57:01, HLA-B*18:01 and HLA-B*08:01 present IAV peptides to stimulate robust $CD8^+$ T cell responses against IAV infection, whereas HLA-A*24:02, HLA-A*01:01, HLA-A*68:01, HLA-B*15:01 often stimulate more limited $CD8^+$ T cell responses specific to IAV (Quinones-Parra et al., 2014). In addition, HLA-A*24:02 was reported to be associated with severe pH1N1 disease and it is an allele that highly expressed in Indigenous Australians and Alaskans (Clemens et al., 2016; Hertz et al., 2013). Hence, the lack of immunodominant epitope presentation by this HLA, especially in the absence of other HLAs that present immunodominant epitopes, such as HLA-A*02:01, HLA-B*08:01, HLA-B*15:01, HLA-B*35:03 (Burrows et al., 1992; Gotch et al., 1987; E. Grant et al., 2013; Wu et al., 2011), may indicate that HLA-A*24:02 does not present an immunodominant IAV epitope and therefore plays a limited role during an anti-IAV cellular immune response. Additionally, Quinones-Parra *et al*. (Quinones-Parra et al., 2014) investigated pre-existing memory pools specific for conserved H7N9 epitopes and found eight conserved NP epitopes included an HLA-A*24:02-restricted epitope NP_{39-47} (A*24:02-NP_{39}). They then showed that $CD8^+$ T cell responses to six of the eight conserved epitopes, however, no $CD8^+$ T cell specific for A*24:02-NP_{39} was detected ex vivo, suggesting that

although NP_{39-47} is a conserved epitope, it is a weak one that do not elicit significant $CD8^+$ T cell response. Such $CD8^+$ T cell responses are believed less protective. My results might at least partially explain why Indigenous Australians were more susceptible to severe IAV infection and had higher mortality rate than other Australian populations during the 2009 H1N1 pandemics (Kelly et al., 2009; Trauer et al., 2011). To date, researchers have mainly focused on assessing immunogenic epitopes for common HLA molecules, such as HLA-A*02:01, with much less attention paid to the HLA molecules associated with Indigenous Australians.

Immunodominance has been studied for decades. In many cases, removing the most dominant T cell epitope enables the T cells specific to the subdominant epitopes to expand more completely (Kim et al., 2011; Thomas et al., 2007). Although the exact mechanisms associated with this phenomenon remain poorly understood, several factors have been shown to influence it, such as peptide-binding ability, T cell competition for particular pMHC-I on the APC surface, dominant T cells actively suppress other T cell development, and other factors (Kim et al., 2011). For example, Kedl *et al.* generated $CD8^+$ T cells to dominant epitope SIINFEKL (ova8) and subdominant epitope KRVVFDKL from Ovalbumin in $H\text{-}2^b$ mice; when high-affinity TCR transgenic T cells (OT1 T cells) for ova8 were transferred, they completely inhibited the response of host OVA-specific T cell response to either epitope due to APC level competition (Kedl et al., 2000). However, in our case, no functional immunodominant $CD8^+$ T cell responses were discovered, indicating that other mechanisms rather than APC level competition are more likely.

Early evidence demonstrated that T cell precursor frequency and the efficiency of peptide generation could influence immunodominance hierarchy (Wallace et al., 2000). For example, Day *et al.* found that co-expression of $H2K^k$ and $H2D^b$ greatly diminished $CD8^+$ T cell response to the $H2D^b$-restricted immunodominant epitope $PA_{224-233}$, as part of the T cell repertoire was deleted by having $H2K^k$, while T cell responses to $H2D^b$ restricted $NP_{366-374}$ remained unaltered (Day et al., 2011). However, a more recently study from Neller *et al.* demonstrated that T cell precursor frequency might not correlate closely with immunodominance hierarchy

after pathogen challenge (Neller et al., 2015). It is possible that none of the epitopes I identified in this study could stimulate an immunodominant response.

However, MHC restriction should be the most significant determining factor although often under-considered and sometimes not considered, especially in syngeneic murine systems when MHC are pre-fixed. In human, as HLA is so polymorphic, the overall immunodominance hierarchy is shaped up by the $CD8^+$ T cell responses restricted to all the involved HLA alleles expressed by the individual.

For example, HLA-A*02:01-$M1_{58-66}$ complexes stimulate an immunodominant $CD8^+$ T cell response in many HLA-A*02:01 donors, but not in those who also express HLA-A*01:01, HLA-B*08:01, HLA-B*15:01, HLA-B*18:01, HLA-B*35:03 (Wu et al., 2011). Additionally, some epitopes can be restricted to different HLA alleles. For example, $M1_{125-134}$ has been reported as an HLA-A*33:01 epitope (Alexander et al., 2010), however, in this study, I showed that this same epitope can be restricted to HLA-A*33:03. Therefore, it is envisaged, if one individual expressed both HLA-A*33:03 and HLA-A*33:01, the response to $M1_{125-134}$ might be boosted into an immunodominant status.

HLA combinations have been shown to be one of the most important elements contributing to $CD8^+$ T cell immunodominance hierarchy (Akram et al., 2012). Akram *et al.* demonstrated during IAV infection in HLA transgenic mice, only certain combinations of HLA allele co-expression enabled immunodominant $CD8^+$ T cell responses. For instance, the IAV immunodominant $CD8^+$ T cell response could only be detected in IAV-infected HLA-B*7/HLA-B*27 transgenic mice but not in HLA-A*2/ HLA-B*7 or HLA-A*2/HLA-B*27 mice (Akram et al., 2013). Moreover, Boon *et al.* reported that HLA alleles were not used equally and there was a hierarchy existed between HLA alleles; such as HLA-B*27:05 and HLA-B*35:01 were preferentially used in IAV-specific $CD8^+$ T cell response, and HLA-B*08:01 and HLA-A*01:01 seemed to contribute less (Boon et al., 2004). According to the above results, co-expression of certain allele may determine not only which HLA may present immunodominant $CD8^+$ T cell response but also whether there is immunodominant $CD8^+$ T cell response at all. In HIV studies, epitopes restricted by HLA-B molecules were dramatically more frequently recognised than those

presented by HLA-A or HLA-C molecules (Bihl et al., 2006). In our case, the study subject expresses HLA-A*24:02, HLA-A*33:03, HLA-B*44:03, HLA-B*46:01, HLA-Cw*01:02, HLA-Cw*07:01. It seems to be the case that such set of HLA wasn't able to support an immunodominant $CD8^+$ T cell response during IAV infection.

It is also worth taking infection exposure and vaccination history into consideration, as a specific viral strain might affect the outcome of $CD8^+$ T cell response, even the previous immunodominance hierarchy. Although little is known about the precise IAV exposure history of this donor, I have compared the conservancy of novel epitopes among all the IAV strains circulated in Australia in the past 25 years and found three out of the seven identified novel epitopes are almost 100% conserved among these strains (Table 4.2). These results suggest that my assessment is valid even though only one IAV strain (PR8) was used for conducting the experiments in this study.

Chronic virus infections, such as HCMV are characterised by the accumulation of antigen-specific $CD8^+$ T cells specific for immunodominant epitopes (Karrer et al., 2003). However, IAV usually causes acute infection, which might not allow $CD8^+$ T cells with a particular specificity to accumulate significantly. Therefore, if one does not possess a set of HLAs that is able to elicit a robust IAV-specific $CD8^+$ T cell response, such individual may have a higher risk for developing severe IAV-related diseases. My present results provide better understanding of IAV-specific $CD8^+$ T cell responses in humans, especially in high risk groups with HLAs that do not present major $CD8^+$ T cell epitopes.

In this chapter, the novel peptides discovered are presented by HLA-B*44:03, HLA-A*33:03. According to IEDB, there is no HLA-B*44:03 restricted IAV immunodominant $CD8^+$ T cell epitopes published previously; moreover, no HLA-A*33:03 restricted IAV epitope have been identified so far. It is possible that the set of HLA alleles this individual expresses failed to present any immunodominant epitope, resulting a broad-based, relatively low-magnitude $CD8^+$ T cell response during IAV infection. Although I have only studied one case on the broad-based $CD8^+$ T cell responses without the typical immunodominance hierarchy, I believe this phenomenon might be wider spread than previously expected as the published

studies only focused on a relatively small numbers of HLA alleles. It is possible that many other HLA alleles, just like the alleles HLA-A*33:03 and HLA-B*44:03 investigated in this study, might not present IAV epitopes that are capable of stimulating immunodominant response likely because their peptide motifs are also too stringent. It would be interesting and worthwhile to carry out a large-scale screen to identify the HLAs associated with such a response in future. Such knowledge may allow us to predict high-risk individuals during IAV infection.

Chapter 5: CD8$^+$ T cell response to alternative reading frame peptides

5.1 Introduction

Viral specific $CD8^+$ T cells recognise virus-derived pMHC-I complexes on antigen presenting cells. The MHC-I antigen processing and presentation pathway uses nearly all endogenous polypeptides as a source to produce antigenic peptides. MHC-I molecules not only select peptides from protein that are regulary turned over (Admon et al., 2003; Yewdell et al., 1988) but also from defective ribosomal products (DRiPs) (Anton et al., 2014; Princiotta et al., 2003; Schubert et al., 2000; Yewdell et al., 1996). During immunosurveillance, $CD8^+$ T cells recognise DRiPs arising from open reading frames (ORFs) (Anton et al., 2014), alternative reading frames (ARFs) (Chen et al., 2001), ribosomal frameshifting (Bullock et al., 1996), alternative initiation on bona fide mRNAs (Yewdell, 2007), and all other errors made as a result of abnormal transcription, translation, posttranslational protein folding and maturation (Anton et al., 2014).

$CD8^+$ T cell epitopes derived from ARF translation are an essential class of DRiPs. It has been reported in research conducted on viruses, cancers and autoimmune diseases (Bullock et al., 1996; Ho et al., 2006; Saulquin et al., 2002; Wang et al., 1996), that $CD8^+$ T cells survey more comprehensive peptide repertoire than originally thought. For example, Maness and colleagues reported that SIV-infected Mamu-B*17 macaques made strong $CD8^+$ T cell responses against an ARF peptide cRW9 (RHLAFKCLW) (Maness et al., 2007). Moreover, the cRW9-specific $CD8^+$ T cell response successfully inhibited SIV replication, indicating that ARF peptide-specific $CD8^+$ T cells could play a part in controlling viral replication (Maness et al., 2007). Recently, Zanker *et al*. described an ARF-encoded immunodominant epitope NS1-$ARF2_{1\text{-}8}$ restricted by H2-Ld from IAV, which is a bona fide DRiP as no biological function can be detected for the NS1-$ARF2_{1\text{-}14}$ precursor (Zanker et al., 2019). Therefore, for generating the most effective $CD8^+$ T cell-based vaccines, it is important to cover the broadest possible range of viral peptides.

Over the past decades, the vast majority of $CD8^+$ T cell recognised peptides are linear peptides, which is true for both viral or tumour antigens (Boon et al., 2002;

Wu et al., 2011), and including those after post-translational modifications (PTMs) (Doyle et al., 2001; Engelhard et al., 2002). For example, protein derived synthetic overlapping peptides or predicted epitopes were often used to identify $CD8^+$ T cell response to viruses such as influenza (Grant et al., 2013; Wu et al., 2011) and tumour-specific T cell responses (Novellino et al., 2005; Stevanovic, 2002). However, this "norm" was challenged when Hanada *et al*. demonstrated the first case in which $CD8^+$ T cells responded to a peptide composed of two fragments originally separated in the parental protein (Hanada et al., 2004). They showed that a $CD8^+$ T cell clone (C2) recognised the fibroblast growth factor 5 (FGF-5) derived 9mer peptide generated by two non-contiguous segments of the parental protein. This 9mer peptide (NTYASPRFK) was formed by NTYAS and PRFK, after excision of 40 amino acid in between (Hanada et al., 2004). Spliced T cell epitopes have been reported for a few pathogens and autoantigens (Mannering et al., 2018; Vigneron et al., 2018), however, no influenza virus-derived spliced peptide has been identified so far. Hence, it would be fascinating to see such observations during influenza virus infection.

Some polypeptides undergo post-translational modifications before they form mature proteins. Post-translational modifications were found in many diseases such as cancer (Bode et al., 2004), infectious (W. Chen et al., 1999) and autoimmune diseases (Mamula et al., 1999). It has been demonstrated that $CD8^+$ T cells specifically recognise some post-translationally modified peptides (Doyle et al., 2001; Engelhard et al., 2002; Petersen et al., 2009). For instance, Chen *et al.* reported that sulfhydryl modification of cysteine (cysteinylation and dimerization) influenced the antigenicity and immunogenicity of two cysteine-containing IAV peptides $NP_{37\text{-}47}$ (FYIQMCTEL) and $NP_{218\text{-}226}$ (AYERMCNIL) (W. Chen et al., 1999). Moreover, Mannering *et al.* reported that a $CD4^+$ T cell clone recognised an HLA-DR4 restricted insulin A-chain 1-13 epitope (KRGIVEQCCTSICSL) which encompasses a vicinal disulphide bond between two adjacent cysteine residues; T cell recognition relied on a vicinal disulphide bond formation between two neighbouring cysteine residues (Mannering et al., 2005). The immunogenic potential of PTMs have been undoubtedly established, thus, future study should pay more attention to the contribution of PTM in antigenic repertoire.

Synthetic peptide has been used for understanding T cell specificity. Solid-Phase Peptide Synthesis (SPPS) was introduced to rapidly synthesise peptides (Merrifield, 1963). A high throughput approach of multiple parallel SPPS in a 96-well format is the synthesis of peptides on amino-functionalized polyethylene (PE) rods, known as pins (Geysen et al., 1984), which has been widely used in large scale of T cell epitope screening (Made et al., 2014; Maeji et al., 1990). However, peptide impurities usually are part of the process, such as salts, missing amino acids (incomplete coupling), uncoupled chemical protecting groups, and other modifications (de Beukelaar et al., 2007). In addition, various side-reactions could also happen during such peptide synthesis leading to peptide impurities (D'Hondt et al., 2014; de Beukelaar et al., 2007; Verbeke et al., 2015), especially in the peptides with lower purity (Verbeke et al., 2015).

In Chapter 4, I described a broad-based $CD8^+$ T cell response in a donor that was targeted to nine IAV proteins without showing a significant immunodominance hierarchy. However, the NP- and NS1-specific $CD8^+$ T cell responses were not fully elucidated using synthetic 18mer overlapping peptides. Although I have identified a novel minimal epitope ($NP_{319-330}$, Chapter 4, Figure 4.4c-i), I hypothesised that another NP-derived epitope was missed because the identified NP peptide response was significantly lower than that stimulated by rVV-NP infected APC (Figure 5.1a). Similarly, only a small response of NS1-specific $CD8^+$ T cells was identified from two neighbouring 18mer peptides (Chapter 4, Figure 4.3). Such small T cell populations were enriched by the novel T cell sorting method (Huang et al., 2019), and the minimal epitopes were then identified(Chapter 4, Figure 4.4e-i). However, the major epitopes targeted by an NS1 response were not identified. Hence, this chapter will be further assessing the missed NP and NS1 responses.

5.2 Results

5.2.1 Assessing the missed CD8$^+$ T cell epitopes from NP and NS1 specific CD8$^+$ T cells

The observed CD8$^+$ T cell responses stimulated by the NP 18mer overlapping peptides, NP 313-330 (9%) and NP 319-336 (13%) were both lower than that stimulated by rVV-NP infected APC (20.5%) (Figure 5.1a). This result indicated that a population of NP-specific CD8$^+$ T cells was missed. The missed NP-specific CD8$^+$ T cell population was further confirmed by testing the different length of NP protein encoded by full length rVV-NP, rVV-1/3-NP (NP 1-168), rVV-2/3-NP (NP 147-315) and rVV-3/3-NP (NP 298-496). As shown in Figure 5.1c, CD8$^+$ T cells responded to rVV-2/3-NP (5.18%), rVV-3/3-NP (6.24%), $NP_{319-330}$ (6.3%), and rVV-2/3 + 3/3-NP (11.3%), indicating that the CD8$^+$ T cell response stimulated by rVV-2/3-NP (NP 147-315) was missed by the 18mer overlapping peptide screen because the only positive NP response identified by that in Chapter 4 (Figure 4.4c-i) was $NP_{319-330}$ which is located in the rVV-3/3-NP fragment (NP 298-496). Additionally, for NS1-specific CD8$^+$ T cells obviously there was only a tiny portion (less than 1%) of NS1-specific CD8$^+$ T cells was identified during the 18mer overlapping peptide screening (Figure 5.1b), indicating that the major CD8$^+$ T cell response was missed.

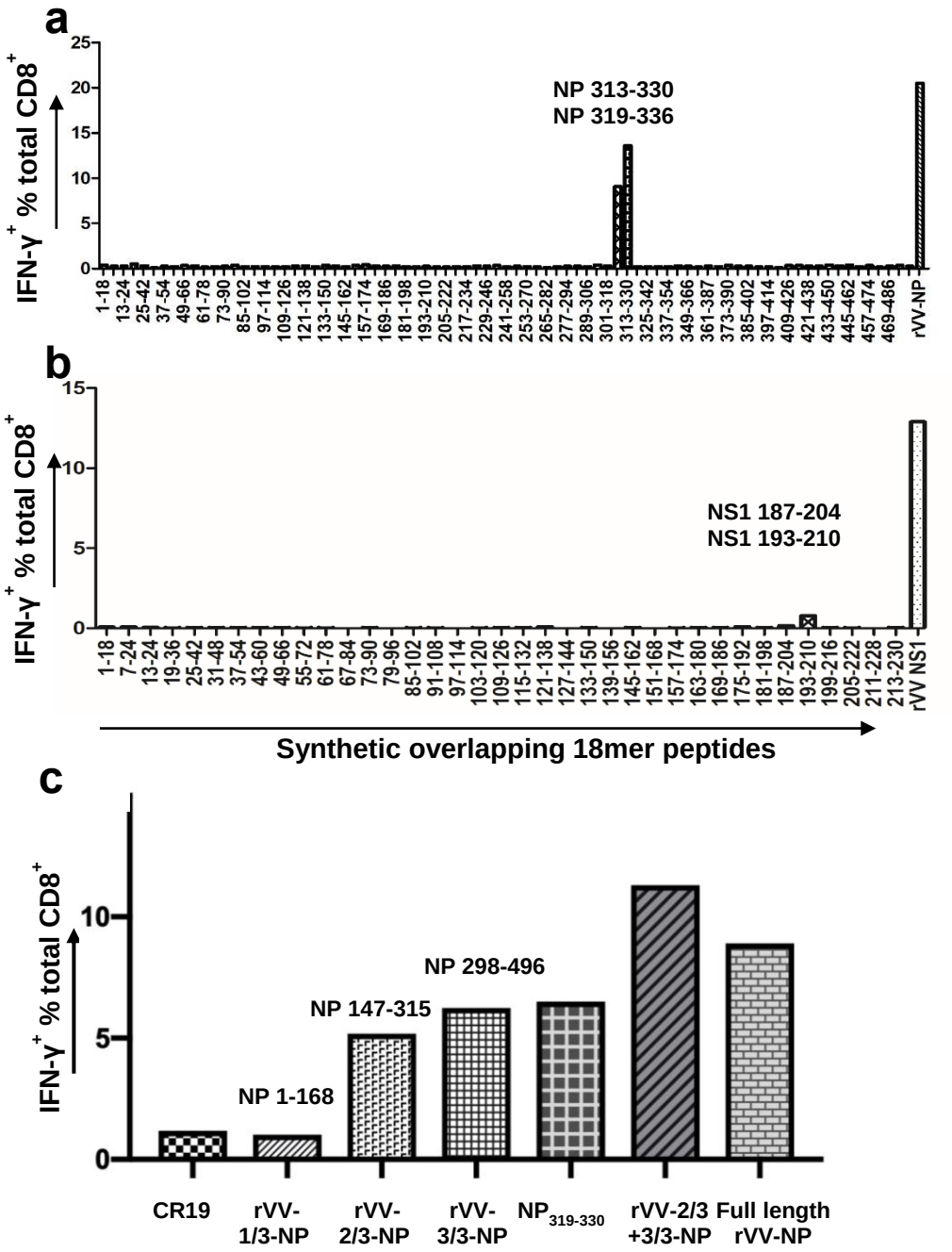

Figure 5.1. Partially missed CD8⁺ T cell epitopes from NP and NS1 specific CD8⁺ T cells

(a-b), CD8⁺ T cell responses to NP and NS1 18mer overlapping peptides; **(c),** CD8⁺ T cell response to $NP_{319-330}$ and the three NP fragments encoded by rVV-1/3-NP [a], rVV-2/3-NP[b] and rVV-3/3-NP[c] represent NP 1-168, NP 147-315 and NP 298-496, respectively and full-length rVV-NP (NP1-496). rVV-2/3 + 3/3 -NP means CD8⁺ T cell response to rVV-2/3-NP infected APCs and rVV-3/3-NP APCs mix with 1:1 ratio.

[a] rVV-1/3-NP means recombinant vaccinia virus (rVV) encoded with NP 1-168;

[b]rVV-2/3-NP means recombinant vaccinia virus (rVV) encoded with NP 147-315;

[c]rVV-3/3-NP means recombinant vaccinia virus (rVV) encoded with NP 298-496;

Note: Figure 5.1a and figure 5.1b are the same data set that were used in the Figure 4.3

5.2.2 NP and NS1 specific $CD8^+$ T cell response to ARF peptides

According to the above analysis, I believed that both NP and NS1 18mer peptide screen missed specific $CD8^+$ T cell responses. It is hard to believe that the 18mer overlapping peptides could miss any linear epitopes. I, therefore, considered the three other possibilities: ARF epitopes, spliced epitopes, and post-translationally modified epitopes. As our laboratory recently reported an ARF-encoded immunodominant epitope NS1-$ARF2_{1-8}$ (Zanker et al., 2019), I then figured that ARF might be the easiest option to test first. All the ARF peptides from NP and NS1 were predicted according to the peptide-binding motifs and predicted ARF sequences with a putative start codon (http://www.syfpeithi.de/index.html) (see Appendix Table 5.1 for more detail). As both NP and NS1 specific $CD8^+$ T cells are restricted by HLA-B*44:03 which has stringent peptide-binding motifs requiring a Glutamate (E) in position two and a Tyrosine (Y), or phenylalanine (F) and less often tryptophan (W) at the C-terminus. Hence, only seven ARF peptides were predicted and synthesised (Table 5.1) and tested by the bulk $CD8^+$ T cell line (the same T cells used in Chapter 4, Figure 4.2) which was restimulated by IAV (PR8) infected C1R-B*44:03. As shown in Figure 5.2, $CD8^+$ T cells responded to five out of the total 7 predicted ARF peptides. Among the five, two peptides are predicted from the reverse ARF, i.e. from 3' to 5' translation.

Table 5.1. Synthetic ARF peptide origins and sequences

ARF peptides	sequence	mRNA area	T cell response
PR8[a] NP[b] ARF-F2[c] p1 [d] (14-24)	Q**E**LLMKECAT**F**	NP 147-315	YES
PR8 NP ARF-F2 p2 (19-29)	K**E**CATFSKGN**F**	NP 147-315	NO
PR8 NP ARF-F2 p3 (17-24)	K**E**KYPCF**Y**	NP 147-315	YES
PR8 NP ARFR-F1[e] p1 (3-12)	K**E**GTIGLAA**F**	NP 1-168	NO
PR8 NP ARFR-F1 p2 (40-51)	A**E**STILSIVKL**F**	NP 314-496	YES
PR8 NP ARFR-F3 p1 (32-41)	D**E**FSHPLSV**Y**	NP 314-496	YES
PR8 NS1 ARF-F3 p1 (8-16)	A**E**SGRPSL**Y**	NS1	YES

Note: [a]IAV strain, [b]IAV protein, [c]ARF-F2: alternative reading frame (5'-3' frame 2), [d]p1: predicted peptide 1, [e]ARFR-F1: alternative reading frame (3'-5' frame 1)

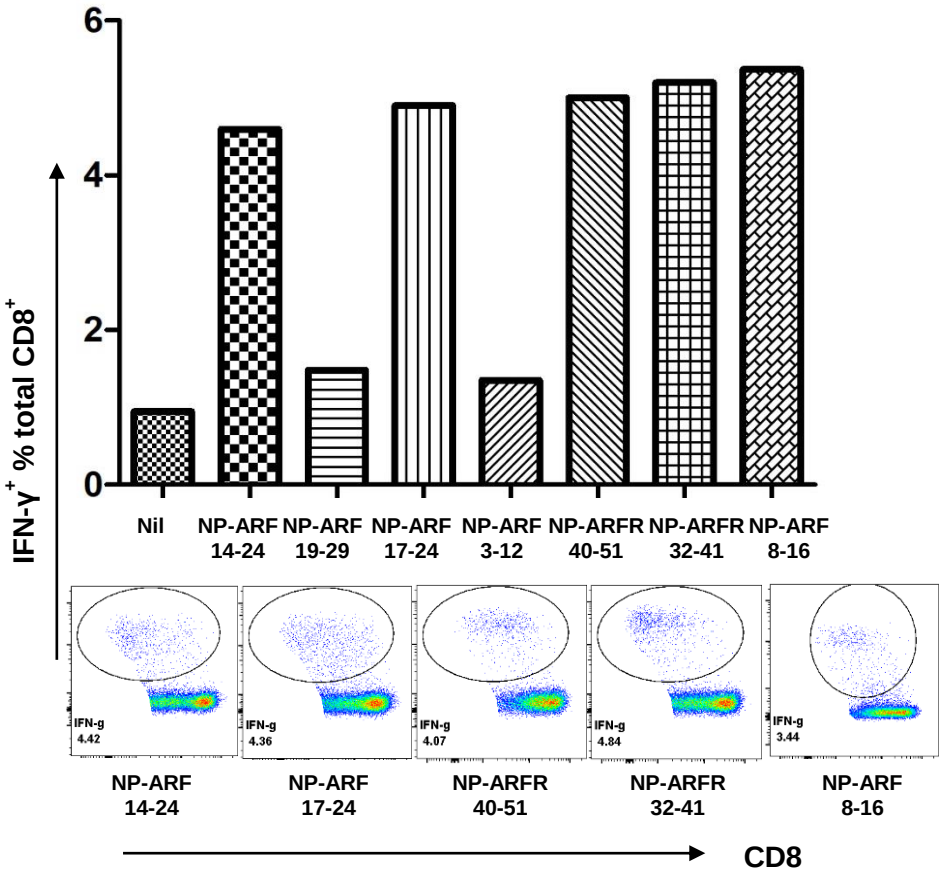

Figure 5.2. CD8+ T cell populations in a bulk CD8+ T cell line responded to five ARF peptides

APCs were pulsed with each of the predicted ARF peptides before being co-cultured with antigen-specific CD8+ T cells. The CD8+ T cell response was assessed by a standard ICS for IFN-γ production.

5.2.3 The impurities of synthetic peptides influence the outcome of CD8$^+$ T cell response

To further confirm and quantitatively assess these CD8$^+$ T cell responses specific to the above ARF peptides, peptide titration experiments were performed using CD8$^+$ T cells specific to the well-studied HLA-A*02:01-restricted IAV epitope M1$_{58-66}$ as a positive control. APCs were pulsed with serially diluted peptides to activate ARF-peptide specific CD8$^+$ T cells. As shown in Figure 5.3a, the responses to these ARF peptides were quite similar and none of the ARF peptides titrated as well as M1$_{58-66}$. Due to similar CD8$^+$ T cell responses in magnitude were observed for all five active ARF peptides and none of them titrated well in a quantitative assessment, I concerned the possibility that these peptides might be cross-contaminated by an unknown peptide. Hence, I permutated and combined the above positive ARF peptides (Appendix Table 5.2) to test whether there was one or multiple CD8$^+$ T cell populations in the culture. Unfortunately, the observed CD8$^+$ T cell responses to individual ARF peptides could not add up using any two different ARF peptides in combination, indicating that there was likely only one antigenic CD8$^+$ T cell population in the culture and the peptides might be contaminated by an active one.

To confirm my prediction and to avoid HPLC-purification caused cross-contamination, I had the above five pin ARF peptides re-synthesised as individual crude peptides and tested side-by-side with the pin ARF peptides using the same CD8$^+$ T cell line. Surprisingly, none of the newly synthesised peptides was recognised by the CD8$^+$ T cells (Figure 5.3c), indicating that CD8$^+$ T cells did not recognise the aforementioned ARF peptide sequences. Gathering these results together, I then considered that all the five ARF peptides might have been contaminated by an unknown peptide, and CD8$^+$ T cells actually recognised a contaminant peptide rather than the ARF peptides. This T cell line was stimulated by PR8 infected APCs and they never encountered any synthetic peptide during its maintenance. As the ARF peptides were ordered and synthesised together with other 87 IAV peptides in the same 96-well format synthesis, I then used this T cell line to screen all the IAV peptides synthesised from the same batch (Appendix

Table 5.3). As shown in Figure 5.3d, this $CD8^+$ T cell line only recognised the five ARF peptides as mentioned above, indicating that these ARF peptides were unlikely to be cross-contaminated by the other IAV peptides during or after the synthesis.

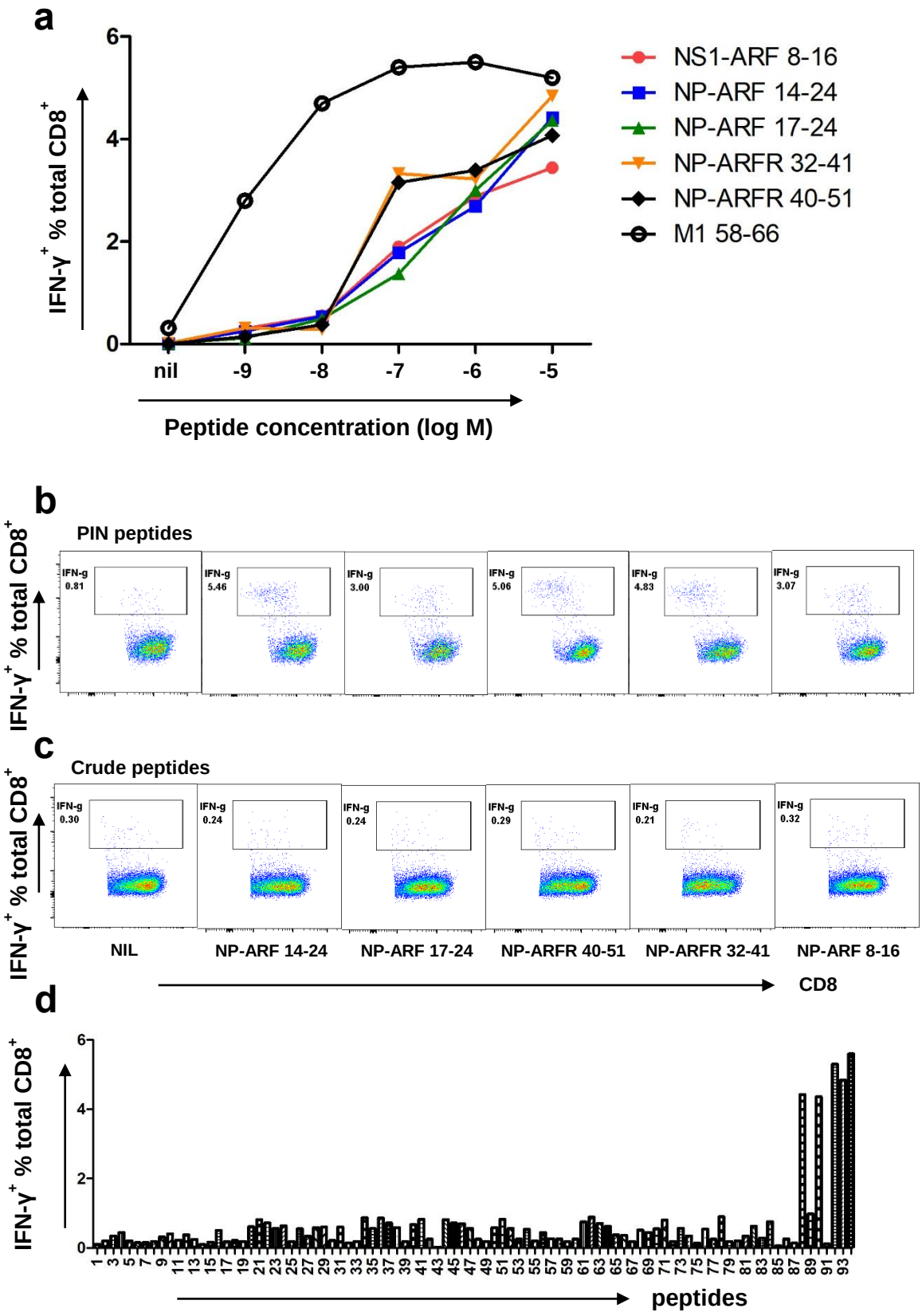
a
IFN-γ+ % total CD8+
6
4
2
0
nil
-9
-8
-7
-6
-5
Peptide concentration (log M)
NS1-ARF 8-16
NP-ARF 14-24
NP-ARF 17-24
NP-ARFR 32-41
NP-ARFR 40-51
M1 58-66
b
PIN peptides
IFN-γ+ % total CD8+
IFN-g 0.81
IFN-g 5.46
IFN-g 3.00
IFN-g 5.06
IFN-g 4.83
IFN-g 3.07
c
Crude peptides
IFN-γ+ % total CD8+
IFN-g 0.30
IFN-g 0.24
IFN-g 0.24
IFN-g 0.29
IFN-g 0.21
IFN-g 0.32
NIL
NP-ARF 14-24
NP-ARF 17-24
NP-ARFR 40-51
NP-ARFR 32-41
NP-ARF 8-16
CD8
d
IFN-γ+ % total CD8+
6
4
2
0
peptides

Figure 5.3. The IAV-specific CD8$^+$ T cells recognise impurity of the five ARF peptides

(a), Standard peptide titrations were performed for the five positive ARF peptides along with M1$_{58\text{-}66}$ and its specific CD8$^+$ T cells serving as a positive control. **(b-c),** CD8$^+$ T cell responses to the two batches of the five ARF peptides: synthetic pin peptides **(b)** and the newly synthesised crude peptides **(c)**. **(d),** CD8$^+$ T cells were used to screen all the pin peptides synthesised together in the same batch with the predicted ARF peptides. CD8$^+$ T cell specificities were assessed by IFN-γ production in a standard ICS assay.

5.2.4 Detection of incomplete ARF peptides by HPLC fractionation coupled with Mass Spectrometry

To know the nature of the active antigenic peptide(s) in the ARF peptides, I decided to fractionate these five ARF peptides using RP-HPLC, and then use the same $CD8^+$ T cell line as a readout tool to identify the active fractions. The prediction was if the ARF peptides were contaminated by the same peptide, the activity in all fraction set should elute at the same time from the HPLC (more detail of HPLC fractionation can be found in Chapter 2, materials and methods section 2.3.5). Surprisingly, no $CD8^+$ T cell response was identified from the NP-ARF17-24 and NP-ARF 8-16 HPLC fractions. ICS analysis of the HPLC fractions of the remaining three ARF peptides (NP-ARFR 32-41, NP-ARFR 40-51, NP-ARF 14-24) revealed that the T cell activating activity was not from the main HPLC peaks. For example, as shown in Figure 5.4, $CD8^+$ T cell response to multiple fractions eluted from 23 min to 25 min from NP-ARFR 40-51, but none of them recognised the fractions derived from the peptide peak (eluted 29.4 min). Similar results were observed for the fractions collected from the other two peptides (NP-ARF 14-24 and NP-ARFR 32-41) (Appendix Figure 5.1). These results indicated that the peptide was likely modified during peptide synthesis and excluded the possibility that the five ARF peptides were contaminated by a single unknown peptide.

To gain more insight into the peptide sequences from the active HPLC fractions, I sampled several fractions (for example in Figure 5.4, fractions eluted at 23.6min, 24.4min, 25.3min and 29.4min from NP-ARFR 40-51) for Mass Spectrometry analysis. According to the Mass Spectrometry analysis, the main peak (29.4 min) revealed the expected peptide sequence AESTILSIVKLF, however, $CD8^+$ T cell failed to recognise this fraction (29.4 min) (Figure 5.4). This result was consistent with Figure 5.3c which revealed that $CD8^+$ T cells were unable to recognise the newly synthesised crude ARF peptide NP-ARFR 40-51 (AESTILSIVKLF). Interestingly, based on the Mass Spectrometry analysis, the positive HPLC fractions (23.6min) identified by the $CD8^+$ T cells suggested a few peptide sequences that were missing amino acid(s) in the intended peptide corresponding to potentially spliced peptides.

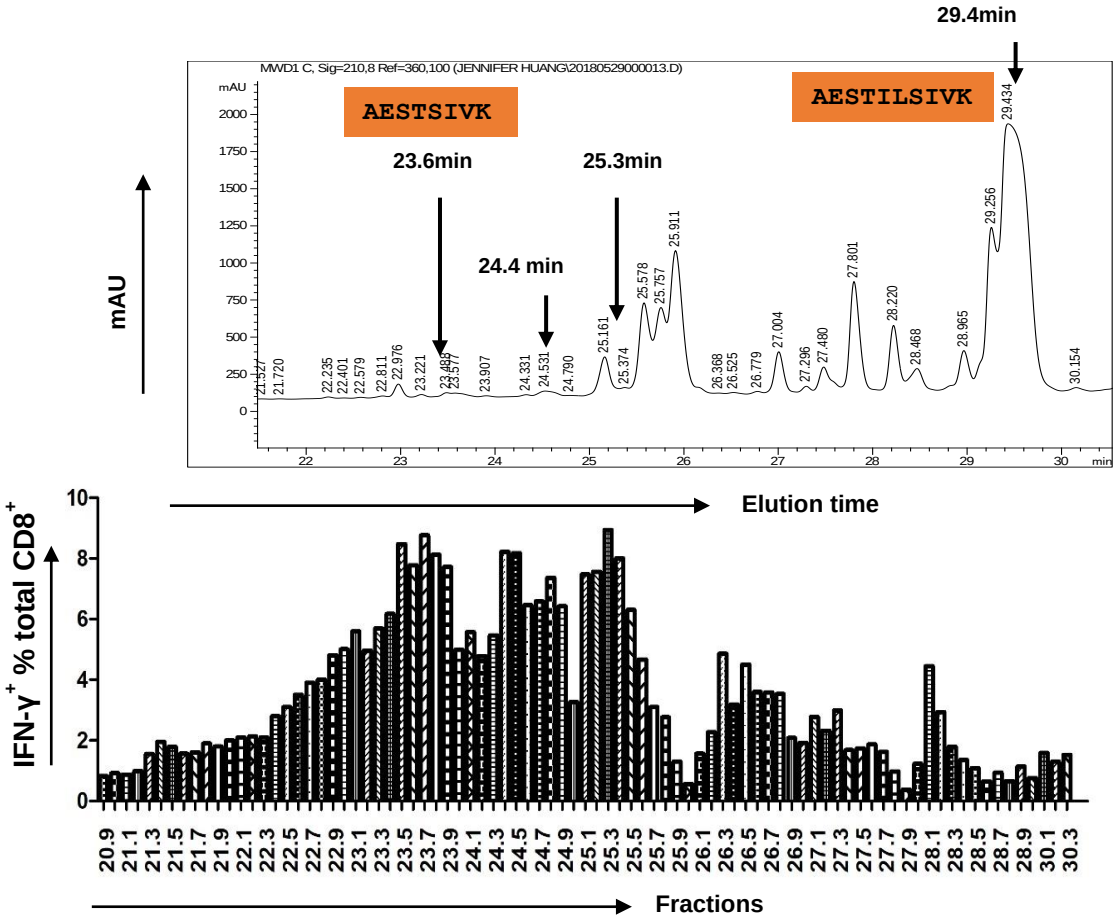

Figure 5.4. Detecting active HPLC fractions from ARF peptide by the IAV-specific CD8$^+$ T cell line

NP-ARFR 40-51 peptide was fractionated on HPLC and the fractions were collected every 0.1min between 10 and 39min, CD8$^+$ T cells were then used to screen all fractions. Four positive representative fractions (23.6min, 24.4min, 25.3min, and 29.4min) were sent to Mass Spectrometry analysis.

5.3 Conclusion, Discussion and Future direction

$CD8^+$ T Cells recognise pMHC-I derived from DRiPs encoded by ORFs or ARFs, or proteins no longer functioning (Anton et al., 2014). Intriguingly, apart from linear peptides (Boon et al., 2002; Wu et al., 2011) and peptides modified by PTMs (Doyle et al., 2001; Engelhard et al., 2002), spliced peptides from tumour antigens and other pathogens are also subject to immunosurveillance by $CD8^+$ T cells (Mannering et al., 2018; Vigneron et al., 2004).

In this chapter, I have further confirmed the observation made in Chapter 4 by showing HLA-B*44:03 restricted NP- and NS1-specific T cell populations initially missed by their 18mer overlapping peptide screen. Furthermore, using rVV-encoded NP fragments, the missed T cell epitope(s) was narrowed down to within NP147-315 (Figure 5.1c). I, therefore, considered ARF peptide encoded by *NP* mRNA, including those within this sequence might be one of the possibilities that stimulate the T cell population missed by the 18mer screen. I then found that $CD8^+$ T cells responded to four predicted NP derived ARF peptides and one NS1 derived ARF peptide (Figure 5.2). However, these T cell responses could not add up when APCs were pulsed by two different ARF peptides. Such results indicated that the antigen-specific $CD8^+$ T cells probably recognise only one predicted ARF peptide rather than five or the occurrence of peptide cross-contamination. Moreover, the peptide titration curves of all five pin ARF peptides were very similar (Figure 5.3a) and the same $CD8^+$ T cells failed to recognise newly synthesised five crude ARF peptides with the same sequences (Figure 5.3c). I have then excluded the possibility of peptide cross-contamination during pin-peptide synthesis (Figure 5.3d). Based on Hanada and colleagues' finding, this result suggested that the $CD8^+$ T cells probably recognised something else, such as truncated or synthesis-modified peptides, rather than the predicted ARF peptide sequence. I then used HPLC fractionation and Mass Spectrometry to analyse active fractions (Figure 5.4). Mass Spectrometry analysis suggested that this particular $CD8^+$ T cell might have recognised "internally truncated" ARF peptides (Figure 5.4), which functionally resemble spliced peptides. I have now had these peptides synthesised and they will be screened once this thesis is submitted.

Several studies reported that impurities in synthetic peptides influence T cell responses (Currier et al., 2008; D'Hondt et al., 2014; de Beukelaar et al., 2007). Beukelaar *et al*. found three peptides recognised by $CD8^+$ T cells, however, the T cell responses could not be confirmed when re-synthesised peptides from the same manufacturer with a higher purity (de Beukelaar et al., 2007). They subsequently compared three synthetic peptide batches and found abundant differences among them, such as omissions of amino acids in the primary peptide sequences (de Beukelaar et al., 2007). Furthermore, Chen and colleagues demonstrated that $CD8^+$ T cells recognised a peptide containing a cyclized asparagine residue which occurred as a side reaction during peptide synthesis rather than the parental peptide containing unmodified asparagine (Chen et al., 1996). In our case, $CD8^+$ T cells responded to five synthetic ARF pin-peptides. However, these responses could not be confirmed when peptide re-synthesised by the same manufacturer with a different chemistry. Base on finding from Beukelaar *et al.* and Chen *et al*. and my Mass Spectrometry analysis (Figure 5.4), there is a high possibility that my $CD8^+$ T cells recognised one of the truncated peptides generated during peptide synthesis rather than the originally predicted ARF peptide sequence.

Hypothetically, peptide splicing could happen in any proteins' proteasome-degraded fragments in a cell. This hypothesis was supported by Liepe *et al*. recent work, as they detected that the proteasome-generated spliced peptide pool could potentially represent about one-third of the diversity of the entire HLA-I ligands and one-fourth of the abundance of total HLA-I peptidomes (Liepe et al., 2016). Therefore, I believe that such spliced epitopes can also be recognised by IAV-specific $CD8^+$ T cells. However, only a handful of spliced peptides have been reported so far and they mainly derived from tumour-associated antigens, this is largely due to the detection of spliced peptides was limited by the laborious isolation of T cell clones from patients' PBMCs (Michaux et al., 2014; Vigneron et al., 2004; Warren et al., 2006). Platteel *et al*. developed a reverse immunology-based multi-level method to detect proteasome-generated spliced epitopes (Platteel et al., 2017). Based on this approach (Figure 5.5), they were able to identify two spliced epitopes using a murine Listeria monocytogenes infection model (Platteel et al., 2017).

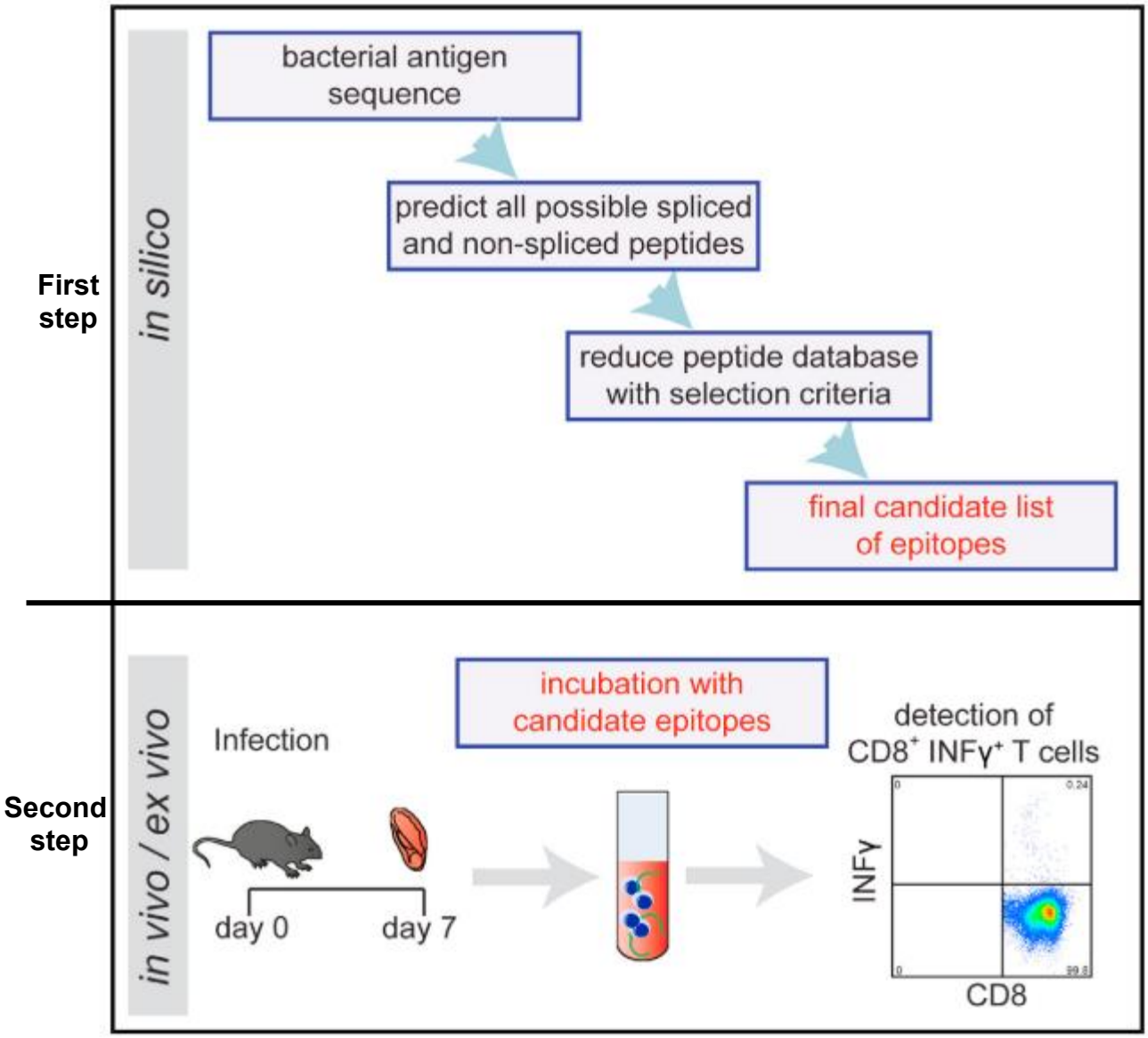

Figure 5.5. A systematic approach for identifying immunogenic spliced peptides

In brief, the two-step systematic approach was developed to identify immunogenic spliced peptides. The first step, predicting a complete list by computing all potential spliced peptides from an antigen of interest and creating a final candidate epitope list. The second step, using antigen-specific $CD8^+$ T cells to identify immunogenic spliced peptides from the final candidate peptide list. Adapted from (Platteel et al., 2017)

Since the DRiP hypothesis was proposed in 1996, a vast number of studies have addressed the role of DRiPs as the source of viral antigenic peptides for $CD8^+$ T cell immunosurveillance (Wei et al., 2019). For effective immune surveillance, it is essential to include a wide-range of peptides presented by MHC-I molecules. ARF-encoded polypeptides, as a likely understudied and underestimated source of novel epitopes, enhance epitope repertoire available for T cell recognition from pathogens and tumours. A study from Maness *et al*. demonstrated that DRiPs encoded by ARFs induced highly effective antiviral T cell responses. More recently, Zanker *et al*. described an ARF-encoded epitope NS1-$ARF2_{1-8}$ as the missed immunodominant determinant in IAV-infected BALB/c mice, suggesting that many biologically relevant peptides could be generated from ARF DRiPs. In this case, a group of $CD8^+$ T cells failed to recognise any of the synthetic overlapping 18mer peptides, strongly implied that such T cell population might respond to epitopes from unconventional antigen source. Additionally, my preliminary results indicated that such $CD8^+$ T cell might recognise internally truncated ARF peptides, likely as by-products generated during pin-peptide synthesis. Therefore, my work in this chapter, when completed, could provide insights into IAV ARF transcription, translation and potentially spliced ARF epitope generation during IAV infection. This observation also indicates that the peptide repertoire recognised by $CD8^+$ T cells during IAV infection is broader than originally thought. Importantly, such T cell response might be worth considering as part of future vaccine design.

As I only synthesised a few selected spliced peptides base on the Mass Spectrometry analysis (Appendix Table 5.4), it is possible that I could potentially miss the real $CD8^+$ T cell epitopes. If my $CD8^+$ T cells fail to recognise any of the synthesised “spliced” peptides (Appendix Table 5.4), I will then have the others also synthesised and tested. I could also create a complete list of theoretically possible spliced peptides from NP and NS1 proteins using the method described in Figure 5.5, including all reading frames. If $CD8^+$ T cells can recognise the above synthesised truncated ARF peptides (or spliced ARF peptides) from the predicted candidate list, one more experiment will be needed to test whether such antigenic peptides can be naturally presented by APCs. Therefore, HPLC fractionation of peptides extracted from PR8, rVV-NS1 and rVV-NP infected C1R-B*44:03 cells will be performed, ICS will be used to detect the positive HPLC fractions and Mass

Spectrometry will be conducted to analyse the peptide sequence of the positive fractions. I will also generate a T2-B*44:03 cell line to increase the chance of directly identifying peptides from above-mentioned HPLC fractions. If $CD8^+$ T cells can't recognise either the above-mentioned synthesised or the predicted spliced peptides, I will then turn to epitope post-translational modifications.

Chapter 6: Conclusion, Discussion, and Future directions

The major goal of this thesis was to characterise novel human $CD8^+$ T cell epitopes from PBMCs collected from a healthy individual with a broad-based IAV-specific $CD8^+$ T cell response, which I believe was achieved. The pursuit of broad-based IAV-specific $CD8^+$ T cell response led to some important scientific observations and insights. First of all, to initiate such a pursuit, I created and optimised a $CD8^+$ T cell enrichment method to enable establishing single or multiple-specificity $CD8^+$ T cell lines from the initial bulk culture with minimal T cell purity. This method was successfully established and proven to be very useful in my study (Huang et al., 2019). It is highly likely that such a novel T cell enrichment method will be useful to many world-wide who have difficulties to expand antigen-specific T cells or T cell clones. Second, the demonstration of broad-based $CD8^+$ T cell response to IAV provided nice evidence that such broad-based T cell response does not only occur in IAV-specific $CD4^+$ T cell compartment (L. Chen et al., 2017). Third, I observed a population of $CD8^+$ T cells failed to recognised NP and NS1 derived 18mer overlapping peptides; this observation will allow for the subsequent investigation into potentially diverse antigenic-peptide sources, such as ARF or spliced peptides, neither has been reported for human anti-IAV $CD8^+$ T cell response.

6.1 The important role of CD3CD8 downregulation based $CD8^+$ T cell enrichment method

In **Chapter 3**, I have established and optimised a novel $CD8^+$ T cell enrichment method based on $CD8^+$ T cell activation-induced CD3CD8 downregulation. I have successfully demonstrated that this method is able to enrich $CD8^+$ T cells from established immunodominant $CD8^+$ T cell culture, single IAV protein-specific $CD8^+$ T cell cultures as well as low purity polyclonal T cell cultures.

Cell lines or clones derived from antiviral $CD8^+$ T cells have been employed as indispensable tools for understanding how antigen-specific responses influence disease progression, and for treating intractable diseases, such as using adoptive cell therapy for treating cancers (Rosenberg et al., 2004). However, establishing $CD8^+$ T cell lines or clones has been empirical, especially when it comes to expanding rather rare antigen-specific $CD8^+$ T cells. This is due to the extremely

low precursor frequencies as antigen-specific $CD8^+$ T cells are approximately 1 in 10^6 $CD8^+$ T cells (Rizzuto et al., 2009). Therefore, developing a $CD8^+$ T cell enrichment method is of more than academic interest, because it can facilitate the isolation and expansion of rare antigen-specific $CD8^+$ T cells potentially for treating difficult-diseases.

Until recently, tetramer staining is the most applied $CD8^+$ T cell enrichment method. However, it was demonstrated that pMHC tetramers underestimated antigen-reactive T cells and missed fully functional T cells (Rius et al., 2018) as these T cells expressed lower TCR (Rius et al., 2018). In addition, Hickey and colleagues recently developed a tool for isolating and enriching antigen-specific T cells (Hickey et al., 2018). This method is mainly depended on magnetic particles conjugated with peptide-loaded MHC molecules that enable antigen-specific T cell binding and selection (Hickey et al., 2018). However, the major limitation of this method is that only a few antigen-specificities can be investigated simultaneously.

In summary, my work from **Chapter 3** shows that CD3CD8 downregulation guided sorting allows for enriching low purity/frequency $CD8^+$ T cells (less than 0.5%), which is useful for establishing $CD8^+$ T cell lines with single or multiple-specificities. Hence, based on this method, I was able to investigate a broad-based IAV-specific $CD8^+$ T cell response in **Chapter 4**.

6.2 The role of atypical immunodominance hierarchy in IAV-specific CD8$^+$ T cells.

In the **Fourth Chapter**, I show that a broad-based CD8$^+$ T cell response to nine IAV proteins without a typical immunodominance hierarchy. I also discovered seven highly conserved novel IAV epitopes which are restricted to HLA-A*33:03 and HLA-B*44:03. Additionally, I show *in vitro* that the magnitude of the CD8$^+$ T cell responses to these epitopes was not correlated with the speed of their antigen presentation assessed by a BFA kinetics assay.

Immunodominance has been studied for decades with the vast majority of research conducted in syngeneic murine models, in which the MHC class I alleles are limited to three or even two, such as in B6 mice. As a result, in such models the MHC alleles expressed are rarely considered as major factors that influences immunodominance hierarchy. However, in studies based on human samples, the influence of HLA on immunodominance is of great importance. It is highly possible that some individuals may express a set of HLA molecules that maybe unable to present any CD8$^+$ T cell epitope to induce functional immunodominant response during IAV infection. For example, the epitopes identified from this study subject are restricted by HLA-A*33:03, HLA-A*24:02 and HLA-B*44:03. Based on IEDB search, only nine HLA-B*44:03 restricted IAV epitopes have been published in the database, however, none are immunodominant IAV epitopes; additionally, no HLA-A*33:03 restricted IAV epitopes have been identified (https://www.iedb.org/home_v3.php). According to data in **Figure 4.2 of Chapter 4,** the primary polyclonal CD8$^+$ T cell responses to the HLA-A*33:03 restricted M1 and NA were quite small (0.8% and 0.6%, respectively), thus, it would not be easy to identify their minimal epitopes without any further enrichment. It might be the case that such smaller responses could be overlooked due to lack of T cell enrichment technique in the previous studies. Additionally, *HLA-A*33:03* is a relatively rare allele as only 0.4% of Australians express HLA-A*33:03 while 26% Australians express HLA-A*02:01 (http://www.allelefrequencies.net/default.asp). Moreover, only a handful of potential HLA-A*33:03-restricted epitopes were predicted according to the consensus IEDB method (http://tools.iedb.org/mhci/),

and peptide binding-motifs at position 9 is Arginine, indicating that HLA-A*33:03 peptide-binding motifs might not be easily satisfied by IAV sequences. These *in silico* results further explain why no HLA-A*33:03 restricted IAV epitope is published so far.

In our case, the haplotypes of this study subject are *HLA-A*24:02/HLA-B*46:01, HLA-A*33:03/HLA-B*44:03.* The most common haplotypes of Australian aboriginal populations are *HLA-A*24:02/HLA-B*15:25*, *HLA-A*24:02/HLA-B*40:01*, and *HLA-A*24:02/HLA-Cw*03:03* (X. Gao et al., 2000), therefore, this individual is unlikely an Australian aborigine. However, studies showed that individuals expressing HLA-A*24:02 showed very limited HLA-A*24:02-restricted $CD8^+$ T cell response during IAV infection (Quinones-Parra et al., 2014). This is also an allele that highly expressed in Indigenous Alaskans (Clemens et al., 2016), which was reported to be associated with severe pH1N1 related diseases and had higher hospitalisation and mortality rates during 2009 pH1N1 pandemic (Hertz et al., 2013). My results in **Chapter 4** show that such individual's HLA combination is likely the reason for a broad-based $CD8^+$ T cell response to IAV. Therefore, such findings may also partially explain why Indigenous Australians were more susceptible to severe IAV infection and had higher mortality rate than other Australian populations. Additionally, as a majority of studies examined the commonly expressed HLA alleles, such as HLA-A*02:01, little is known about the peptides presented by HLAs specific to Indigenous population. As only one individual has been studied in this chapter, further work should include more PBMC samples to identify and characterise epitopes restricted by HLAs expressed by the Indigenous population.

A comprehensive study of immunodominant IAV-specific $CD8^+$ T cell response is critical to understanding and potentially manipulating the cellular immunity to IAV, especially in relation to developing vaccines that stimulate effective IAV-specific $CD8^+$ T cell responses. However, based on my study in **Chapter 4**, some individuals may only show a broad-based response without significant immunodominant T cell population (**Chapter 4, Figure 4.2**). Specific vaccines that can boost an individual's immune response may require to prevent infection or limit infection severity in an IAV epidemics. Thus, the investigation of atypical immunodominance hierarchy in this study may provide insight for future vaccine

development, particularly for people who may never develop immunodominant $CD8^+$ T cell responses to IAV naturally.

Collectively, my work from **Chapter 4** reported the first case of broad-based $CD8^+$ T cell response to IAV and the first HLA-A*33:03-restricted IAV $CD8^+$ T cell epitope. This work also affirms the important role of studying IAV-specific $CD8^+$ T cell response in individuals with uncommon HLA alleles or haplotypes.

6.3 The importance of ARF epitopes recognise by $CD8^+$ T cells

In the **fifth Chapter,** I tried to work out the HLA-B*44:03-restricted NP- and NS1-specific responses observed in **Chapter 4** using rVV-NP and rVV-NS1 infection, but missed by 18mer overlapping peptide screen. I conducted experiments to exclude the possibility of peptide cross-contamination. So, I considered ARF peptides encoded by these genes as a possibility. As HLA-B*44:03 requires stringent peptide-binding motif, there were only a few peptides predicted to potentially able to bind this HLA. Pin-peptides were synthesised and they were able to activate some IAV-specific T cells. Critically, when these peptides were re-synthesised as crude peptides using different chemistry, the same T cells failed to recognise any of the new peptides. Preliminary studies suggested that the $CD8^+$ T cells may recognise internally truncated ARF peptides (functionally equal to spliced ARF peptides) generated during pin-peptide synthesis but not the crude peptide synthesis. Using HPLC fractionation combined with mass spectrometry analysis, a number of internally truncated ARF peptides were identified. However, due to the time constraint, I was unable to validate these findings by specifically synthesising such truncated ARF peptides.

DRiPs encoded by ARF are another antigen source and part of immunosurveillance. Therefore, it is of great importance to reconsider the approach of immunogenic peptide identification. Recently, our laboratory reported an ARF-encoded immunodominant epitope H-$2L^d$/NS1-$ARF2_{1-8}$ by screening predicted IAV ARF peptides. This newly identified $CD8^+$ T cell epitope is a bona

fide DRiP as no biological function was detected from the NS1-ARF2$_{1-14}$ precursor (D. J. Zanker et al., 2019). Moreover, the IAV ARF2$_{1-8}$ epitope generation from its NS gene or from a recombinant "self-gene" (eGFP gene in which ARF2$_{1-8}$ was inserted in its ARF) was enhanced by IAV infection (D. J. Zanker et al., 2019), indicating that virus infection could potentially cause autoimmune response by enhancing ARF DRiP generation. In addition to ARF DRiPs, other DRiPs such as tumour derived spliced peptides (Hanada et al., 2004; Vigneron et al., 2004), bacteria (Listeria monocytogenes) derived spliced peptides (Platteel et al., 2017) have been shown to be immunogenic, and such peptides are predicted to potentially account for 1/3 of the total antigenic peptide pool (Liepe et al., 2016). Hence, it is possible and highly likely spliced ARF peptides will be part of the immunosurveillance during pathogen infection or tumorigenesis although no such example has been yet reported (Anton et al., 2014; Mannering et al., 2018; Vigneron et al., 2018).

During the investigation of the missed NP- and NS1-derived epitopes, I had several hypotheses to potentially explain my results. The first one was that the IAV-specific CD8$^+$ T cells actually responded to an unknown contaminant peptide rather than the predicted ARF peptides. However, this concern was excluded as the active HPLC fractions derived from each individual ARF peptide eluded at different time, indicating they are possessing different peptide sequences (**Chapter 5, Figure 5.4**).

Post-translational modifications can happen to individual amino acid side chains and affect the immunogenicity of peptides (Engelhard et al., 2006; Petersen et al., 2009). Some PTMs can occur automatically under physiological conditions such as cysteinylation (W. Chen et al., 1999) and isoaspartyl formation (Najbauer et al., 1996). For instance, CD8$^+$ T cells recognised two synthetic cysteine-containing peptides were underestimated as subdominant status due to sulfhydryl modification of cysteine in the absence of reducing agents (W. Chen et al., 1999). Although I have not yet investigated the possibility of PTM peptides in **Chapter 5**, this remains a possibility as it is possible that those CD8$^+$ T cells could recognise post-translational modified ARF as two active ARF peptides contain cysteine (NP-ARF 14-24 and NP-ARF 17-24). Interestingly, there is no such report currently in the literature.

I then hypothesised that the predicted ARF peptides might have been modified by a chemical group during peptide synthesis, such as the reported HLA-B*57:01/peptide-abacavir complex (Illing et al., 2012; Illing et al., 2013). In such a scenario, it is possible that different peptide sequences modified by the same chemical group likely at the same position might be able to activate $CD8^+$ T cells in a similar fashion. It has been reported that peptide impurities occurred during synthesis due to incomplete coupling sequences such as missing amino acids (de Beukelaar et al., 2007), or incomplete sidechain deprotection (W. Chen et al., 1996). Based on my preliminary data (**Chapter 5, Figure 5.4**), it is most likely that the IAV-specific $CD8^+$ T cells recognise internally truncated (spliced) ARF peptides generated during pin-peptide synthesis as part of the impurity rather than the originally predicted ARF sequences.

In the near future, IAV-specific $CD8^+$ T cells will be used to screen the synthetic internally truncated ARF peptides (Appendix Table 5.4). It is possible that I could potentially miss the real $CD8^+$ T cell epitope as only selected truncated ARF peptides were synthesised based on Mass Spectrometry analysis. Therefore, if $CD8^+$ T cell fails to recognise any of these synthetic peptides, I will then create a complete candidate list of all theoretically possible truncated ARF peptides from NP and NS1 proteins. If both approaches fail to identify the missing $CD8^+$ T cell response, I will turn to epitope post-translational modification. However, if $CD8^+$ T cells are able to recognise the synthesised truncated ARF peptides or peptides from the predicated candidate list, further experiments will be performed to confirm whether such peptides can be naturally presented by IAV infected APCs.

In summary, my work in **Chapter 5**, when finished, could provide insights into the generation of ARF or spliced ARF peptides after IAV infection. The relevant knowledge of IAV ARF peptides could add another dimension to designing $CD8^+$ T cell-based IAV vaccines.

6.4 Conclusion

IAV-specific $CD8^+$ T cells play a critical role in virus clearance. My findings in this thesis demonstrate a novel $CD8^+$ T cell enrichment approach which showed great capacity to enrich low purity antigen-specific $CD8^+$ T cells (**Chapter 3**). Such method facilitated my investigation into a broad-based $CD8^+$ T cell response to IAV and allowed further characterisation of novel $CD8^+$ T cell epitopes derived from IAV (**Chapter 4**). An interesting observation was made in **Chapter 5** in the process trying to define the missing $CD8^+$ T cell epitopes in NP- and NS1-specific $CD8^+$ T cell responses in **Chapter 4**. My preliminary results (**Chapter 5, Figure 5.4**) indicate that these $CD8^+$ T cells may recognise internally truncated ARF peptides generated during pin-peptide synthesis, however, due to limited time further experiments will be conducted to confirm such findings after thesis submission.

In summary, my method will allow researchers to enrich low and rare antigen-specific $CD8^+$ T cells for future studies and potential therapeutic applications; and my other findings will provide better understanding towards broad-based $CD8^+$ T cell response to IAV, which may aid future vaccine development.

References

Admon, A., Barnea, E., & Ziv, T. (2003). Tumor antigens and proteomics from the point of view of the major histocompatibility complex peptides. *Mol Cell Proteomics, 2*(6), 388-398. doi:10.1074/mcp.R300004-MCP200

Ahmed, R., Oldstone, M. B., & Palese, P. (2007). Protective immunity and susceptibility to infectious diseases: lessons from the 1918 influenza pandemic. *Nat Immunol, 8*(11), 1188-1193. doi:10.1038/ni1530

Akram, A., & Inman, R. D. (2012). Immunodominance: a pivotal principle in host response to viral infections. *Clin Immunol, 143*(2), 99-115. doi:10.1016/j.clim.2012.01.015

Akram, A., & Inman, R. D. (2013). Co-expression of HLA-B7 and HLA-B27 alleles is associated with B7-restricted immunodominant responses following influenza infection. *Eur J Immunol, 43*(12), 3254-3267. doi:10.1002/eji.201343597

Alexander, J., Bilsel, P., del Guercio, M. F., Marinkovic-Petrovic, A., Southwood, S., Stewart, S., . . . Sette, A. (2010). Identification of broad binding class I HLA supertype epitopes to provide universal coverage of influenza A virus. *Hum Immunol, 71*(5), 468-474.

Anderton, S. M. (2004). Post-translational modifications of self antigens: implications for autoimmunity. *Curr Opin Immunol, 16*(6), 753-758. doi:10.1016/j.coi.2004.09.001

Anton, L. C., & Yewdell, J. W. (2014). Translating DRiPs: MHC class I immunosurveillance of pathogens and tumors. *J Leukoc Biol, 95*(4), 551-562. doi:10.1189/jlb.1113599

Arcaro, A., Gregoire, C., Bakker, T. R., Baldi, L., Jordan, M., Goffin, L., . . . Luescher, I. F. (2001). CD8beta endows CD8 with efficient coreceptor function by coupling T cell receptor/CD3 to raft-associated CD8/p56(lck) complexes. *J Exp Med, 194*(10), 1485-1495.

Bach, F. H., & van Rood, J. J. (1976). The major histocompatibility complex--genetics and biology. (First of three parts). *N Engl J Med, 295*(15), 806-813. doi:10.1056/nejm197610072951504

Banchereau, J., Briere, F., Caux, C., Davoust, J., Lebecque, S., Liu, Y. J., . . . Palucka, K. (2000). Immunobiology of dendritic cells. *Annu Rev Immunol, 18*, 767-811. doi:10.1146/annurev.immunol.18.1.767

Banchereau, J., & Steinman, R. M. (1998). Dendritic cells and the control of immunity. *Nature, 392*(6673), 245-252. doi:10.1038/32588

Baumgarth, N., Herman, O. C., Jager, G. C., Brown, L., Herzenberg, L. A., & Herzenberg, L. A. (1999). Innate and acquired humoral immunities to influenza virus are mediated by distinct arms of the immune system. *Proc Natl Acad Sci U S A, 96*(5), 2250-2255. doi:10.1073/pnas.96.5.2250

Baumgarth, N., Herman, O. C., Jager, G. C., Brown, L. E., Herzenberg, L. A., & Chen, J. (2000). B-1 and B-2 cell-derived immunoglobulin M antibodies are nonredundant components of the protective response to influenza virus infection. *J Exp Med, 192*(2), 271-280. doi:10.1084/jem.192.2.271

Bautista, E., Chotpitayasunondh, T., Gao, Z., Harper, S. A., Shaw, M., Uyeki, T. M., . . . Nicholson, K. G. (2010). Clinical aspects of pandemic 2009 influenza A (H1N1) virus infection. *N Engl J Med, 362*(18), 1708-1719. doi:10.1056/NEJMra1000449

Bell, M. J., Burrows, J. M., Brennan, R., Miles, J. J., Tellam, J., McCluskey, J., . . . Burrows, S. R. (2009). The peptide length specificity of some HLA class I alleles is very broad and includes peptides of up to 25 amino acids in length. *Mol Immunol, 46*(8-9), 1911-1917. doi:10.1016/j.molimm.2008.12.003

Belz, G. T., Stevenson, P. G., & Doherty, P. C. (2000). Contemporary analysis of MHC-related immunodominance hierarchies in the CD8+ T cell response to influenza A viruses. *J Immunol, 165*(5), 2404-2409. doi:10.4049/jimmunol.165.5.2404

Bender, B. S., Croghan, T., Zhang, L., & Small, P. A., Jr. (1992). Transgenic mice lacking class I major histocompatibility complex-restricted T cells have delayed viral clearance and increased mortality after influenza virus challenge. *J Exp Med, 175*(4), 1143-1145. doi:10.1084/jem.175.4.1143

Bennink, J. R., Yewdell, J. W., & Gerhard, W. (1982). A viral polymerase involved in recognition of influenza virus-infected cells by a cytotoxic T-cell clone. *Nature, 296*(5852), 75-76. doi:10.1038/296075a0

Bertrand, F. E., Eckfeldt, C. E., Fink, J. R., Lysholm, A. S., Pribyl, J. A., Shah, N., & LeBien, T. W. (2000). Microenvironmental influences on human B-cell development. *Immunol Rev, 175*, 175-186.

Bhardwaj, N., Bender, A., Gonzalez, N., Bui, L. K., Garrett, M. C., & Steinman, R. M. (1994). Influenza virus-infected dendritic cells stimulate strong proliferative and cytolytic responses from human CD8+ T cells. *J Clin Invest, 94*(2), 797-807. doi:10.1172/jci117399

Bierer, B. E., Sleckman, B. P., Ratnofsky, S. E., & Burakoff, S. J. (1989). The biologic roles of CD2, CD4, and CD8 in T-cell activation. *Annu Rev Immunol, 7*, 579-599. doi:10.1146/annurev.iy.07.040189.003051

Bihl, F., Frahm, N., Di Giammarino, L., Sidney, J., John, M., Yusim, K., . . . Brander, C. (2006). Impact of HLA-B alleles, epitope binding affinity, functional avidity, and viral coinfection on the immunodominance of virus-specific CTL responses. *J Immunol, 176*(7), 4094-4101. doi:10.4049/jimmunol.176.7.4094

Bishop, J. F., Murnane, M. P., & Owen, R. (2009). Australia's winter with the 2009 pandemic influenza A (H1N1) virus. *N Engl J Med, 361*(27), 2591-2594. doi:10.1056/NEJMp0910445

Bjorkman, P. J., Saper, M. A., Samraoui, B., Bennett, W. S., Strominger, J. L., & Wiley, D. C. (1987a). The foreign antigen binding site and T cell recognition regions of class I histocompatibility antigens. *Nature, 329*(6139), 512-518. doi:10.1038/329512a0

Bjorkman, P. J., Saper, M. A., Samraoui, B., Bennett, W. S., Strominger, J. L., & Wiley, D. C. (1987b). Structure of the human class I histocompatibility antigen, HLA-A2. *Nature, 329*(6139), 506-512. doi:10.1038/329506a0

Blum, J. S., Wearsch, P. A., & Cresswell, P. (2013). Pathways of antigen processing. *Annu Rev Immunol, 31*, 443-473. doi:10.1146/annurev-immunol-032712-095910

Bode, A. M., & Dong, Z. (2004). Post-translational modification of p53 in tumorigenesis. *Nat Rev Cancer, 4*(10), 793-805. doi:10.1038/nrc1455

Boon, A. C., De Mutsert, G., Fouchier, R. A., Sintnicolaas, K., Osterhaus, A. D., & Rimmelzwaan, G. F. (2004). Preferential HLA usage in the influenza virus-specific CTL response. *J Immunol, 172*(7), 4435-4443. doi:10.4049/jimmunol.172.7.4435

Boyle, L. H., Hermann, C., Boname, J. M., Porter, K. M., Patel, P. A., Burr, M. L., . . . Trowsdale, J. (2013). Tapasin-related protein TAPBPR is an additional component of the MHC class I presentation pathway. *Proc Natl Acad Sci U S A, 110*(9), 3465-3470. doi:10.1073/pnas.1222342110

Bullock, T. N., & Eisenlohr, L. C. (1996). Ribosomal scanning past the primary initiation codon as a mechanism for expression of CTL epitopes encoded in alternative reading frames. *J Exp Med, 184*(4), 1319-1329. doi:10.1084/jem.184.4.1319

Burnet, F. M. (1976). A modification of Jerne's theory of antibody production using the concept of clonal selection. *CA Cancer J Clin, 26*(2), 119-121.

Burrows, S. R., Rodda, S. J., Suhrbier, A., Geysen, H. M., & Moss, D. J. (1992). The specificity of recognition of a cytotoxic T lymphocyte epitope. *Eur J Immunol, 22*(1), 191-195. doi:10.1002/eji.1830220128

Burrows, S. R., Silins, S. L., Moss, D. J., Khanna, R., Misko, I. S., & Argaet, V. P. (1995). T cell receptor repertoire for a viral epitope in humans is diversified by tolerance to a background major histocompatibility complex antigen. *J Exp Med, 182*(6), 1703-1715.

Butcher, E. C., & Picker, L. J. (1996). Lymphocyte homing and homeostasis. *Science, 272*(5258), 60-66.

Cantrell, D. A., Davies, A. A., & Crumpton, M. J. (1985). Activators of protein kinase C down-regulate and phosphorylate the T3/T-cell antigen receptor complex of human T lymphocytes. *Proc Natl Acad Sci U S A, 82*(23), 8158-8162.

Cardinaud, S., Moris, A., Fevrier, M., Rohrlich, P. S., Weiss, L., Langlade-Demoyen, P., . . . Habel, A. (2004). Identification of cryptic MHC I-restricted epitopes encoded by HIV-1 alternative reading frames. *J Exp Med, 199*(8), 1053-1063. doi:10.1084/jem.20031869

Chang, S. C., Momburg, F., Bhutani, N., & Goldberg, A. L. (2005). The ER aminopeptidase, ERAP1, trims precursors to lengths of MHC class I peptides by a "molecular ruler" mechanism. *Proc Natl Acad Sci U S A, 102*(47), 17107-17112. doi:10.1073/pnas.0500721102

Chaplin, D. D. (2010). Overview of the immune response. *J Allergy Clin Immunol, 125*(2 Suppl 2), S3-23. doi:10.1016/j.jaci.2009.12.980

Chen, L., Anthony, A., Oveissi, S., Huang, M., Zanker, D., Xiao, K., . . . Chen, W. (2017). Broad-Based CD4(+) T Cell Responses to Influenza A Virus in a Healthy Individual Who Lacks Typical Immunodominance Hierarchy. *Front Immunol, 8*, 375. doi:10.3389/fimmu.2017.00375

Chen, L., Zanker, D., Xiao, K., Wu, C., Zou, Q., & Chen, W. (2014). Immunodominant CD4+ T-cell responses to influenza A virus in healthy individuals focus on matrix 1 and nucleoprotein. *J Virol, 88*(20), 11760-11773. doi:10.1128/jvi.01631-14

Chen, W., Anton, L. C., Bennink, J. R., & Yewdell, J. W. (2000). Dissecting the multifactorial causes of immunodominance in class I-restricted T cell responses to viruses. *Immunity, 12*(1), 83-93.

Chen, W., Calvo, P. A., Malide, D., Gibbs, J., Schubert, U., Bacik, I., . . . Yewdell, J. W. (2001). A novel influenza A virus mitochondrial protein that induces cell death. *Nat Med, 7*(12), 1306-1312. doi:10.1038/nm1201-1306

Chen, W., Ede, N. J., Jackson, D. C., McCluskey, J., & Purcell, A. W. (1996). CTL recognition of an altered peptide associated with asparagine bond rearrangement. Implications for immunity and vaccine design. *J Immunol, 157*(3), 1000-1005.

Chen, W., Jin, W., Hardegen, N., Lei, K. J., Li, L., Marinos, N., . . . Wahl, S. M. (2003). Conversion of peripheral CD4+CD25- naive T cells to CD4+CD25+ regulatory T cells by TGF-beta induction of transcription factor Foxp3. *J Exp Med, 198*(12), 1875-1886. doi:10.1084/jem.20030152

Chen, W., Pang, K., Masterman, K. A., Kennedy, G., Basta, S., Dimopoulos, N., . . . Yewdell, J. W. (2004). Reversal in the immunodominance hierarchy in secondary

CD8+ T cell responses to influenza A virus: roles for cross-presentation and lysis-independent immunodomination. *J Immunol, 173*(8), 5021-5027.

Chen, W., Yewdell, J. W., Levine, R. L., & Bennink, J. R. (1999). Modification of cysteine residues in vitro and in vivo affects the immunogenicity and antigenicity of major histocompatibility complex class I-restricted viral determinants. *J Exp Med, 189*(11), 1757-1764.

Chidgzey, P. J., Davis, S., Williams, P., & Reeve, C. (2015). An outbreak of influenza A (H1N1) virus in a remote Aboriginal community post-pandemic: implications for pandemic planning and health service policy. *Aust N Z J Public Health, 39*(1), 15-20. doi:10.1111/1753-6405.12295

Chothia, C., Boswell, D. R., & Lesk, A. M. (1988). The outline structure of the T-cell alpha beta receptor. *Embo j, 7*(12), 3745-3755.

Clemens, E. B., Grant, E. J., Wang, Z., Gras, S., Tipping, P., Rossjohn, J., . . . Kedzierska, K. (2016). Towards identification of immune and genetic correlates of severe influenza disease in Indigenous Australians. *Immunol Cell Biol, 94*(4), 367-377. doi:10.1038/icb.2015.93

Clevers, H., Alarcon, B., Wileman, T., & Terhorst, C. (1988). The T cell receptor/CD3 complex: a dynamic protein ensemble. *Annu Rev Immunol, 6*, 629-662. doi:10.1146/annurev.iy.06.040188.003213

Davis, M. M., & Bjorkman, P. J. (1988). T-cell antigen receptor genes and T-cell recognition. *Nature, 334*(6181), 395-402. doi:10.1038/334395a0

Day, E. B., Charlton, K. L., La Gruta, N. L., Doherty, P. C., & Turner, S. J. (2011). Effect of MHC class I diversification on influenza epitope-specific CD8+ T cell precursor frequency and subsequent effector function. *J Immunol, 186*(11), 6319-6328. doi:10.4049/jimmunol.1000883

de Beukelaar, J. W., Gratama, J. W., Smitt, P. A., Verjans, G. M., Kraan, J., Luider, T. M., & Burgers, P. C. (2007). The impact of impurities in synthetic peptides on the outcome of T-cell stimulation assays. *Rapid Commun Mass Spectrom, 21*(7), 1282-1288. doi:10.1002/rcm.2958

Delves, P. J., & Roitt, I. M. (2000). The immune system. First of two parts. *N Engl J Med, 343*(1), 37-49. doi:10.1056/nejm200007063430107

Deng, Y., Yewdell, J. W., Eisenlohr, L. C., & Bennink, J. R. (1997). MHC affinity, peptide liberation, T cell repertoire, and immunodominance all contribute to the paucity of MHC class I-restricted peptides recognized by antiviral CTL. *J Immunol, 158*(4), 1507-1515.

Di Carluccio, A. R., Triffon, C. F., & Chen, W. (2018). Perpetual complexity: predicting human CD8(+) T-cell responses to pathogenic peptides. *Immunol Cell Biol, 96*(4), 358-369. doi:10.1111/imcb.12019

Diedrich, G., Bangia, N., Pan, M., & Cresswell, P. (2001). A role for calnexin in the assembly of the MHC class I loading complex in the endoplasmic reticulum. *J Immunol, 166*(3), 1703-1709. doi:10.4049/jimmunol.166.3.1703

Doherty, P. C., Topham, D. J., & Tripp, R. A. (1996). Establishment and persistence of virus-specific CD4+ and CD8+ T cell memory. *Immunol Rev, 150*, 23-44.

Doms, R. W., Russ, G., & Yewdell, J. W. (1989). Brefeldin A redistributes resident and itinerant Golgi proteins to the endoplasmic reticulum. *J Cell Biol, 109*(1), 61-72. doi:10.1083/jcb.109.1.61

Doyle, H. A., & Mamula, M. J. (2001). Post-translational protein modifications in antigen recognition and autoimmunity. *Trends Immunol, 22*(8), 443-449.

Echevarria-Zuno, S., Mejia-Arangure, J. M., Mar-Obeso, A. J., Grajales-Muniz, C., Robles-Perez, E., Gonzalez-Leon, M., . . . Borja-Aburto, V. H. (2009). Infection and death from influenza A H1N1 virus in Mexico: a retrospective analysis. *Lancet, 374*(9707), 2072-2079. doi:10.1016/s0140-6736(09)61638-x

Elkington, R., Walker, S., Crough, T., Menzies, M., Tellam, J., Bharadwaj, M., & Khanna, R. (2003). Ex vivo profiling of CD8+-T-cell responses to human cytomegalovirus reveals broad and multispecific reactivities in healthy virus carriers. *J Virol, 77*(9), 5226-5240. doi:10.1128/jvi.77.9.5226-5240.2003

Engelhard, V. H., Altrich-Vanlith, M., Ostankovitch, M., & Zarling, A. L. (2006). Post-translational modifications of naturally processed MHC-binding epitopes. *Curr Opin Immunol, 18*(1), 92-97. doi:10.1016/j.coi.2005.11.015

Engelhard, V. H., Brickner, A. G., & Zarling, A. L. (2002). Insights into antigen processing gained by direct analysis of the naturally processed class I MHC associated peptide repertoire. *Mol Immunol, 39*(3-4), 127-137.

Falk, K., Rotzschke, O., Stevanovic, S., Jung, G., & Rammensee, H. G. (1991). Allele-specific motifs revealed by sequencing of self-peptides eluted from MHC molecules. *Nature, 351*(6324), 290-296. doi:10.1038/351290a0

Falk, K., Rotzschke, O., Takiguchi, M., Grahovac, B., Gnau, V., Stevanovic, S., . . . Rammensee, H. G. (1994). Peptide motifs of HLA-A1, -A11, -A31, and -A33 molecules. *Immunogenetics, 40*(3), 238-241.

Falo, L. D., Jr., Colarusso, L. J., Benacerraf, B., & Rock, K. L. (1992). Serum proteases alter the antigenicity of peptides presented by class I major histocompatibility complex molecules. *Proc Natl Acad Sci U S A, 89*(17), 8347-8350. doi:10.1073/pnas.89.17.8347

Flint, S. M., Davis, J. S., Su, J. Y., Oliver-Landry, E. P., Rogers, B. A., Goldstein, A., . . . Tong, S. Y. (2010). Disproportionate impact of pandemic (H1N1) 2009 influenza on Indigenous people in the Top End of Australia's Northern Territory. *Med J Aust, 192*(10), 617-622.

Gao, G. F., & Jakobsen, B. K. (2000). Molecular interactions of coreceptor CD8 and MHC class I: the molecular basis for functional coordination with the T-cell receptor. *Immunol Today, 21*(12), 630-636.

Gao, R., Cao, B., Hu, Y., Feng, Z., Wang, D., Hu, W., . . . Shu, Y. (2013). Human infection with a novel avian-origin influenza A (H7N9) virus. *N Engl J Med, 368*(20), 1888-1897. doi:10.1056/NEJMoa1304459

Gao, X., Lester, S., Veale, A., Boettcher, B., Currie, B., McCluskey, J., & Chelvanayagam, G. (2000). *HLA class I alleles in Australian aborigines and their peptide binding profiles*, Tokyo.

Garcia-Hernandez Mde, L., Hamada, H., Reome, J. B., Misra, S. K., Tighe, M. P., & Dutton, R. W. (2010). Adoptive transfer of tumor-specific Tc17 effector T cells controls the growth of B16 melanoma in mice. *J Immunol, 184*(8), 4215-4227. doi:10.4049/jimmunol.0902995

Gerhard, W., Mozdzanowska, K., Furchner, M., Washko, G., & Maiese, K. (1997). Role of the B-cell response in recovery of mice from primary influenza virus infection. *Immunol Rev, 159*, 95-103.

Goldberg, A. L., & St John, A. C. (1976). Intracellular protein degradation in mammalian and bacterial cells: Part 2. *Annu Rev Biochem, 45*, 747-803. doi:10.1146/annurev.bi.45.070176.003531

Gooding, L. R., & O'Connell, K. A. (1983). Recognition by cytotoxic T lymphocytes of cells expressing fragments of the SV40 tumor antigen. *J Immunol, 131*(5), 2580-2586.

Gotch, F., Rothbard, J., Howland, K., Townsend, A., & McMichael, A. (1987). Cytotoxic T lymphocytes recognize a fragment of influenza virus matrix protein in association with HLA-A2. *Nature, 326*(6116), 881-882. doi:10.1038/326881a0

Grant, E., Wu, C., Chan, K. F., Eckle, S., Bharadwaj, M., Zou, Q. M., . . . Chen, W. (2013). Nucleoprotein of influenza A virus is a major target of immunodominant CD8+ T-cell responses. *Immunol Cell Biol, 91*(2), 184-194. doi:10.1038/icb.2012.78

Grant, E. J., Chen, L., Quinones-Parra, S., Pang, K., Kedzierska, K., & Chen, W. (2014). T-cell immunity to influenza A viruses. *Crit Rev Immunol, 34*(1), 15-39.

Gras, S., Kedzierski, L., Valkenburg, S. A., Laurie, K., Liu, Y. C., Denholm, J. T., . . . Kedzierska, K. (2010). Cross-reactive CD8+ T-cell immunity between the pandemic H1N1-2009 and H1N1-1918 influenza A viruses. *Proc Natl Acad Sci U S A, 107*(28), 12599-12604. doi:10.1073/pnas.1007270107

Grebe, K. M., Yewdell, J. W., & Bennink, J. R. (2008). Heterosubtypic immunity to influenza A virus: where do we stand? *Microbes Infect, 10*(9), 1024-1029. doi:10.1016/j.micinf.2008.07.002

Greenbaum, J. A., Kotturi, M. F., Kim, Y., Oseroff, C., Vaughan, K., Salimi, N., . . . Peters, B. (2009). Pre-existing immunity against swine-origin H1N1 influenza viruses in the general human population. *Proc Natl Acad Sci U S A, 106*(48), 20365-20370. doi:10.1073/pnas.0911580106

Grufman, P., Wolpert, E. Z., Sandberg, J. K., & Karre, K. (1999). T cell competition for the antigen-presenting cell as a model for immunodominance in the cytotoxic T lymphocyte response against minor histocompatibility antigens. *Eur J Immunol, 29*(7), 2197-2204. doi:10.1002/(sici)1521-4141(199907)29:07<2197::Aid-immu2197>3.0.Co;2-b

Guermonprez, P., Valladeau, J., Zitvogel, L., Thery, C., & Amigorena, S. (2002). Antigen presentation and T cell stimulation by dendritic cells. *Annu Rev Immunol, 20*, 621-667. doi:10.1146/annurev.immunol.20.100301.064828

Halenius, A., Gerke, C., & Hengel, H. (2015). Classical and non-classical MHC I molecule manipulation by human cytomegalovirus: so many targets-but how many arrows in the quiver? *Cell Mol Immunol, 12*(2), 139-153. doi:10.1038/cmi.2014.105

Hamada, H., Bassity, E., Flies, A., Strutt, T. M., Garcia-Hernandez Mde, L., McKinstry, K. K., . . . Dutton, R. W. (2013). Multiple redundant effector mechanisms of CD8+ T cells protect against influenza infection. *J Immunol, 190*(1), 296-306. doi:10.4049/jimmunol.1200571

Hamilton-Easton, A., & Eichelberger, M. (1995). Virus-specific antigen presentation by different subsets of cells from lung and mediastinal lymph node tissues of influenza virus-infected mice. *J Virol, 69*(10), 6359-6366.

Hanada, K., Yewdell, J. W., & Yang, J. C. (2004). Immune recognition of a human renal cancer antigen through post-translational protein splicing. *Nature, 427*(6971), 252-256. doi:10.1038/nature02240

Harrington, L. E., Hatton, R. D., Mangan, P. R., Turner, H., Murphy, T. L., Murphy, K. M., & Weaver, C. T. (2005). Interleukin 17-producing CD4+ effector T cells develop via a

lineage distinct from the T helper type 1 and 2 lineages. *Nat Immunol, 6*(11), 1123-1132. doi:10.1038/ni1254

Hermann, C., van Hateren, A., Trautwein, N., Neerincx, A., Duriez, P. J., Stevanovic, S., . . . Boyle, L. H. (2015). TAPBPR alters MHC class I peptide presentation by functioning as a peptide exchange catalyst. *Elife, 4*. doi:10.7554/eLife.09617

Hertz, T., Oshansky, C. M., Roddam, P. L., DeVincenzo, J. P., Caniza, M. A., Jojic, N., . . . Corey, L. (2013). HLA targeting efficiency correlates with human T-cell response magnitude and with mortality from influenza A infection. *Proc Natl Acad Sci U S A, 110*(33), 13492-13497. doi:10.1073/pnas.1221555110

Hewitt, E. W. (2003). The MHC class I antigen presentation pathway: strategies for viral immune evasion. *Immunology, 110*(2), 163-169. doi:10.1046/j.1365-2567.2003.01738.x

Hickey, J. W., & Schneck, J. P. (2018). Enrich and Expand Rare Antigen-specific T Cells with Magnetic Nanoparticles. *J Vis Exp*(141). doi:10.3791/58640

Hillaire, M. L., Vogelzang-van Trierum, S. E., Kreijtz, J. H., de Mutsert, G., Fouchier, R. A., Osterhaus, A. D., & Rimmelzwaan, G. F. (2013). Human T-cells directed to seasonal influenza A virus cross-react with 2009 pandemic influenza A (H1N1) and swine-origin triple-reassortant H3N2 influenza viruses. *J Gen Virol, 94*(Pt 3), 583-592. doi:10.1099/vir.0.048652-0

Holler, P. D., & Kranz, D. M. (2003). Quantitative analysis of the contribution of TCR/pepMHC affinity and CD8 to T cell activation. *Immunity, 18*(2), 255-264.

Howarth, M., Williams, A., Tolstrup, A. B., & Elliott, T. (2004). Tapasin enhances MHC class I peptide presentation according to peptide half-life. *Proc Natl Acad Sci U S A, 101*(32), 11737-11742. doi:10.1073/pnas.0306294101

Huang, M., Zhang, J., & Chen, W. (2019). FACS isolation of low percentage human antigen-specific CD8(+) T cells based on activation-induced CD3 and CD8 downregulation. *J Immunol Methods*. doi:10.1016/j.jim.2019.06.013

Hughes, E. A., & Cresswell, P. (1998). The thiol oxidoreductase ERp57 is a component of the MHC class I peptide-loading complex. *Curr Biol, 8*(12), 709-712.

Ibe, M., Moore, Y. I., Miwa, K., Kaneko, Y., Yokota, S., & Takiguchi, M. (1996). Role of strong anchor residues in the effective binding of 10-mer and 11-mer peptides to HLA-A*2402 molecules. *Immunogenetics, 44*(4), 233-241.

Ilca, F. T., Neerincx, A., Wills, M. R., de la Roche, M., & Boyle, L. H. (2018). Utilizing TAPBPR to promote exogenous peptide loading onto cell surface MHC I molecules. *Proc Natl Acad Sci U S A, 115*(40), E9353-e9361. doi:10.1073/pnas.1809465115

Illing, P. T., Vivian, J. P., Dudek, N. L., Kostenko, L., Chen, Z., Bharadwaj, M., . . . McCluskey, J. (2012). Immune self-reactivity triggered by drug-modified HLA-peptide repertoire. *Nature, 486*(7404), 554-558. doi:10.1038/nature11147

Illing, P. T., Vivian, J. P., Purcell, A. W., Rossjohn, J., & McCluskey, J. (2013). Human leukocyte antigen-associated drug hypersensitivity. *Curr Opin Immunol, 25*(1), 81-89. doi:10.1016/j.coi.2012.10.002

Jackson, H. M., Dimopoulos, N., Chen, Q., Luke, T., Yee Tai, T., Maraskovsky, E., . . . Chen, W. (2004). A robust human T-cell culture method suitable for monitoring CD8+ and CD4+ T-cell responses from cancer clinical trial samples. *J Immunol Methods, 291*(1-2), 51-62. doi:10.1016/j.jim.2004.04.017

Jagger, B. W., Wise, H. M., Kash, J. C., Walters, K. A., Wills, N. M., Xiao, Y. L., . . . Digard, P. (2012). An overlapping protein-coding region in influenza A virus segment 3 modulates the host response. *Science, 337*(6091), 199-204. doi:10.1126/science.1222213

Janeway, C. A., Jr. (1992). The T cell receptor as a multicomponent signalling machine: CD4/CD8 coreceptors and CD45 in T cell activation. *Annu Rev Immunol, 10*, 645-674. doi:10.1146/annurev.iy.10.040192.003241

Jardetzky, T. S., Lane, W. S., Robinson, R. A., Madden, D. R., & Wiley, D. C. (1991). Identification of self peptides bound to purified HLA-B27. *Nature, 353*(6342), 326-329. doi:10.1038/353326a0

Jiang, J., Natarajan, K., Boyd, L. F., Morozov, G. I., Mage, M. G., & Margulies, D. H. (2017). Crystal structure of a TAPBPR-MHC I complex reveals the mechanism of peptide editing in antigen presentation. *Science, 358*(6366), 1064-1068. doi:10.1126/science.aao5154

Kane, L. P., Lin, J., & Weiss, A. (2000). Signal transduction by the TCR for antigen. *Curr Opin Immunol, 12*(3), 242-249.

Karrer, U., Sierro, S., Wagner, M., Oxenius, A., Hengel, H., Koszinowski, U. H., . . . Klenerman, P. (2003). Memory inflation: continuous accumulation of antiviral CD8+ T cells over time. *J Immunol, 170*(4), 2022-2029. doi:10.4049/jimmunol.170.4.2022

Kedl, R. M., Rees, W. A., Hildeman, D. A., Schaefer, B., Mitchell, T., Kappler, J., & Marrack, P. (2000). T cells compete for access to antigen-bearing antigen-presenting cells. *J Exp Med, 192*(8), 1105-1113. doi:10.1084/jem.192.8.1105

Kelly, H., Mercer, G., & Cheng, A. (2009). Quantifying the risk of pandemic influenza in pregnancy and indigenous people in Australia in 2009. *Euro Surveill, 14*(50).

Kim, P. S., Lee, P. P., & Levy, D. (2011). A theory of immunodominance and adaptive regulation. *Bull Math Biol, 73*(7), 1645-1665. doi:10.1007/s11538-010-9585-5

Klein, J., & Sato, A. (2000). The HLA system. First of two parts. *N Engl J Med, 343*(10), 702-709. doi:10.1056/nejm200009073431006

Koivunen, E., Arap, W., Rajotte, D., Lahdenranta, J., & Pasqualini, R. (1999). Identification of receptor ligands with phage display peptide libraries. *J Nucl Med, 40*(5), 883-888.

Koutsakos, M., Illing, P. T., Nguyen, T. H. O., Mifsud, N. A., Crawford, J. C., Rizzetto, S., . . . Kedzierska, K. (2019). Human CD8(+) T cell cross-reactivity across influenza A, B and C viruses. *Nat Immunol, 20*(5), 613-625. doi:10.1038/s41590-019-0320-6

Koutsakos, M., Nguyen, T. H., Barclay, W. S., & Kedzierska, K. (2016). Knowns and unknowns of influenza B viruses. *Future Microbiol, 11*(1), 119-135. doi:10.2217/fmb.15.120

Krammer, F. (2019). The human antibody response to influenza A virus infection and vaccination. *Nat Rev Immunol, 19*(6), 383-397. doi:10.1038/s41577-019-0143-6

Krammer, F., Smith, G. J. D., Fouchier, R. A. M., Peiris, M., Kedzierska, K., Doherty, P. C., . . . Garcia-Sastre, A. (2018). Influenza. *Nat Rev Dis Primers, 4*(1), 3. doi:10.1038/s41572-018-0002-y

Krangel, M. S. (1987). Endocytosis and recycling of the T3-T cell receptor complex. The role of T3 phosphorylation. *J Exp Med, 165*(4), 1141-1159.

Kreijtz, J. H., de Mutsert, G., van Baalen, C. A., Fouchier, R. A., Osterhaus, A. D., & Rimmelzwaan, G. F. (2008). Cross-recognition of avian H5N1 influenza virus by

human cytotoxic T-lymphocyte populations directed to human influenza A virus. *J Virol, 82*(11), 5161-5166. doi:10.1128/jvi.02694-07

Krogsgaard, M., Li, Q. J., Sumen, C., Huppa, J. B., Huse, M., & Davis, M. M. (2005). Agonist/endogenous peptide-MHC heterodimers drive T cell activation and sensitivity. *Nature, 434*(7030), 238-243. doi:10.1038/nature03391

Kubo, R. T., Sette, A., Grey, H. M., Appella, E., Sakaguchi, K., Zhu, N. Z., . . . et al. (1994). Definition of specific peptide motifs for four major HLA-A alleles. *J Immunol, 152*(8), 3913-3924.

Kuhns, M. S., & Davis, M. M. (2012). TCR Signaling Emerges from the Sum of Many Parts. *Front Immunol, 3*, 159. doi:10.3389/fimmu.2012.00159

La Gruta, N. L., Turner, S. J., & Doherty, P. C. (2004). Hierarchies in cytokine expression profiles for acute and resolving influenza virus-specific CD8+ T cell responses: correlation of cytokine profile and TCR avidity. *J Immunol, 172*(9), 5553-5560. doi:10.4049/jimmunol.172.9.5553

La Ruche, G., Tarantola, A., Barboza, P., Vaillant, L., Gueguen, J., & Gastellu-Etchegorry, M. (2009). The 2009 pandemic H1N1 influenza and indigenous populations of the Americas and the Pacific. *Euro Surveill, 14*(42). doi:10.2807/ese.14.42.19366-en

Lacey, S. F., Villacres, M. C., La Rosa, C., Wang, Z., Longmate, J., Martinez, J., . . . Diamond, D. J. (2003). Relative dominance of HLA-B*07 restricted CD8+ T-lymphocyte immune responses to human cytomegalovirus pp65 in persons sharing HLA-A*02 and HLA-B*07 alleles. *Hum Immunol, 64*(4), 440-452.

Laugel, B., van den Berg, H. A., Gostick, E., Cole, D. K., Wooldridge, L., Boulter, J., . . . Sewell, A. K. (2007). Different T cell receptor affinity thresholds and CD8 coreceptor dependence govern cytotoxic T lymphocyte activation and tetramer binding properties. *J Biol Chem, 282*(33), 23799-23810. doi:10.1074/jbc.M700976200

Lee, L. Y., Ha do, L. A., Simmons, C., de Jong, M. D., Chau, N. V., Schumacher, R., . . . Dong, T. (2008). Memory T cells established by seasonal human influenza A infection cross-react with avian influenza A (H5N1) in healthy individuals. *J Clin Invest, 118*(10), 3478-3490. doi:10.1172/jci32460

Leone, P., Shin, E. C., Perosa, F., Vacca, A., Dammacco, F., & Racanelli, V. (2013). MHC class I antigen processing and presenting machinery: organization, function, and defects in tumor cells. *J Natl Cancer Inst, 105*(16), 1172-1187. doi:10.1093/jnci/djt184

Leslie, A. J., Pfafferott, K. J., Chetty, P., Draenert, R., Addo, M. M., Feeney, M., . . . Goulder, P. J. (2004). HIV evolution: CTL escape mutation and reversion after transmission. *Nat Med, 10*(3), 282-289. doi:10.1038/nm992

Lester, S., Cassidy, S., Humphreys, I., Bennett, G., Hurley, C. K., Boettcher, B., & McCluskey, J. (1995). Evolution in HLA-DRB1 and major histocompatibility complex class II haplotypes of Australian aborigines. Definition of a new DRB1 allele and distribution of DRB1 gene frequencies. *Hum Immunol, 42*(2), 154-160.

Lienert, K., McCluskey, J., Bennett, G., Fowler, C., & Russ, G. (1995). HLA class I variation in Australian aborigines: characterization of allele B*1521. *Tissue Antigens, 45*(1), 12-17.

Liepe, J., Marino, F., Sidney, J., Jeko, A., Bunting, D. E., Sette, A., . . . Mishto, M. (2016). A large fraction of HLA class I ligands are proteasome-generated spliced peptides. *Science, 354*(6310), 354-358. doi:10.1126/science.aaf4384

Liu, J., Zhang, S., Tan, S., Yi, Y., Wu, B., Cao, B., . . . Gao, G. F. (2012). Cross-allele cytotoxic T lymphocyte responses against 2009 pandemic H1N1 influenza A virus among HLA-A24 and HLA-A3 supertype-positive individuals. *J Virol, 86*(24), 13281-13294. doi:10.1128/jvi.01841-12

Liu, K., & Nussenzweig, M. C. (2010). Origin and development of dendritic cells. *Immunol Rev, 234*(1), 45-54. doi:10.1111/j.0105-2896.2009.00879.x

Luescher, I. F., Romero, P., Kuznetsov, D., Rimoldi, D., Coulie, P., Cerottini, J. C., & Jongeneel, C. V. (1996). HLA photoaffinity labeling reveals overlapping binding of homologous melanoma-associated gene peptides by HLA-A1, HLA-A29, and HLA-B44. *J Biol Chem, 271*(21), 12463-12471.

Malik, A., Adland, E., Laker, L., Kloverpris, H., Fardoos, R., Roider, J., . . . Goulder, P. J. R. (2017). Immunodominant cytomegalovirus-specific CD8+ T-cell responses in sub-Saharan African populations. *PLoS One, 12*(12), e0189612. doi:10.1371/journal.pone.0189612

Mamula, M. J., Gee, R. J., Elliott, J. I., Sette, A., Southwood, S., Jones, P. J., & Blier, P. R. (1999). Isoaspartyl post-translational modification triggers autoimmune responses to self-proteins. *J Biol Chem, 274*(32), 22321-22327. doi:10.1074/jbc.274.32.22321

Mannering, S. I., Harrison, L. C., Williamson, N. A., Morris, J. S., Thearle, D. J., Jensen, K. P., . . . Purcell, A. W. (2005). The insulin A-chain epitope recognized by human T cells is posttranslationally modified. *J Exp Med, 202*(9), 1191-1197. doi:10.1084/jem.20051251

Mannering, S. I., So, M., Elso, C. M., & Kay, T. W. H. (2018). Shuffling peptides to create T-cell epitopes: does the immune system play cards? *Immunol Cell Biol, 96*(1), 34-40. doi:10.1111/imcb.1015

Martini, M., Gazzaniga, V., Bragazzi, N. L., & Barberis, I. (2019). The Spanish Influenza Pandemic: a lesson from history 100 years after 1918. *J Prev Med Hyg, 60*(1), E64-e67. doi:10.15167/2421-4248/jpmh2019.60.1.1205

Matsuzaki, Y., Katsushima, N., Nagai, Y., Shoji, M., Itagaki, T., Sakamoto, M., . . . Nishimura, H. (2006). Clinical features of influenza C virus infection in children. *J Infect Dis, 193*(9), 1229-1235. doi:10.1086/502973

McCluskey, J., & Peh, C. A. (1999). The human leucocyte antigens and clinical medicine: an overview. *Rev Immunogenet, 1*(1), 3-20.

McKinstry, K. K., Dutton, R. W., Swain, S. L., & Strutt, T. M. (2013). Memory CD4 T cell-mediated immunity against influenza A virus: more than a little helpful. *Arch Immunol Ther Exp (Warsz), 61*(5), 341-353. doi:10.1007/s00005-013-0236-z

McMichael, A. J., Gotch, F. M., Noble, G. R., & Beare, P. A. (1983). Cytotoxic T-cell immunity to influenza. *N Engl J Med, 309*(1), 13-17. doi:10.1056/nejm198307073090103

Merad, M., Sathe, P., Helft, J., Miller, J., & Mortha, A. (2013). The dendritic cell lineage: ontogeny and function of dendritic cells and their subsets in the steady state and the inflamed setting. *Annu Rev Immunol, 31*, 563-604. doi:10.1146/annurev-immunol-020711-074950

Miceli, M. C., & Parnes, J. R. (1991). The roles of CD4 and CD8 in T cell activation. *Semin Immunol, 3*(3), 133-141.

Miceli, M. C., von Hoegen, P., & Parnes, J. R. (1991). Adhesion versus coreceptor function of CD4 and CD8: role of the cytoplasmic tail in coreceptor activity. *Proc Natl Acad Sci U S A, 88*(7), 2623-2627. doi:10.1073/pnas.88.7.2623

Michaux, A., Larrieu, P., Stroobant, V., Fonteneau, J. F., Jotereau, F., Van den Eynde, B. J., . . . Vigneron, N. (2014). A spliced antigenic peptide comprising a single spliced amino acid is produced in the proteasome by reverse splicing of a longer peptide fragment followed by trimming. *J Immunol, 192*(4), 1962-1971. doi:10.4049/jimmunol.1302032

Milner, E., Barnea, E., Beer, I., & Admon, A. (2006). The turnover kinetics of major histocompatibility complex peptides of human cancer cells. *Mol Cell Proteomics, 5*(2), 357-365. doi:10.1074/mcp.M500241-MCP200

Mori, I., Komatsu, T., Takeuchi, K., Nakakuki, K., Sudo, M., & Kimura, Y. (1995). In vivo induction of apoptosis by influenza virus. *J Gen Virol, 76 (Pt 11)*, 2869-2873. doi:10.1099/0022-1317-76-11-2869

Morozov, G. I., Zhao, H., Mage, M. G., Boyd, L. F., Jiang, J., Dolan, M. A., . . . Margulies, D. H. (2016). Interaction of TAPBPR, a tapasin homolog, with MHC-I molecules promotes peptide editing. *Proc Natl Acad Sci U S A, 113*(8), E1006-1015. doi:10.1073/pnas.1519894113

Mosmann, T. R., Cherwinski, H., Bond, M. W., Giedlin, M. A., & Coffman, R. L. (1986). Two types of murine helper T cell clone. I. Definition according to profiles of lymphokine activities and secreted proteins. *J Immunol, 136*(7), 2348-2357.

Mozdzanowska, K., Furchner, M., Zharikova, D., Feng, J., & Gerhard, W. (2005). Roles of CD4+ T-cell-independent and -dependent antibody responses in the control of influenza virus infection: evidence for noncognate CD4+ T-cell activities that enhance the therapeutic activity of antiviral antibodies. *J Virol, 79*(10), 5943-5951. doi:10.1128/jvi.79.10.5943-5951.2005

Muramoto, Y., Noda, T., Kawakami, E., Akkina, R., & Kawaoka, Y. (2013). Identification of novel influenza A virus proteins translated from PA mRNA. *J Virol, 87*(5), 2455-2462. doi:10.1128/jvi.02656-12

Najbauer, J., Orpiszewski, J., & Aswad, D. W. (1996). Molecular aging of tubulin: accumulation of isoaspartyl sites in vitro and in vivo. *Biochemistry, 35*(16), 5183-5190. doi:10.1021/bi953063g

Neller, M. A., Ladell, K., McLaren, J. E., Matthews, K. K., Gostick, E., Pentier, J. M., . . . Miles, J. J. (2015). Naive CD8(+) T-cell precursors display structured TCR repertoires and composite antigen-driven selection dynamics. *Immunol Cell Biol, 93*(7), 625-633. doi:10.1038/icb.2015.17

Oldstone, M. B., Lewicki, H., Borrow, P., Hudrisier, D., & Gairin, J. E. (1995). Discriminated selection among viral peptides with the appropriate anchor residues: implications for the size of the cytotoxic T-lymphocyte repertoire and control of viral infection. *J Virol, 69*(12), 7423-7429.

Orr, H. T., Lancet, D., Robb, R. J., Lopez de Castro, J. A., & Strominger, J. L. (1979). The heavy chain of human histocompatibility antigen HLA-B7 contains an immunoglobulin-like region. *Nature, 282*(5736), 266-270. doi:10.1038/282266a0

Ortmann, B., Copeman, J., Lehner, P. J., Sadasivan, B., Herberg, J. A., Grandea, A. G., . . . Cresswell, P. (1997). A critical role for tapasin in the assembly and function of multimeric MHC class I-TAP complexes. *Science, 277*(5330), 1306-1309. doi:10.1126/science.277.5330.1306

Ostroumov, D., Fekete-Drimusz, N., Saborowski, M., Kuhnel, F., & Woller, N. (2018). CD4 and CD8 T lymphocyte interplay in controlling tumor growth. *Cell Mol Life Sci, 75*(4), 689-713. doi:10.1007/s00018-017-2686-7

Palese, P., & Schulman, J. L. (1976). Mapping of the influenza virus genome: identification of the hemagglutinin and the neuraminidase genes. *Proc Natl Acad Sci U S A, 73*(6), 2142-2146.

Pang, K. C., Wei, J. Q., & Chen, W. (2006). Dynamic quantification of MHC class I-peptide presentation to CD8+ T cells via intracellular cytokine staining. *J Immunol Methods, 311*(1-2), 12-18. doi:10.1016/j.jim.2006.01.008

Pannetier, C., Cochet, M., Darche, S., Casrouge, A., Zoller, M., & Kourilsky, P. (1993). The sizes of the CDR3 hypervariable regions of the murine T-cell receptor beta chains vary as a function of the recombined germ-line segments. *Proc Natl Acad Sci U S A, 90*(9), 4319-4323. doi:10.1073/pnas.90.9.4319

Park, H., Li, Z., Yang, X. O., Chang, S. H., Nurieva, R., Wang, Y. H., . . . Dong, C. (2005). A distinct lineage of CD4 T cells regulates tissue inflammation by producing interleukin 17. *Nat Immunol, 6*(11), 1133-1141. doi:10.1038/ni1261

Parkin, J., & Cohen, B. (2001). An overview of the immune system. *Lancet, 357*(9270), 1777-1789. doi:10.1016/s0140-6736(00)04904-7

Petersen, J., Purcell, A. W., & Rossjohn, J. (2009). Post-translationally modified T cell epitopes: immune recognition and immunotherapy. *J Mol Med (Berl), 87*(11), 1045-1051. doi:10.1007/s00109-009-0526-4

Peterson, R. A. (2012). Regulatory T-cells: diverse phenotypes integral to immune homeostasis and suppression. *Toxicol Pathol, 40*(2), 186-204. doi:10.1177/0192623311430693

Platteel, A. C. M., Liepe, J., Textoris-Taube, K., Keller, C., Henklein, P., Schalkwijk, H. H., . . . Sijts, A. (2017). Multi-level Strategy for Identifying Proteasome-Catalyzed Spliced Epitopes Targeted by CD8(+) T Cells during Bacterial Infection. *Cell Rep, 20*(5), 1242-1253. doi:10.1016/j.celrep.2017.07.026

Princiotta, M. F., Finzi, D., Qian, S. B., Gibbs, J., Schuchmann, S., Buttgereit, F., . . . Yewdell, J. W. (2003). Quantitating protein synthesis, degradation, and endogenous antigen processing. *Immunity, 18*(3), 343-354.

Quinones-Parra, S., Grant, E., Loh, L., Nguyen, T. H., Campbell, K. A., Tong, S. Y., . . . Kedzierska, K. (2014). Preexisting CD8+ T-cell immunity to the H7N9 influenza A virus varies across ethnicities. *Proc Natl Acad Sci U S A, 111*(3), 1049-1054. doi:10.1073/pnas.1322229111

Rammensee, H., Bachmann, J., Emmerich, N. P., Bachor, O. A., & Stevanovic, S. (1999). SYFPEITHI: database for MHC ligands and peptide motifs. *Immunogenetics, 50*(3-4), 213-219.

Rist, M. J., Theodossis, A., Croft, N. P., Neller, M. A., Welland, A., Chen, Z., . . . Burrows, S. R. (2013). HLA peptide length preferences control CD8+ T cell responses. *J Immunol, 191*(2), 561-571. doi:10.4049/jimmunol.1300292

Rius, C., Attaf, M., Tungatt, K., Bianchi, V., Legut, M., Bovay, A., . . . Sewell, A. K. (2018). Peptide-MHC Class I Tetramers Can Fail To Detect Relevant Functional T Cell Clonotypes and Underestimate Antigen-Reactive T Cell Populations. *J Immunol, 200*(7), 2263-2279. doi:10.4049/jimmunol.1700242

Rizzuto, G. A., Merghoub, T., Hirschhorn-Cymerman, D., Liu, C., Lesokhin, A. M., Sahawneh, D., . . . Houghton, A. N. (2009). Self-antigen-specific CD8+ T cell

precursor frequency determines the quality of the antitumor immune response. *J Exp Med, 206*(4), 849-866. doi:10.1084/jem.20081382

Robey, E., & Fowlkes, B. J. (1994). Selective events in T cell development. *Annu Rev Immunol, 12*, 675-705. doi:10.1146/annurev.iy.12.040194.003331

Robinson, J., Guethlein, L. A., Cereb, N., Yang, S. Y., Norman, P. J., Marsh, S. G. E., & Parham, P. (2017). Distinguishing functional polymorphism from random variation in the sequences of >10,000 HLA-A, -B and -C alleles. *PLoS Genet, 13*(6), e1006862. doi:10.1371/journal.pgen.1006862

Rosenberg, S. A., Yang, J. C., & Restifo, N. P. (2004). Cancer immunotherapy: moving beyond current vaccines. *Nat Med, 10*(9), 909-915. doi:10.1038/nm1100

Sadasivan, B., Lehner, P. J., Ortmann, B., Spies, T., & Cresswell, P. (1996). Roles for calreticulin and a novel glycoprotein, tapasin, in the interaction of MHC class I molecules with TAP. *Immunity, 5*(2), 103-114.

Sakaguchi, S., Sakaguchi, N., Asano, M., Itoh, M., & Toda, M. (2011). Pillars article: immunologic self-tolerance maintained by activated T cells expressing IL-2 receptor alpha-chains (CD25). Breakdown of a single mechanism of self-tolerance causes various autoimmune diseases. J. Immunol. 1995. *J Immunol, 186*(7), 3808-3821.

Salter, R. D., Benjamin, R. J., Wesley, P. K., Buxton, S. E., Garrett, T. P., Clayberger, C., . . . Parham, P. (1990). A binding site for the T-cell co-receptor CD8 on the alpha 3 domain of HLA-A2. *Nature, 345*(6270), 41-46. doi:10.1038/345041a0

Saulquin, X., Scotet, E., Trautmann, L., Peyrat, M. A., Halary, F., Bonneville, M., & Houssaint, E. (2002). +1 Frameshifting as a novel mechanism to generate a cryptic cytotoxic T lymphocyte epitope derived from human interleukin 10. *J Exp Med, 195*(3), 353-358. doi:10.1084/jem.20011399

Saunders-Hastings, P. R., & Krewski, D. (2016). Reviewing the History of Pandemic Influenza: Understanding Patterns of Emergence and Transmission. *Pathogens, 5*(4). doi:10.3390/pathogens5040066

Saveanu, L., Carroll, O., Lindo, V., Del Val, M., Lopez, D., Lepelletier, Y., . . . van Endert, P. M. (2005). Concerted peptide trimming by human ERAP1 and ERAP2 aminopeptidase complexes in the endoplasmic reticulum. *Nat Immunol, 6*(7), 689-697. doi:10.1038/ni1208

Schirmbeck, R., Stober, D., El-Kholy, S., Riedl, P., & Reimann, J. (2002). The immunodominant, Ld-restricted T cell response to hepatitis B surface antigen (HBsAg) efficiently suppresses T cell priming to multiple Dd-, Kd-, and Kb-restricted HBsAg epitopes. *J Immunol, 168*(12), 6253-6262. doi:10.4049/jimmunol.168.12.6253

Schott, E., & Ploegh, H. L. (2002). Mouse MHC class I tetramers that are unable to bind to CD8 reveal the need for CD8 engagement in order to activate naive CD8 T cells. *Eur J Immunol, 32*(12), 3425-3434. doi:10.1002/1521-4141(200212)32:12<3425::aid-immu3425>3.0.co;2-7

Schubert, U., Anton, L. C., Gibbs, J., Norbury, C. C., Yewdell, J. W., & Bennink, J. R. (2000). Rapid degradation of a large fraction of newly synthesized proteins by proteasomes. *Nature, 404*(6779), 770-774. doi:10.1038/35008096

Selman, M., Dankar, S. K., Forbes, N. E., Jia, J. J., & Brown, E. G. (2012). Adaptive mutation in influenza A virus non-structural gene is linked to host switching and

induces a novel protein by alternative splicing. *Emerg Microbes Infect, 1*(11), e42. doi:10.1038/emi.2012.38

Sercarz, E. E., Lehmann, P. V., Ametani, A., Benichou, G., Miller, A., & Moudgil, K. (1993). Dominance and crypticity of T cell antigenic determinants. *Annu Rev Immunol, 11*, 729-766.

Short, K. R., Kedzierska, K., & van de Sandt, C. E. (2018). Back to the Future: Lessons Learned From the 1918 Influenza Pandemic. *Front Cell Infect Microbiol, 8*, 343. doi:10.3389/fcimb.2018.00343

Shrestha, S. S., Swerdlow, D. L., Borse, R. H., Prabhu, V. S., Finelli, L., Atkins, C. Y., . . . Meltzer, M. I. (2011). Estimating the burden of 2009 pandemic influenza A (H1N1) in the United States (April 2009-April 2010). *Clin Infect Dis, 52 Suppl 1*, S75-82. doi:10.1093/cid/ciq012

Sidney, J., Peters, B., Frahm, N., Brander, C., & Sette, A. (2008). HLA class I supertypes: a revised and updated classification. *BMC Immunol, 9*, 1. doi:10.1186/1471-2172-9-1

Simmons, C. P., Bernasconi, N. L., Suguitan, A. L., Mills, K., Ward, J. M., Chau, N. V., . . . Subbarao, K. (2007). Prophylactic and therapeutic efficacy of human monoclonal antibodies against H5N1 influenza. *PLoS Med, 4*(5), e178. doi:10.1371/journal.pmed.0040178

Smith-Garvin, J. E., Koretzky, G. A., & Jordan, M. S. (2009). T cell activation. *Annu Rev Immunol, 27*, 591-619. doi:10.1146/annurev.immunol.021908.132706

Snyder, H. L., Yewdell, J. W., & Bennink, J. R. (1994). Trimming of antigenic peptides in an early secretory compartment. *J Exp Med, 180*(6), 2389-2394. doi:10.1084/jem.180.6.2389

Steinman, R. M. (2012). Decisions about dendritic cells: past, present, and future. *Annu Rev Immunol, 30*, 1-22. doi:10.1146/annurev-immunol-100311-102839

Steinman, R. M., & Cohn, Z. A. (1973). Identification of a novel cell type in peripheral lymphoid organs of mice. I. Morphology, quantitation, tissue distribution. *J Exp Med, 137*(5), 1142-1162. doi:10.1084/jem.137.5.1142

Stockinger, B., Kassiotis, G., & Bourgeois, C. (2004). Homeostasis and T cell regulation. *Curr Opin Immunol, 16*(6), 775-779. doi:10.1016/j.coi.2004.09.003

Sun, J., & Braciale, T. J. (2013). Role of T cell immunity in recovery from influenza virus infection. *Curr Opin Virol, 3*(4), 425-429. doi:10.1016/j.coviro.2013.05.001

Swain, S. L., McKinstry, K. K., & Strutt, T. M. (2012). Expanding roles for CD4(+) T cells in immunity to viruses. *Nat Rev Immunol, 12*(2), 136-148. doi:10.1038/nri3152

Takiguchi, M., Matsuda, T., Tomiyama, H., & Miwa, K. (2000). Analysis of three HLA-A*3303 binding peptide anchors using an HLA-A*3303 stabilization assay. *Tissue Antigens, 55*(4), 296-302.

Taubenberger, J. K., & Kash, J. C. (2010). Influenza virus evolution, host adaptation, and pandemic formation. *Cell Host Microbe, 7*(6), 440-451. doi:10.1016/j.chom.2010.05.009

Taylor, P. M., & Askonas, B. A. (1986). Influenza nucleoprotein-specific cytotoxic T-cell clones are protective in vivo. *Immunology, 58*(3), 417-420.

Teijaro, J. R., Verhoeven, D., Page, C. A., Turner, D., & Farber, D. L. (2010). Memory CD4 T cells direct protective responses to influenza virus in the lungs through helper-independent mechanisms. *J Virol, 84*(18), 9217-9226. doi:10.1128/jvi.01069-10

Tenzer, S., Wee, E., Burgevin, A., Stewart-Jones, G., Friis, L., Lamberth, K., . . . Iversen, A. K. (2009). Antigen processing influences HIV-specific cytotoxic T lymphocyte immunodominance. *Nat Immunol, 10*(6), 636-646. doi:10.1038/ni.1728

Thomas, P. G., Brown, S. A., Keating, R., Yue, W., Morris, M. Y., So, J., . . . Doherty, P. C. (2007). Hidden epitopes emerge in secondary influenza virus-specific CD8+ T cell responses. *J Immunol, 178*(5), 3091-3098.

Toes, R. E., Nussbaum, A. K., Degermann, S., Schirle, M., Emmerich, N. P., Kraft, M., . . . Schild, H. (2001). Discrete cleavage motifs of constitutive and immunoproteasomes revealed by quantitative analysis of cleavage products. *J Exp Med, 194*(1), 1-12. doi:10.1084/jem.194.1.1

Townsend, A. R., Rothbard, J., Gotch, F. M., Bahadur, G., Wraith, D., & McMichael, A. J. (1986). The epitopes of influenza nucleoprotein recognized by cytotoxic T lymphocytes can be defined with short synthetic peptides. *Cell, 44*(6), 959-968. doi:10.1016/0092-8674(86)90019-x

Trauer, J. M., Laurie, K. L., McDonnell, J., Kelso, A., & Markey, P. G. (2011). Differential effects of pandemic (H1N1) 2009 on remote and indigenous groups, Northern Territory, Australia, 2009. *Emerg Infect Dis, 17*(9), 1615-1623. doi:10.3201/eid1709.101196

Treanor, J. (2004). Influenza vaccine--outmaneuvering antigenic shift and drift. *N Engl J Med, 350*(3), 218-220. doi:10.1056/NEJMp038238

Tscharke, D. C., Karupiah, G., Zhou, J., Palmore, T., Irvine, K. R., Haeryfar, S. M., . . . Yewdell, J. W. (2005). Identification of poxvirus CD8+ T cell determinants to enable rational design and characterization of smallpox vaccines. *J Exp Med, 201*(1), 95-104. doi:10.1084/jem.20041912

Turner, S. J., Doherty, P. C., McCluskey, J., & Rossjohn, J. (2006). Structural determinants of T-cell receptor bias in immunity. *Nat Rev Immunol, 6*(12), 883-894. doi:10.1038/nri1977

Udaka, K., Tsomides, T. J., Walden, P., Fukusen, N., & Eisen, H. N. (1993). A ubiquitous protein is the source of naturally occurring peptides that are recognized by a CD8+ T-cell clone. *Proc Natl Acad Sci U S A, 90*(23), 11272-11276. doi:10.1073/pnas.90.23.11272

Valitutti, S., Muller, S., Cella, M., Padovan, E., & Lanzavecchia, A. (1995). Serial triggering of many T-cell receptors by a few peptide-MHC complexes. *Nature, 375*(6527), 148-151. doi:10.1038/375148a0

van de Sandt, C. E., Kreijtz, J. H., de Mutsert, G., Geelhoed-Mieras, M. M., Hillaire, M. L., Vogelzang-van Trierum, S. E., . . . Rimmelzwaan, G. F. (2014). Human cytotoxic T lymphocytes directed to seasonal influenza A viruses cross-react with the newly emerging H7N9 virus. *J Virol, 88*(3), 1684-1693. doi:10.1128/jvi.02843-13

Vasin, A. V., Temkina, O. A., Egorov, V. V., Klotchenko, S. A., Plotnikova, M. A., & Kiselev, O. I. (2014). Molecular mechanisms enhancing the proteome of influenza A viruses: an overview of recently discovered proteins. *Virus Res, 185*, 53-63. doi:10.1016/j.virusres.2014.03.015

Veillette, A., Bookman, M. A., Horak, E. M., & Bolen, J. B. (1988). The CD4 and CD8 T cell surface antigens are associated with the internal membrane tyrosine-protein kinase p56lck. *Cell, 55*(2), 301-308.

Vigneron, N., Stroobant, V., Chapiro, J., Ooms, A., Degiovanni, G., Morel, S., . . . Van den Eynde, B. J. (2004). An antigenic peptide produced by peptide splicing in the proteasome. *Science, 304*(5670), 587-590. doi:10.1126/science.1095522

Vigneron, N., Stroobant, V., Ferrari, V., Abi Habib, J., & Van den Eynde, B. J. (2018). Production of spliced peptides by the proteasome. *Mol Immunol*. doi:10.1016/j.molimm.2018.03.030

Waffarn, E. E., & Baumgarth, N. (2011). Protective B cell responses to flu--no fluke! *J Immunol, 186*(7), 3823-3829. doi:10.4049/jimmunol.1002090

Wallace, M. E., Bryden, M., Cose, S. C., Coles, R. M., Schumacher, T. N., Brooks, A., & Carbone, F. R. (2000). Junctional biases in the naive TCR repertoire control the CTL response to an immunodominant determinant of HSV-1. *Immunity, 12*(5), 547-556. doi:10.1016/s1074-7613(00)80206-x

Wallace, M. E., Keating, R., Heath, W. R., & Carbone, F. R. (1999). The cytotoxic T-cell response to herpes simplex virus type 1 infection of C57BL/6 mice is almost entirely directed against a single immunodominant determinant. *J Virol, 73*(9), 7619-7626.

Wang, R. F., Parkhurst, M. R., Kawakami, Y., Robbins, P. F., & Rosenberg, S. A. (1996). Utilization of an alternative open reading frame of a normal gene in generating a novel human cancer antigen. *J Exp Med, 183*(3), 1131-1140. doi:10.1084/jem.183.3.1131

Wang, Z., Wan, Y., Qiu, C., Quinones-Parra, S., Zhu, Z., Loh, L., . . . Xu, J. (2015). Recovery from severe H7N9 disease is associated with diverse response mechanisms dominated by CD8(+) T cells. *Nat Commun, 6*, 6833. doi:10.1038/ncomms7833

Warren, E. H., Vigneron, N. J., Gavin, M. A., Coulie, P. G., Stroobant, V., Dalet, A., . . . Van den Eynde, B. J. (2006). An antigen produced by splicing of noncontiguous peptides in the reverse order. *Science, 313*(5792), 1444-1447. doi:10.1126/science.1130660

Wegener, A. M., Letourneur, F., Hoeveler, A., Brocker, T., Luton, F., & Malissen, B. (1992). The T cell receptor/CD3 complex is composed of at least two autonomous transduction modules. *Cell, 68*(1), 83-95.

Wells, M. A., Ennis, F. A., & Albrecht, P. (1981). Recovery from a viral respiratory infection. II. Passive transfer of immune spleen cells to mice with influenza pneumonia. *J Immunol, 126*(3), 1042-1046.

Wilkinson, T. M., Li, C. K., Chui, C. S., Huang, A. K., Perkins, M., Liebner, J. C., . . . Xu, X. N. (2012). Preexisting influenza-specific CD4+ T cells correlate with disease protection against influenza challenge in humans. *Nat Med, 18*(2), 274-280. doi:10.1038/nm.2612

Wise, H. M., Foeglein, A., Sun, J., Dalton, R. M., Patel, S., Howard, W., . . . Digard, P. (2009). A complicated message: Identification of a novel PB1-related protein translated from influenza A virus segment 2 mRNA. *J Virol, 83*(16), 8021-8031. doi:10.1128/jvi.00826-09

Wise, H. M., Hutchinson, E. C., Jagger, B. W., Stuart, A. D., Kang, Z. H., Robb, N., . . . Digard, P. (2012). Identification of a novel splice variant form of the influenza A virus M2 ion channel with an antigenically distinct ectodomain. *PLoS Pathog, 8*(11), e1002998. doi:10.1371/journal.ppat.1002998

Wrammert, J., Smith, K., Miller, J., Langley, W. A., Kokko, K., Larsen, C., . . . Wilson, P. C. (2008). Rapid cloning of high-affinity human monoclonal antibodies against influenza virus. *Nature, 453*(7195), 667-671. doi:10.1038/nature06890

Wu, C., Zanker, D., Valkenburg, S., Tan, B., Kedzierska, K., Zou, Q. M., . . . Chen, W. (2011). Systematic identification of immunodominant CD8+ T-cell responses to influenza A virus in HLA-A2 individuals. *Proc Natl Acad Sci U S A, 108*(22), 9178-9183. doi:10.1073/pnas.1105624108

Xiao, Z., Mescher, M. F., & Jameson, S. C. (2007). Detuning CD8 T cells: down-regulation of CD8 expression, tetramer binding, and response during CTL activation. *J Exp Med, 204*(11), 2667-2677. doi:10.1084/jem.20062376

Yap, K. L., & Ada, G. L. (1978). The recovery of mice from influenza A virus infection: adoptive transfer of immunity with influenza virus-specific cytotoxic T lymphocytes recognizing a common virion antigen. *Scand J Immunol, 8*(5), 413-420.

Yap, K. L., Ada, G. L., & McKenzie, I. F. (1978). Transfer of specific cytotoxic T lymphocytes protects mice inoculated with influenza virus. *Nature, 273*(5659), 238-239. doi:10.1038/273238a0

Yewdell, J. W. (2001). Not such a dismal science: the economics of protein synthesis, folding, degradation and antigen processing. *Trends Cell Biol, 11*(7), 294-297.

Yewdell, J. W. (2011). DRiPs solidify: progress in understanding endogenous MHC class I antigen processing. *Trends Immunol, 32*(11), 548-558. doi:10.1016/j.it.2011.08.001

Yewdell, J. W., Anton, L. C., & Bennink, J. R. (1996). Defective ribosomal products (DRiPs): a major source of antigenic peptides for MHC class I molecules? *J Immunol, 157*(5), 1823-1826.

Yewdell, J. W., & Bennink, J. R. (1989). Brefeldin A specifically inhibits presentation of protein antigens to cytotoxic T lymphocytes. *Science, 244*(4908), 1072-1075.

Yewdell, J. W., & Bennink, J. R. (1999). Immunodominance in major histocompatibility complex class I-restricted T lymphocyte responses. *Annu Rev Immunol, 17*, 51-88. doi:10.1146/annurev.immunol.17.1.51

Yewdell, J. W., Bennink, J. R., & Hosaka, Y. (1988). Cells process exogenous proteins for recognition by cytotoxic T lymphocytes. *Science, 239*(4840), 637-640. doi:10.1126/science.3257585

Yewdell, J. W., Schubert, U., & Bennink, J. R. (2001). At the crossroads of cell biology and immunology: DRiPs and other sources of peptide ligands for MHC class I molecules. *J Cell Sci, 114*(Pt 5), 845-851.

York, I. A., & Rock, K. L. (1996). Antigen processing and presentation by the class I major histocompatibility complex. *Annu Rev Immunol, 14*, 369-396. doi:10.1146/annurev.immunol.14.1.369

Yuseff, M. I., Pierobon, P., Reversat, A., & Lennon-Dumenil, A. M. (2013). How B cells capture, process and present antigens: a crucial role for cell polarity. *Nat Rev Immunol, 13*(7), 475-486. doi:10.1038/nri3469

Zanker, D., Xiao, K., Oveissi, S., Guillaume, P., Luescher, I. F., & Chen, W. (2013). An optimized method for establishing high purity murine CD8+ T cell cultures. *J Immunol Methods, 387*(1-2), 173-180. doi:10.1016/j.jim.2012.10.012

Zanker, D. J., Oveissi, S., Tscharke, D. C., Duan, M., Wan, S., Zhang, X., . . . Chen, W. (2019). Influenza A Virus Infection Induces Viral and Cellular Defective Ribosomal

Products Encoded by Alternative Reading Frames. *J Immunol*. doi:10.4049/jimmunol.1900070

Zelnickova, P., Faldyna, M., Stepanova, H., Ondracek, J., & Kovaru, F. (2007). Intracellular cytokine detection by flow cytometry in pigs: fixation, permeabilization and cell surface staining. *J Immunol Methods, 327*(1-2), 18-29. doi:10.1016/j.jim.2007.07.006

Zhu, J., & Paul, W. E. (2008). CD4 T cells: fates, functions, and faults. *Blood, 112*(5), 1557-1569. doi:10.1182/blood-2008-05-078154

Zinkernagel, R. M., Althage, A., Cooper, S., Kreeb, G., Klein, P. A., Sefton, B., . . . Klein, J. (1978). Ir-genes in H-2 regulate generation of anti-viral cytotoxic T cells. Mapping to K or D and dominance of unresponsiveness. *J Exp Med, 148*(2), 592-606.

Zinkernagel, R. M., & Doherty, P. C. (1974). Restriction of in vitro T cell-mediated cytotoxicity in lymphocytic choriomeningitis within a syngeneic or semiallogeneic system. *Nature, 248*(5450), 701-702. doi:10.1038/248701a0

Appendix

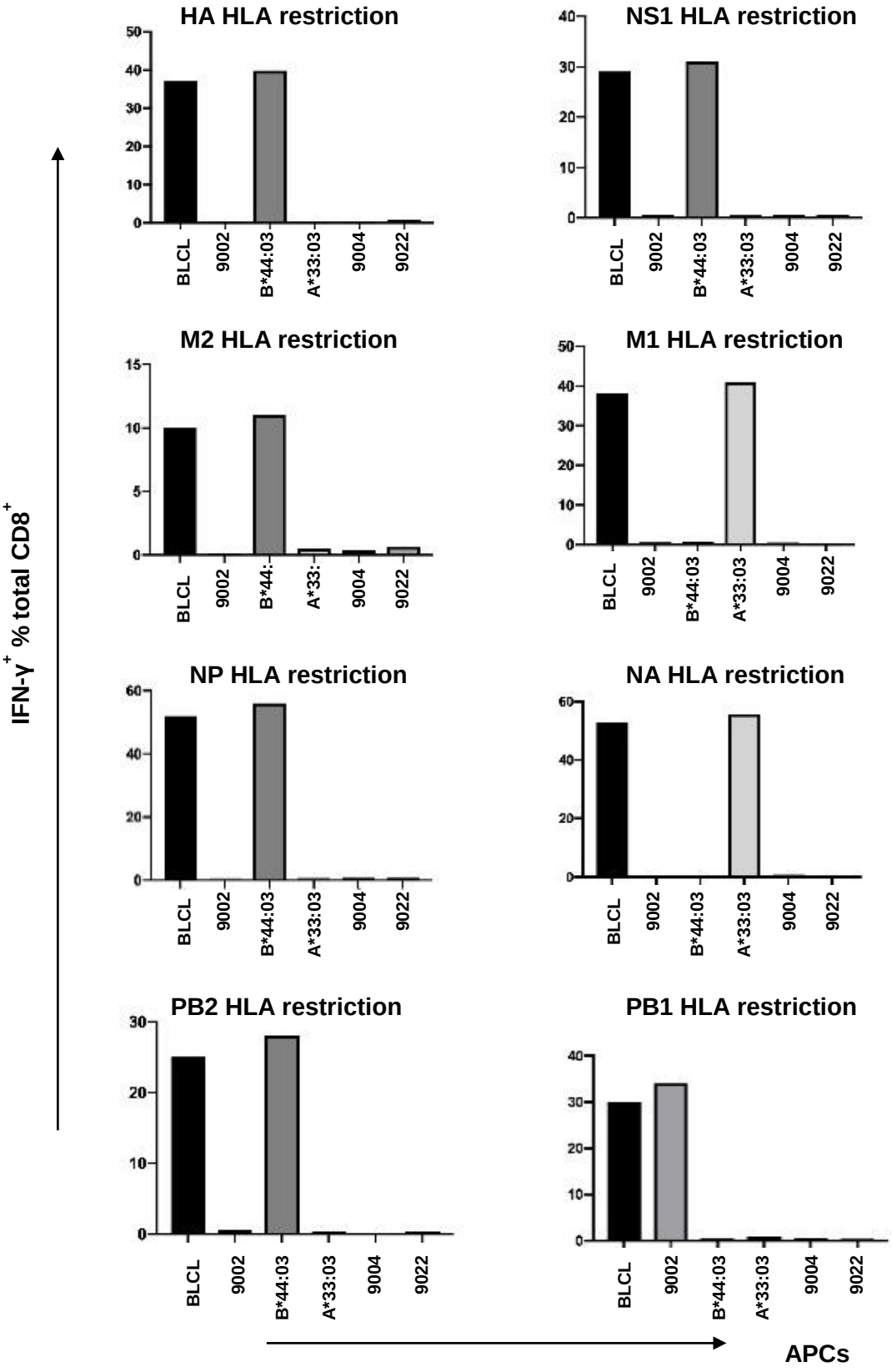
HA HLA restriction
NS1 HLA restriction
M2 HLA restriction
M1 HLA restriction
NP HLA restriction
NA HLA restriction
PB2 HLA restriction
PB1 HLA restriction
IFN-γ+ % total CD8+
BLCL
9002
B*44:03
A*33:03
9004
9022
APCs

Appendix Figure 4.1. HLA restriction of all 18mer peptides identified in Figure 4.3 (Chapter 4)

Partial donor HLA-matched BLCLs were pulsed with 10^{-6}M of relevant 18mer peptides for 1 hour. Later, cells were extensively washed and used as APCs in a co-culture with antigen-specific $CD8^+$ T cells for 4 hours. HLA-restriction was assessed by ICS for production of IFN-γ.

Alternative Reading Frame (ARF) encode NP protein (5'3' Frame 2)[a]
MENARMPLKSEHPSEKMRDGMTKKKMVTMQRLVMMQLIRGQELLFAPEWILGCALMIGTSGGVRMDEK**QELLMKECATFSKGNF**KLLHKKQMLSSKISLFMRIQHTRVNWCGWHAILPHLKIMKIWRLWNQVHLNMGIQRGEHLTMCLSRGGESSSSRTKRQRGESSRTKRQRARSCLPLTMKDLISSETMQRSTTI**KEKYPCFY**
ARF encode NP protein (5'3' Frame 1)
MS**KEGTIGLAAF**SSESSKTPRPWKDTSSGLALSIILMISVLMSDVLPSVFPLNAAIMVVLSKGRFLCTENVGCMLIWPADALCMAQYLLLSSSVLDSIVSIFSLEAIMKLNTLRSSNAAEWHAIHTSMSADRARKVRSSNSAFPGFRLSLTMSSLIHFPFTLLYIGPPVFLGSFPALGCSSRYLFLLSSK**AESTILSIVKLF**WINRPSMILMSLSE
ARF encode NP protein (3'5' Frame 2)
MFSPLYSHMLPMPSVDWCFLHFWSLWPSTCFSVQVYLIPMRQNGMPSTPVDSCVLDSHLV
ARF encode NP protein (3'5' Frame 3)
MACHPHQLTLVCWILIWSDMPDHHVSQTSRCIVTIISLAPDSPYFFFVIKDEFSHPLSVYSPVYRSSSFLRILPRTGMFFKVFISPFVKSREHHSLYC
ARF encode NS1 protein (5'3' Frame 2)
MSANELQTKNMPHSLIGFAEIRNPMRHLK
ARF encode NS1 protein (5'3' Frame 3)
MVHAHTQ**AESGRPSLY**QNGPGDHGME
ARF encode NS1 protein (3'5' Frame 1)
MSWKRRQWMPKKAIYLKA
ARF encode NS1 protein (3'5' Frame 1)
MVKFRQQLLPLRMGHHLVLGLQLVCGHAKESNLPESLTQCLDPLCLCHPAFA

Appendix Table 5.1. The potential ARF peptide sequence predicted from NP and NS1 protein

[a] predicted from bioinformatics website https://www.expasy.org/

NP-ARF 14-24 + NP-ARF 17-24
NP-ARF 14-24 + NP-ARF 40-51
NP-ARF 14-24 + NP-ARF 32-41
NP-ARF 14-24 + NP-ARF 8-16
NP-ARF 17-24 + NP-ARF 40-51
NP-ARF 17-24 + NP-ARF 32-41
NP-ARF 17-24 + NP-ARF 8-16
NP-ARF 40-51 + NP-ARF 32-41
NP-ARF 40-51 + NP-ARF 8-16
NP-ARF 32-41 + NP-ARF 8-16

Appendix Table 5.2. Permutated and combined all the positive ARF peptides

	Protein	Peptide ID	Sequence		Protein	peptide ID	Sequence
1	NP	NP 97-109	YKRVDGKWMRELV	48	NP	NP 102-114 V4	RKWMRELVLYDKE
2	NP	NP 97-109 V3	YRRVGGKWMRELV	49	NP	NP 331-343 V2	MACNSAAFEDLRV
3	NP	NP 98-110 V2	KRVDGKWMRELVL	50	NP	NP 332-344 V2	ACNSAAFEDLRVS
4	NP	NP 98-110 V3	RRVGGKWMRELVL	51	NP	NP 333-345 V2	CNSAAFEDLRVSS
5	NP	NP 99-111 V2	RVDGKWMRELVLY	52	NP	NP 334-346 V2	NSAAFEDLRVSSF
6	NP	NP 99-111 V3	RVGGKWMRELVLY	53	NP	NP 335-347 V2	SAAFEDLRVSSFI
7	NP	NP 100-112 V2	VDGKWMRELVLYD	54	NP	NP 336-348 V2	AAFEDLRVSSFIR
8	NP	NP 100-112 V3	VGGKWMRELVLYD	55	PA	PA 168-178	RARIKTRLFTI
9	NP	NP 101-113 V2	DGKWMRELVLYDK	56	PA	PA 169-178	ARIKTRLFTI
10	NP	NP 101-113 V3	GGKWMRELVLYDK	57	PA	PA 168-177	RARIKTRLFT
11	NP	NP 102-114 V2	GKWMRELVLYDKE	58	PA	PA 167-178	SRARIKTRLFTI
12	NP	NP 102-114 V3	GKWMRELVLYDKD	59	PA	PA 168-179	RARIKTRLFTIR
13	NP	NP 139-151 V1	WHSNLNDTTYQRT	60	PA	PA 167-179	SRARIKTRLFTI
14	NP	NP 140-152 V1	HSNLNDTTYQRTR	61	PA	PA 168-176	RARIKTRLF
15	NP	NP 141-153 V1	SNLNDTTYQRTRA	62	PA	PA 169-176	ARIKTRLF
16	NP	NP 142-154 V1	NLNDTTYQRTRAL	63	PA	PA 168-175	RARIKTRL
17	NP	NP 143-155 V1	LNDTTYQRTRALV	64	PA	PA 167-176	SRARIKTRLF
18	NP	NP 144-156 V1	NDTTYQRTRALVR	65	PA	PA 168-176	RARIKTRLF
19	NP	NP 205-217 V1	NFWRGENGRKTRS	66	PA	PA 167-175	SRARIKTRL
20	NP	NP 206-218 V1	FWRGENGRKTRSA	67	M1	M1 124-134	LASCMGLIYNR
21	NP	NP 207-219 V1	WRGENGRKTRSAY	68	M1	M1 125-134	ASCMGLIYNR
22	NP	NP 208-220 V1	RGENGRKTRSAYE	69	M1	M1 124-133	LASCMGLIYN
23	NP	NP 209-221 V1	GENGRKTRSAYER	70	M1	M1 123-134	ALASCMGLIYNR
24	NP	NP 210-222 V1	ENGRKTRSAYERM	71	M1	M1 124-135	LASCMGLIYNRM
25	NP	NP 211-223 V1	NGRKTRSAYERMC	72	M2	M2 13-21	NEWGCRCNG
26	NP	NP 212-224 V1	GRKTRSAYERMCN	73	M2	M2 14-21	EWGCRCNG
27	NP	NP 213-225 V1	RKTRSAYERMCNI	74	M2	M2 13-20	NEWGCRCN
28	NP	NP 214-226 V1	KTRSAYERMCNIL	75	M2	M2 13-22	NEWGCRCNGS
29	NP	NP 215-227 V1	TRSAYERMCNILK	76	M2	M2 12-21	RNEWGCRCNG
30	NP	NP 216-228 V1	RSAYERMCNILKG	77	M2	M2 7-15	VETPIRNEW
31	NP	NP 331-343 V1	MACHSAAFEDLRL	78	M2	M2 8-15	ETPIRNEW
32	NP	NP 332-344 V1	ACHSAAFEDLRLL	79	M2	M2 7-14	VETPIRNE
33	NP	NP 333-345 V1	CHSAAFEDLRLLS	80	NA	NA 337-346	RYGNGVWIGR
34	NP	NP 334-346 V1	HSAAFEDLRLLSF	81	NA	NA 338-346	YGNGVWIGR
35	NP	NP 335-347 V1	SAAFEDLRLLSFI	82	NA	NA 337-345	RYGNGVWIG
36	NP	NP 336-348 V1	AAFEDLRLLSFIR	83	NA	NA 337-347	RYGNGVWIGRT
37	NP	NP 97-109 V1	YRRVDGKWMRELV	84	NA	NA 336-346	YRYGNGVWIGR
38	NP	NP 97-109 V4	YRRVDRKWMRELV	85	PB1	PB1 498-509	RYGFVANFSMEL
39	NP	NP 98-110 V1	RRVDGKWMRELVL	86	PB1	PB1 499-509	YGFVANFSMEL
40	NP	NP 98-110 V4	RRVDRKWMRELVL	87	PB1	PB1 498-508	RYGFVANFSME
41	NP	NP 99-111 V1	RVDGKWMRELVLY	88	NP	**NP-ARF 14-24**	**QELLMKECATF**
42	NP	NP 99-111 V4	RVDRKWMRELVLY	89	NP	**NP-ARF 19-29**	**KECATFSKGNF**
43	NP	NP 100-112 V1	VDGKWMRELVLYD	90	NP	**NP-ARF 17-24**	**KEKYPCFY**
44	NP	NP 100-110 V4	VDRKWMRELVLYD	91	NP	**NP-ARF 3-12**	**KEGTIGLAAF**

45	NP	NP 101-113 V1	DGKWMRELVLYDK	92	NP	**NP-ARF 40-51**	**AESTILSIVKLF**
46	NP	NP 101-113 V4	DRKWMRELVLYDK	93	NP	**NP-ARF 32-41**	**DEFSHPLSVY**
47	NP	NP 102-114 V1	GKWMRELVLYDKE	94	NP	**NS1 ARF 8-16**	**AESGRPSLY**

Appendix Table 5.3. The whole batch of peptides synthesized with predicted ARF peptides

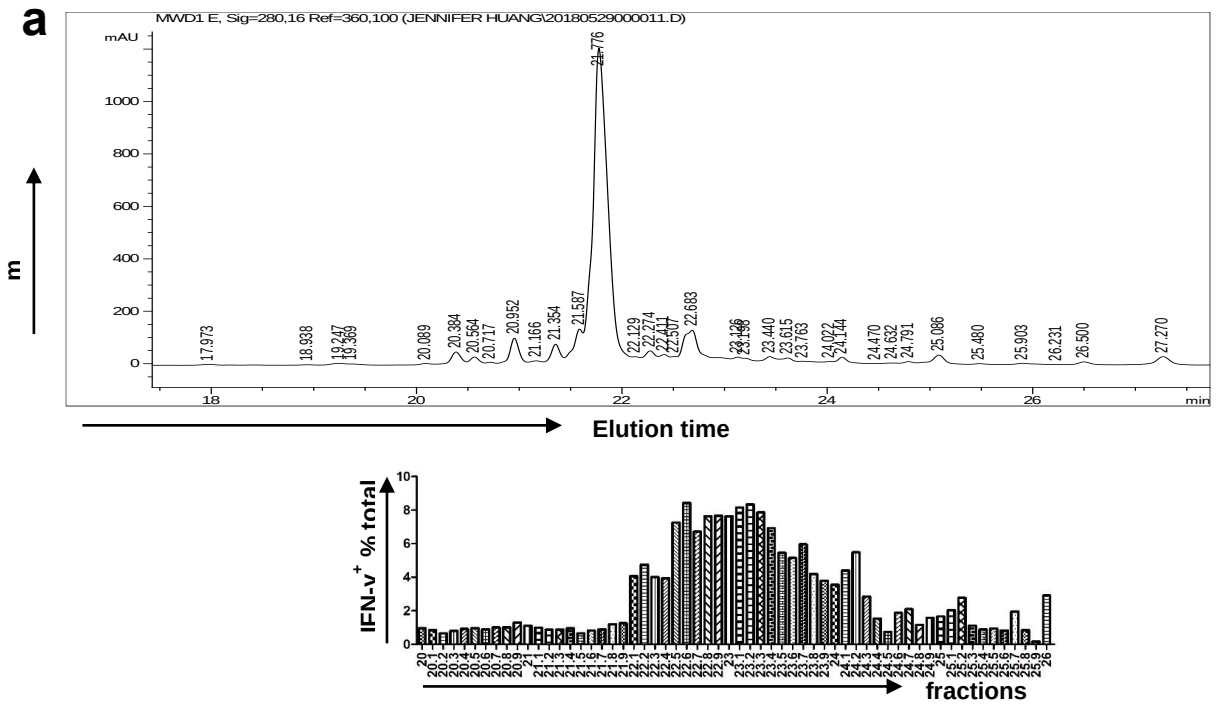
a
MWD1 E, Sig=280,16 Ref=360,100 (JENNIFER HUANG\20180529000011.D)
mAU
m
Elution time
IFN-γ+ % total
fractions

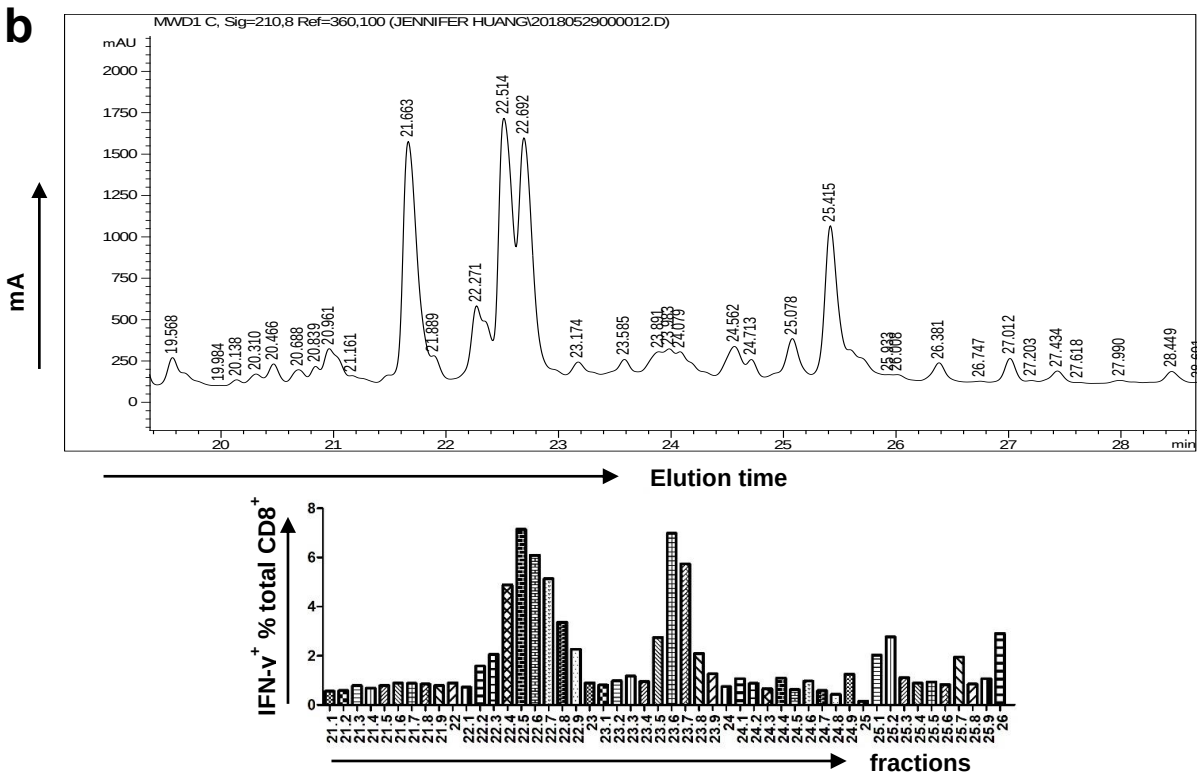
b
MWD1 C, Sig=210,8 Ref=360,100 (JENNIFER HUANG\20180529000012.D)
mAU
mA
Elution time
IFN-γ+ % total CD8+
fractions

Appendix Figure 5.1. Detecting active HPLC fractions from ARF peptide by the IAV-specific CD8$^+$ T cell line

(a), NP-ARFR 32-41 peptide was fractionated on HPLC and the fractions were collected every 0.1min between 10 and 39 min, CD8$^+$ T cells were then used to screen all fractions.
(b), NP-ARF-F2 14-24 peptide was fractionated on HPLC and the fractions were collected every 0.1min between 10 and 39 min, CD8$^+$ T cells were then used to screen all fractions.

peptide number	spliced peptide sequence	original sequence	Truncated positions
10mer	AESTSIVKLF	AEST**IL**SIVKLF	P5,P6
10mer	AESLSIVKLF	AES**TI**LSIVKLF	P4,P5
10mer	AETLSIVKLF	AE**S**T**I**LSIVKLF	P3,P5
10mer	AETISIVKLF	AE**S**TI**L**SIVKLF	P3,P6
10mer	AEILSIVKLF	AE**ST**ILSIVKLF	P3,P4
11mer	AESTLSIVKLF	AEST**I**LSIVKLF	P5
11mer	AESILSIVKLF	AES**TIL**SIVKLF	P4
9mer	AESSIVKLF	AE**STI**LSIVKLF	P4,P5,P6
9mer	AELSIVKLF	AE**STI**LSIVKLF	P3,P4,P5
10mer	AESTLSIVKF	AEST**I**LSIVKLF	P5,P11
9mer	AETSIVKLF	AE**S**T**IL**SIVKLF	P3,P5,P6
8mer	AESTVKLF	AEST**ILSI**VKLF	P5,P6,P7,P8
8mer	AESLVKLF	AES**TI**L**SI**VKLF	P4,P5,P7,P8

Appendix Table 5.4 Selected spliced peptide sequence obtains based on Mass Spectrometry analysis